

**Discovery of 3-((4-Benzylpyridin-2-yl)amino)benzamides as  
Potent GPR52 G Protein-Biased Agonists**

Ryan E. Murphy,<sup>1</sup> Pingyuan Wang,<sup>1</sup> Saghir Ali,<sup>1</sup> Hudson R. Smith, Daniel E. Felsing, Haiying  
Chen, Jia Zhou\* and John A. Allen\*

Center for Addiction Sciences and Therapeutics, Department of Pharmacology and Toxicology,  
University of Texas Medical Branch, Galveston, TX 77555, USA

<sup>1</sup>These authors contributed equally to this work.

***\*Corresponding authors:***

Dr. John A. Allen; Phone: (409) 772-9621; E-mail: [joaallen@utmb.edu](mailto:joaallen@utmb.edu)

Dr. Jia Zhou ; Phone: (409) 772-9748; E-mail: [jizhou@utmb.edu](mailto:jizhou@utmb.edu).

\*J.A.A. and J.Z. are equal contributors and corresponding authors

## ABSTRACT

Orphan GPR52 is emerging as a promising neurotherapeutic target. Optimization of previously reported lead **4a** employing an iterative drug design strategy led to identification of a series of unique GPR52 agonists, such as **10a** (PW0677), **15b** (PW0729) and **24f** (PW0866), with improved potency and efficacy. Intriguingly, compounds **10a** and **24f** showed greater bias for G protein/cAMP signaling and induced significantly less *in vitro* desensitization than parent compound **4a**, indicating that reducing GPR52  $\beta$ -arrestin activity with biased agonism results in sustained GPR52 activation. Further exploration of compounds **15b** and **24f** indicated improved potency and efficacy, excellent target selectivity, but limited brain exposure warranting further optimization. These balanced and biased GPR52 agonists provide important pharmacological tools to study GPR52 activation, signaling bias, and therapeutic potential for neuropsychiatric and neurological diseases.

**Keywords:** G protein-coupled receptor (GPCR); orphan receptor GPR52; agonist; biased agonism; functional selectivity; desensitization; cAMP;  $\beta$ -arrestin; drug discovery; neurotherapeutics; schizophrenia; addiction.

## INTRODUCTION

Orphan G protein-coupled receptors (oGPCRs; e.g., GPR6, GPR12, GPR37, GPR61, GPR88, GPR52, and GPR158) are emerging therapeutic targets for central nervous system (CNS) disorders, such as schizophrenia (SZ), Huntington's disease (HD), Parkinson's disease (PD), Alzheimer's disease (AD), attention deficit hyperactivity disorder (ADHD) as well as metabolic disorders, obesity and cancer.<sup>1-9</sup> GPR52 is an oGPCR that regulates diverse cAMP-mediated pathological and physiological processes.<sup>1</sup> GPR52 was first identified as a novel oGPCR from the GenBank high-throughput genome database in 1999.<sup>10</sup> Considerable effort has been made to determine the tissue distribution and expression of GPR52.<sup>11,12</sup> *In situ* hybridization studies in rats and large-scale RNA sequencing approaches in humans indicate GPR52 is exclusively expressed in the brain, most abundantly in the striatum.<sup>11,12</sup> Anatomical studies have demonstrated that GPR52 is specifically co-expressed with dopamine D2 receptors (D2R) in medium spiny neurons (MSNs) in the striatum.<sup>13</sup> Activated GPR52 couples primarily to G<sub>s</sub> or G<sub>oif</sub> protein that activates adenylyl cyclases to increase cellular cAMP. The G<sub>s</sub>/cAMP signaling pathway of GPR52 may induce a functional crosstalk with the G<sub>i</sub>-coupled D2R,<sup>14</sup> and modulate dopamine signaling in striatal neurons and in the broader corticostriatal brain circuitry.<sup>11,13</sup> Recent human genome-wide association studies (GWAS) have revealed that GPR52 is also a schizophrenia (SZ) risk gene.<sup>15</sup> GPR52-knockout mice display psychosis-related behaviors, whereas transgenic mice overexpressing GPR52 exhibit antipsychotic-like behaviors.<sup>11</sup> These studies collectively suggest that GPR52 agonists may have antipsychotic-like activity. In addition, co-localization of GPR52 with G<sub>s</sub>-coupled dopamine D1 receptors (D1R) in the medial prefrontal cortex suggests a functional role in attention, cognition, and memory.<sup>11,16,17</sup> Based on its co-expression with D2R and D1R, activation of GPR52 could produce antipsychotic effects, improve cognition, and reduce

the effects of psychostimulant drugs. Furthermore, GPR52 was reported to stabilize mutant huntingtin (mHTT) protein, exacerbating the cytotoxicity of mHTT in Huntington's disease (HD).<sup>18-20</sup> Interestingly, knockout of GPR52 or loss of GPR52 function suppresses the accumulation of mHTT in striatal neurons and improves HD-related movement impairments.<sup>18,20</sup> Taken together, these findings indicate that GPR52 agonists could be beneficial for treating SZ, psychotic disorders, or substance use disorders (SUDs). However, GPR52 antagonists could be potential therapeutics for HD.

To date, the endogenous ligand of GPR52 has not been identified. The crystal structure of human GPR52 has been solved in three states: two ligand-free apo states (PDB codes: 6LI1 and 6LI2) and one active state in complex with agonist c17 (**2**) (PDB: 6LI0).<sup>21</sup> In these structures, GPR52 displays an unprecedented phenomenon of self-activation as a result of binding its own extracellular loop 2 (ECL2) as an internal agonist to the classical orthosteric site.<sup>21,22</sup> The lack of known endogenous GPR52 ligands and lack of close homology to known GPCRs poses challenges to fully understanding the functional roles of the receptor. Therefore, development of surrogate ligands is highly desirable for probing the functional activity and therapeutic potential of GPR52.

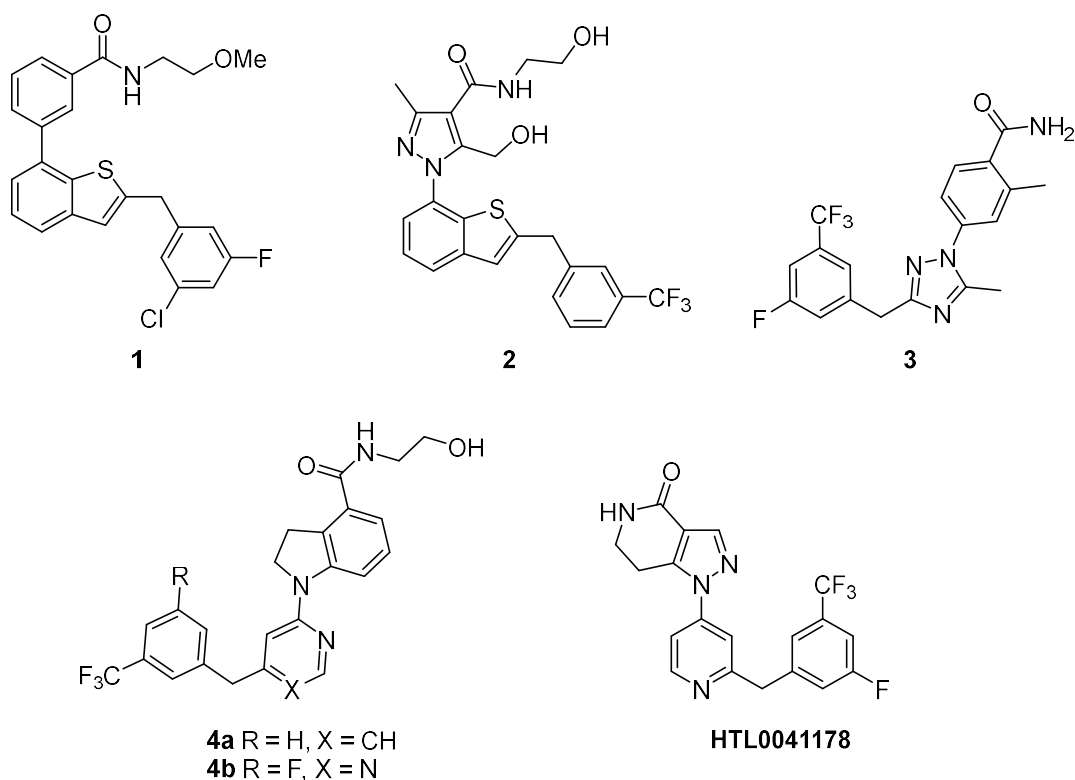


**Figure 1.** Chemical structures of representative GPR52 agonists.

So far, several surrogate ligands as GPR52 agonists have been identified (Figure 1). Setoh et al. identified the first GPR52 agonists, exemplified by compound **1** as a potent GPR52 agonist ( $EC_{50} = 30$  nM) with poor aqueous solubility.<sup>23</sup> Further optimization of compound **1** to improve the aqueous solubility led to the identification of compound **2** with high potency ( $EC_{50} = 21$  nM) and better aqueous solubility (21  $\mu$ g/mL at pH 6.8).<sup>24</sup> In addition, compound **2** dose-dependently inhibited methamphetamine-induced hyperlocomotion in mice, a preclinical model for antipsychotic activity. Tokumaru et al. reported a series of 4-azolyl-benzamide analogues as GPR52 agonists, exemplified by compound **3** with high potency ( $EC_{50} = 75$  nM).<sup>25</sup> In animal models, compound **3** dose-dependently demonstrated antipsychotic activity and improved cognitive functions.<sup>26</sup> Arena Pharmaceuticals disclosed a series of indoline-4-carboxamides as GPR52 agonists, exemplified by a representative compound **4a**.<sup>27</sup> Recently, Sosei Heptares reported an additional series of GPR52 agonists with a similar pharmacophore, exemplified by

**HTL0041178**.<sup>28</sup> Phase I clinical trials have begun with compound HTL0048149 (structure not disclosed) as the first-in-class GPR52 agonist from Sosei Heptares for the treatment of SZ positive, negative, and cognitive symptoms, potentially without the adverse effects accompanied by currently available antipsychotics.<sup>29</sup> Some additional GPR52 modulators have been disclosed in recent patents.<sup>30,31</sup>

Notably, prior SAR and pharmacology studies of these compounds strictly focused on GPR52 agonist activity for the canonical G protein  $G_{s/olf}$  cAMP pathway. However, most activated GPCRs also universally couple to the  $\beta$ -arrestin proteins, which control receptor trafficking and desensitization and may propagate receptor signaling pathways distinct from G proteins.<sup>32-34</sup> Agonists that activate receptors to signal primarily via G proteins versus  $\beta$ -arrestin are known as biased agonists,<sup>35</sup> which may improve agonist efficacy and/or reduce side effects induced by unbiased receptor ligands.<sup>36-39</sup> Therefore, development of potent and highly selective GPR52 agonists, including biased agonists, will provide useful pharmacological tools for elucidating GPR52 function as well as provide promising drug leads for the treatment of various CNS diseases.

Inspired by the understudied physiology of GPR52 and the potential neurotherapeutic applications of GPR52 agonists, we focused our drug discovery program on developing novel potent and selective GPR52 agonists. In our previous work, compound **4a** was selected as the lead for further systematic SAR studies to identify more potent compounds.<sup>40,41</sup> This prior optimization of compound **4a** led to the identification of a series of 1-(pyrimidin-4-yl)indoline-4-carboxamides as selective GPR52 agonists, exemplified by compound **4b** with improved efficacy, along with excellent target specificity and pharmacokinetic (PK) profiles. Further studies of amphetamine-induced hyperlocomotor behavior in mice revealed that compound **4b** exhibited antipsychotic-like activity.<sup>40</sup>

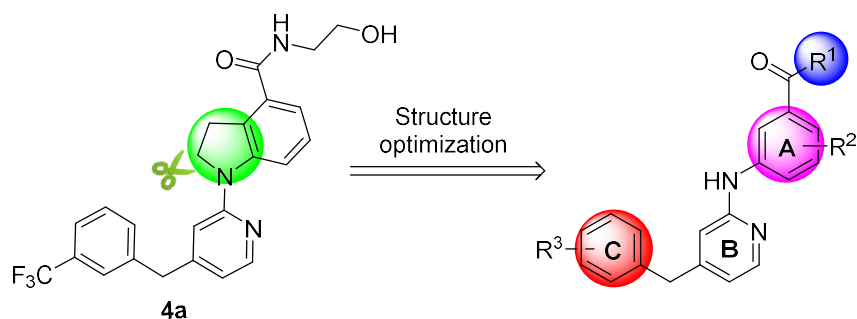


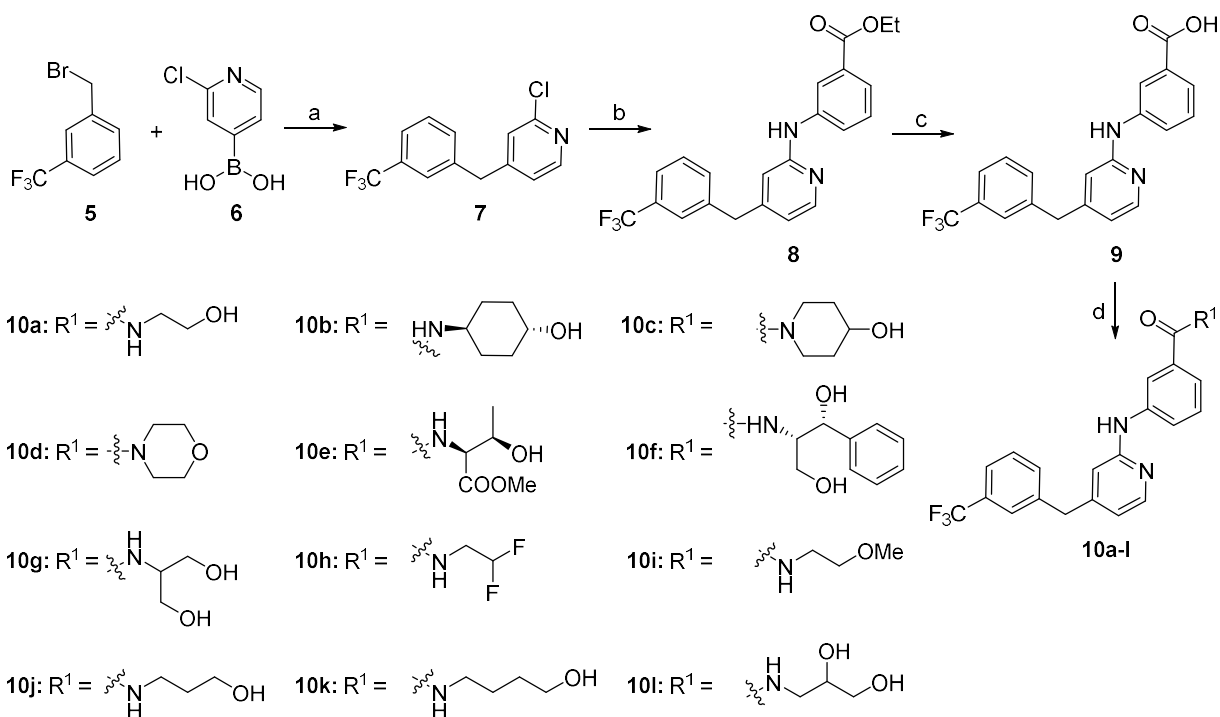
**Figure 2.** Proposed design strategy and structural modifications to **4a**.

In our continued research toward developing novel GPR52 agonists based on the lead **4a** (Figure 2), we first opened the indoline ring moiety (highlighted in green) to enhance the flexibility of the molecules with a truncated scaffold and to expose an additional NH that could form new hydrogen bonds to improve the potency. In addition, we employed systematic medicinal chemistry around the aminoalcohol group ( $R^1$ ) and substituents on ring A and ring C ( $R^2$  and  $R^3$ , respectively) of **4a** (Figure 2; aminoalcohol sidechain highlighted in blue, ring A highlighted in magenta, ring C highlighted in red). Remarkably, the opening of the indoline ring resulted in GPR52 biased agonism relative to parent compound **4a**, with significantly increased G protein signaling potency and efficacy but decreased potency for  $\beta$ -arrestin recruitment. The most biased of these compounds also displayed reduced GPR52 agonist-induced desensitization, which allowed for sustained cAMP signaling. To our knowledge, these are among the first biased ligands for any oGPCR and the first biased agonists for GPR52.

## RESULTS AND DISCUSSION

**Chemistry.** All compounds described herein were synthesized following the synthetic procedures depicted in Schemes 1-4. The intermediate **7** was prepared by Suzuki C-C coupling reaction using commercially available 1-(bromomethyl)-3-(trifluoromethyl)benzene **5** and (2-chloropyridin-4-yl)boronic acid **6** in the presence of  $\text{Pd}(\text{PPh}_3)_4$  (Scheme 1).<sup>27</sup> The palladium catalyzed C-N coupling reaction between intermediate **7** and ethyl 3-aminobenzoate provided

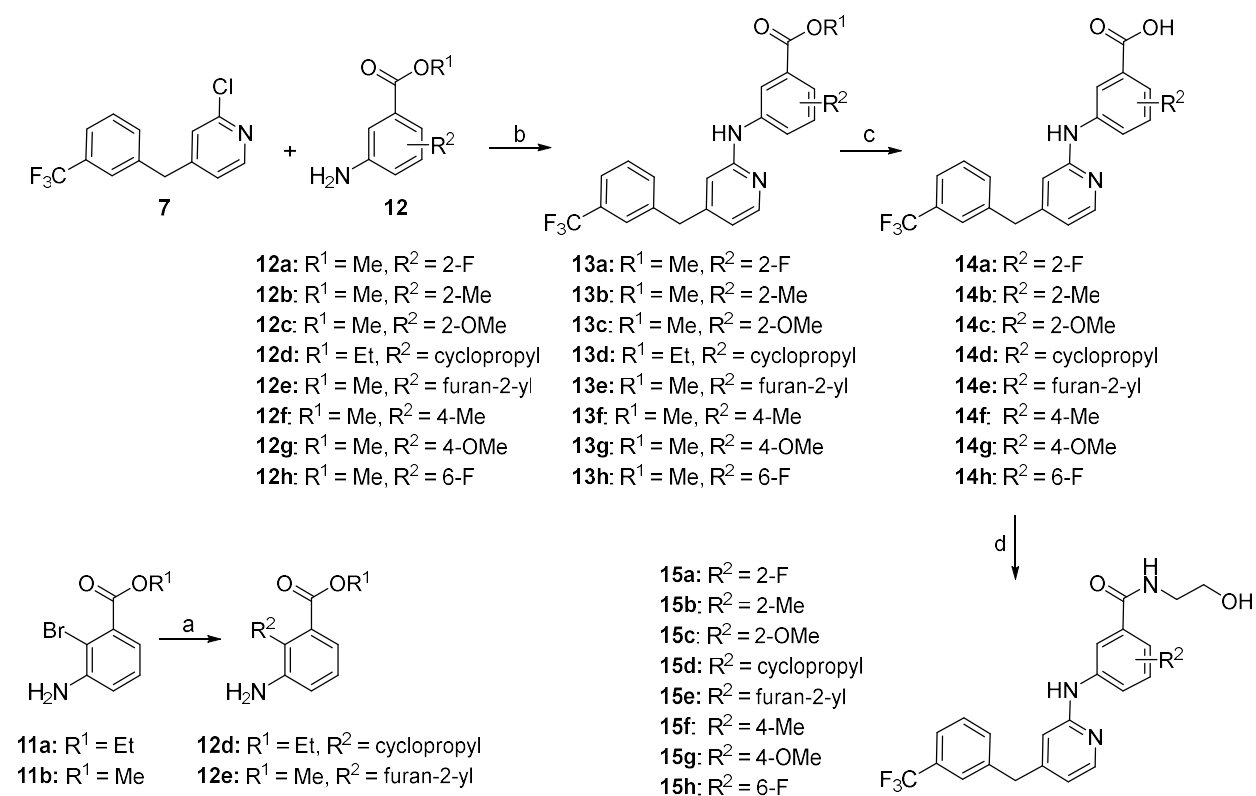
intermediate **8**, which subsequently underwent ester hydrolysis to yield intermediate **9**. Compounds **10a-l** were synthesized through the amide coupling between the intermediate **9** and corresponding amino derivatives.



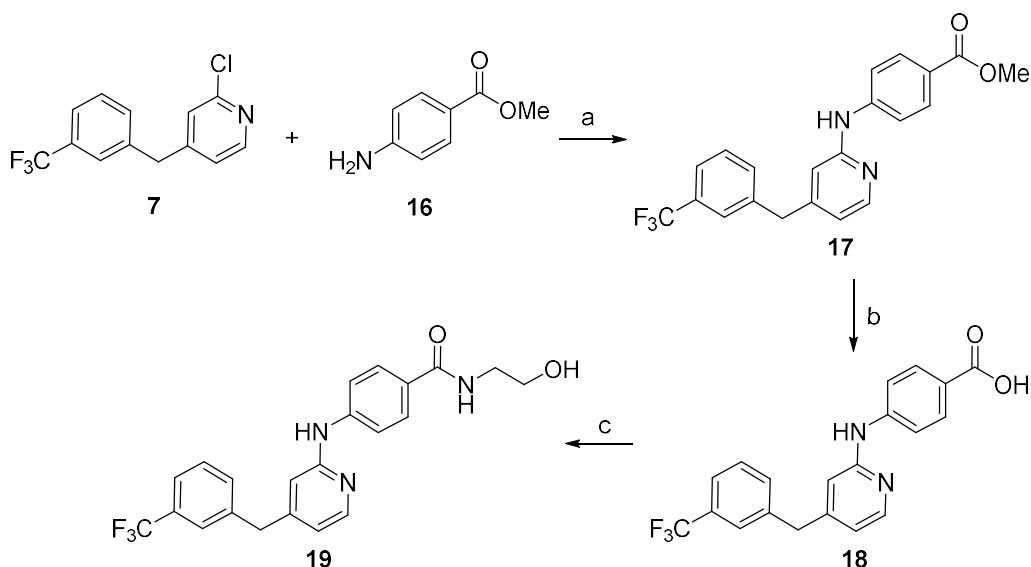
**Scheme 1.** Synthesis of compounds **10a-l**. Reagents and conditions: (a) Pd(PPh<sub>3</sub>)<sub>4</sub>, Na<sub>2</sub>CO<sub>3</sub>, toluene, EtOH, 85 °C, 1.5 h, 48%; (b) ethyl 3-aminobenzoate, Pd(OAc)<sub>2</sub>, XantPhos, Cs<sub>2</sub>CO<sub>3</sub>, 1,4-dioxane, 100 °C, 12 h, 76%; (c) i) 4 N NaOH, EtOH, reflux, 2 h; ii) 2 N HCl, 80%; (d) R<sup>1</sup>H, EDCl, DMAP, HOBT, DMF, rt, 12 h, 41-87%.

Compounds **12d** and **12e** were produced via palladium catalyzed cross-coupling reaction of **11a** and **11b** with cyclopropylboronic acid or furan-2-ylboronic acid, respectively (Scheme 2). The intermediates **13a-h** were synthesized using intermediate **7** and a set of intermediates **12a-h** following the synthetic procedure of intermediate **8**. Ester hydrolysis of intermediates **13a-h** led to compounds **14a-h**, which subsequently coupled with 2-aminoethan-1-ol to provide the final compounds **15a-h**. Compound **19** was prepared following similar synthetic procedures to compound **10a** (Scheme 3). The C-N coupling reaction between intermediate **7** and methyl 4-

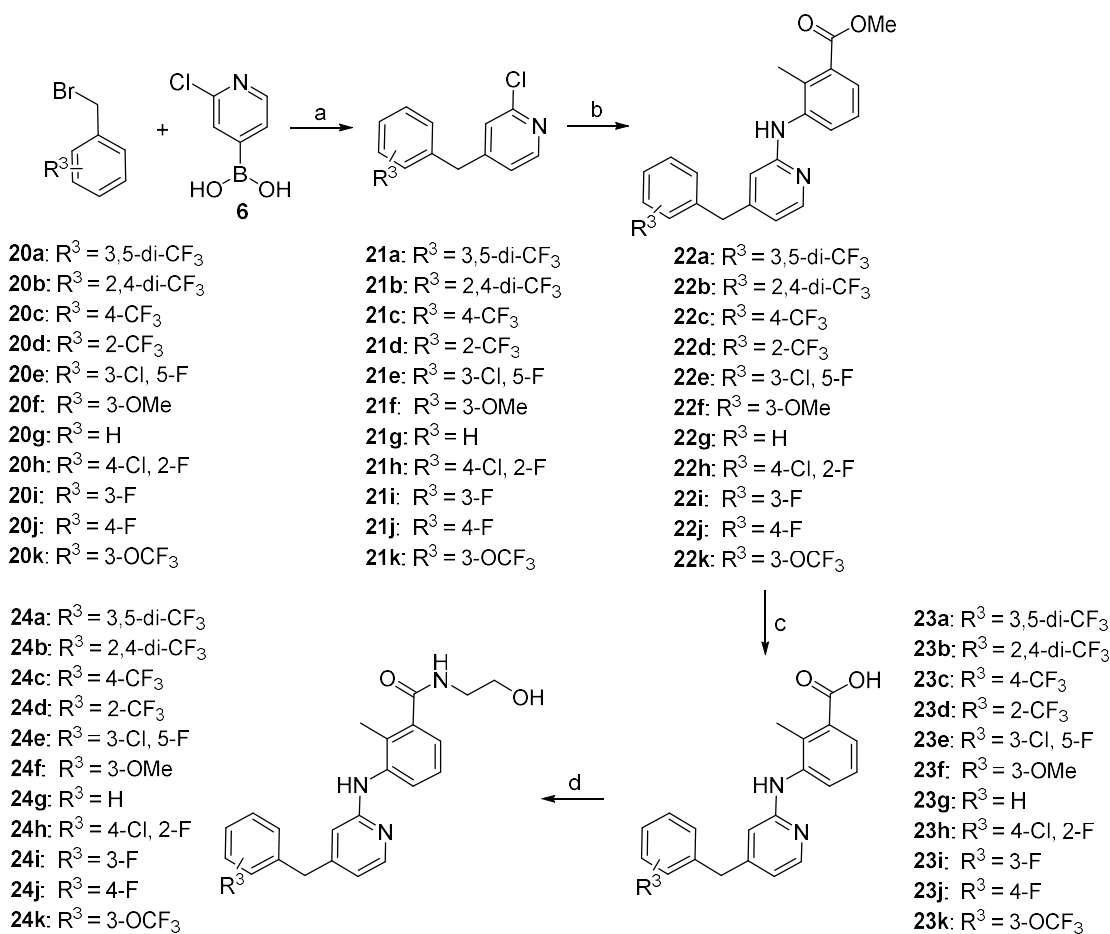
aminobenzoate **16** afforded intermediate **17**, which upon ester hydrolysis provided intermediate **18**. Finally, condensation of intermediate **18** with 2-aminoethan-1-ol furnished the targeted compound **19**.



**Scheme 2.** Synthesis of compounds **15a-h**. Reagents and conditions: (a) cyclopropylboronic acid or furan-2-ylboronic acid, Pd(dppf)<sub>2</sub>Cl<sub>2</sub>, K<sub>3</sub>PO<sub>4</sub>, 1,4-dioxane, H<sub>2</sub>O, 85 °C, 12 h, 47% for **12d**, 60% for **12e**; (b) Pd(OAc)<sub>2</sub>, XantPhos, Cs<sub>2</sub>CO<sub>3</sub>, 1,4-dioxane, 100 °C, 12 h, 37-81%; (c) i) 2 N NaOH, EtOH, reflux, 2 h; ii) 2 N HCl, 79-94%; (d) NH<sub>2</sub>CH<sub>2</sub>CH<sub>2</sub>OH, EDCI, DMAP, HOBt, DMF, rt, 12 h, 38-86%.



**Scheme 3.** Synthesis of compound **19**. Reagents and conditions: (a) Pd(OAc)<sub>2</sub>, XantPhos, Cs<sub>2</sub>CO<sub>3</sub>, 1,4-dioxane, 100 °C, 12 h, 87%; (b) i) 4 N NaOH, EtOH, reflux, 2 h; ii) 2 N HCl, 91%; (c) NH<sub>2</sub>CH<sub>2</sub>CH<sub>2</sub>OH, EDCI, DMAP, HOBt, DMF, rt, 12 h, 77%.

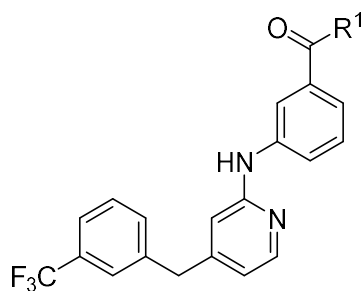


**Scheme 4.** Synthesis of compound **24a-k**. Reagents and conditions: (a) Pd(PPh<sub>3</sub>)<sub>4</sub>, Na<sub>2</sub>CO<sub>3</sub>, toluene, EtOH, 85 °C, 1.5 h, 53-93%; (b) methyl 3-amino-2-methylbenzoate, Pd(OAc)<sub>2</sub>, XantPhos, Cs<sub>2</sub>CO<sub>3</sub>, 1,4-dioxane, 100 °C, 12 h, 65-83%; (c) i) 2 N NaOH, EtOH, reflux, 2 h; ii) 2 N HCl, 73-93%; (d) R<sup>1</sup>H, EDCl, DMAP, HOBt, DMF, rt, 12 h, 38-93%.

The intermediates **21a-k** were prepared following the synthetic procedure of intermediate **7** using commercially available **6** with **20a-k** (Scheme 4). Following the synthetic route of intermediate **8**, intermediates **22a-k** were obtained using methyl 3-amino-2-methylbenzoate and **21a-k**. Hydrolysis of methyl esters **22a-k** led to the formation of corresponding acid **23a-k**. The targeted compounds **24a-k** were accessed following the same synthetic procedure as compound **10a**, using intermediates **23a-k** and 2-aminoethan-1-ol.

***In Vitro* Evaluation of GPR52 G Protein-Mediated cAMP Activities.** All the compounds were evaluated for their GPR52 agonist activity based on cAMP production using the GloSensor cAMP assay, and the results are summarized in Tables 1-3. Reported GPR52 agonist **4a** was resynthesized and used as the parent scaffold and reference compound (EC<sub>50</sub> = 119 nM, when screened in our assay in a 12-point concentration-response). Interestingly, GPR52 expression alone significantly elevated basal cAMP more than 20-fold over both empty vector control and G<sub>s</sub>-coupled D1R, indicating that GPR52 has high constitutive activity for cAMP signaling (Supplementary Figure 1A). The GloSensor cAMP assay used for GPR52 screening provided a consistent, robust agonist signal for all compounds described herein, although the limited aqueous solubility of compound **4a** caused visible precipitation and decreased signal at high concentrations (Supplementary Figure 1B).

**Table 1. EC<sub>50</sub> and E<sub>max</sub> of compounds 10a-l**



Compound	R <sup>1</sup>	ClogP <sup>a</sup>	EC <sub>50</sub> (nM) <sup>b</sup>	E <sub>max</sub> (%) <sup>b</sup>
<b>4a</b>		4.10	119 ± 18	100 ± 5
<b>10a</b>		4.16	282 ± 46	197 ± 26
<b>10b</b>		5.47	467 ± 60	131 ± 13
<b>10c</b>		5.03	672 ± 134	99 ± 12
<b>10d</b>		4.91	774 ± 124	93 ± 7
<b>10e</b>		4.09	448 ± 59	164 ± 12
<b>10f</b>		5.26	862 ± 157	188 ± 11
<b>10g</b>		3.52	220 ± 39	214 ± 19
<b>10h</b>		5.43	638 ± 137	152 ± 7
<b>10i</b>		4.81	252 ± 54	131 ± 15
<b>10j</b>		4.55	220 ± 43	129 ± 7
<b>10k</b>		4.94	198 ± 37	129 ± 8
<b>10l</b>		3.52	286 ± 3	268 ± 12

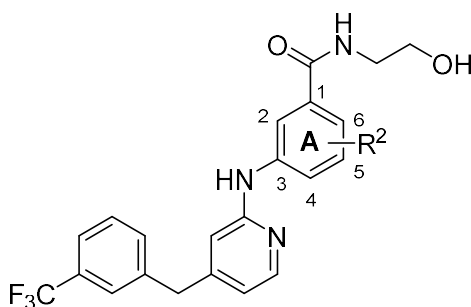
<sup>a</sup>ClogP is calculated from a web calculator: <http://biosig.unimelb.edu.au/pkcsmprediction>.

<sup>b</sup>Values are mean ± SEM from n ≥ 3 independent experiments. E<sub>max</sub> (%) is the efficacy maximum of the compounds in the cAMP assay relative to compound **4a** as 100% and DMSO as 0%.

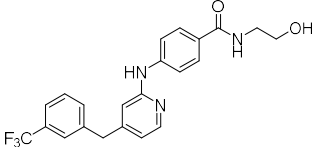
We embarked on a systematic structure-activity relationship (SAR) study, at the outset exploring the indoline ring moiety of compound **4a** (Figure 2, highlighted in green) (Table 1).

Opening of indoline ring led to the formation of compound **10a** ( $EC_{50} = 282$  nM,  $E_{max} = 197\%$ ), which demonstrated a 2.4-fold decrease in potency but a significant increase in efficacy compared to reference **4a**. To probe the flexibility of the side chain ( $R^1$ ), the aminoalcohol was replaced with a set of cycloalkanes **10b-d** or appended with substituents on the aminoalcohol side chain **10e-g**. Compounds **10b-g** displayed reduced potency in comparison to **4a**, ranging from a 1.8- to 7.2-fold shift. Incorporation of fluorine or group of fluorine atoms in a molecule may increase the potency and the permeability, reduce the pKa and clearance, and restrict the conformation.<sup>42,43</sup> Therefore, we leveraged the application of fluorine in our medicinal chemistry campaign. Replacing the hydroxy group of the aminoalcohol of **10a** with difluoro afforded compound **10h**. In contrast to our expectation, compound **10h** displayed a 4.8-fold potency loss and a slight decrease in efficacy compared to **4a**. Swapping the hydroxy group of the aminoalcohol of **10a** with a methoxy group yielded compound **10i** ( $EC_{50} = 252$  nM), which showed a slight decrease in potency versus **4a**. Extending the alkyl chain of the aminoalcohol of **10a** led to compounds **10j-l**, which exhibited similar potency to **10a**. Collectively, none of compounds **10a-l** displayed improved potency over **4a**. Therefore, we decided to use the aminoalcohol as the optimal side chain for further modifications.

**Table 2.  $EC_{50}$  and  $E_{max}$  of compounds 15a-h and 19**



Compound	$R^2$	ClogP <sup>a</sup>	$EC_{50}$ (nM) <sup>b</sup>	$E_{max}$ (%) <sup>b</sup>
----------	-------	--------------------	-----------------------------	----------------------------

<b>4a</b>	Indoline	4.10	119 ± 18	100 ± 5
<b>10a</b>	H	4.16	282 ± 46	197 ± 26
<b>15a</b>	2-F	4.30	342 ± 78	134 ± 2
<b>15b</b>	2-Me	4.47	47 ± 8	143 ± 5
<b>15c</b>	2-OMe	4.17	64 ± 19	149 ± 8
<b>15d</b>	2-cyclopropyl	5.03	30 ± 9	146 ± 9
<b>15e</b>	2-(furan-2-yl)	5.42	84 ± 12	147 ± 6
<b>15f</b>	4-Me	4.47	984 ± 18	94 ± 6
<b>15g</b>	4-OMe	4.17	1432 ± 207	111 ± 7
<b>15h</b>	6-F	4.30	229 ± 38	126 ± 9
<b>19</b>		4.16	1086 ± 85	115 ± 10

<sup>a</sup>ClogP is calculated from a web calculator: <http://biosig.unimelb.edu.au/pkcsml/prediction>.

<sup>b</sup>Values are mean ± SEM from  $n \geq 3$  independent experiments.  $E_{\max}$  (%) is the efficacy maximum of the compounds in the cAMP assay relative to compound **4a** as 100% and DMSO as 0%.

Having optimized the side chain, we next turned our attention to the role of substituents on ring A of **10a**, and the results are summarized in Table 2. Appending substitutions at the 2-position led to compounds **15a-e**, which demonstrated increased potency, except **15a**, but slightly reduced efficacy relative to **10a**. Notably, **15b** ( $EC_{50} = 47$  nM,  $E_{\max} = 143\%$ ) and **15d** ( $EC_{50} = 30$  nM,  $E_{\max} = 146\%$ ) displayed the best improvement in potency. Addition of substituents at the 4-position of ring A provided compounds **15f** and **15g**. However, substitution at the 4-position of ring A was not tolerated and led to a significant decrease in potency. In addition, introduction of fluorine at the 6-position of ring A afforded compound **15h**, which significantly lost efficacy compared to **10a** ( $E_{\max} = 126\%$  and  $197\%$ , respectively) but had minimal effect on potency. Transposition of amide from the 1-position to the 6-position on ring A yielded compound **19** that exhibited a substantial loss in potency relative to both **4a** and **10a**, though it still retained efficacy comparable to **4a**. Taken together, small alkyl groups (e.g., methyl, cyclopropyl) on the 2-position of ring A

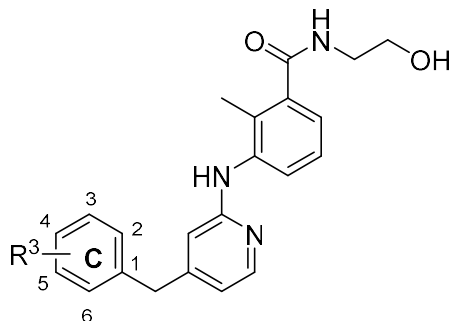
were found to improve potency over both **4a** and **10a**, while maintaining the increased efficacy of the open-ring **10a** for GPR52 cAMP signaling.

By taking advantage of the results presented in Tables 1 and 2, we established the aminoalcohol as a privileged side chain and the methyl group at the 2-position of ring A as a principal substituent to further investigate the effects of substitutions on ring C of **15b** (Table 3). Introduction of an additional CF<sub>3</sub> group led to compound **24a** (3,5-di-CF<sub>3</sub>), which displayed a 4-fold loss in potency (EC<sub>50</sub> = 211 nM) compared to **15b**. Conversely, compound **24b** (2,4-di-CF<sub>3</sub>) maintained potency (EC<sub>50</sub> = 52 nM). Transposition of the CF<sub>3</sub> group from the 3-position to the 2- or 4-position led to compounds **24c** and **24d**, respectively. Interestingly, these mono-CF<sub>3</sub> substitutions in **24c** and **24d** showed a 3-fold decrease in potency compared to **24b** with both additions. Installation of Cl at the 3-position and F at the 5-position on ring C provided compound **24e** that exhibited similar activity (EC<sub>50</sub> = 46 nM) to **15b**. In contrast, compound **24h** containing Cl at the 4-position and F at the 2-position on ring C demonstrated a reduction in potency (EC<sub>50</sub> = 235 nM). To investigate the effects of steric hindrance caused by the substituents at the 3-position of ring C, compounds **24f**, **24g**, **24i**, and **24k** were designed and synthesized, which mainly displayed good potency in the order OCF<sub>3</sub> > CF<sub>3</sub> > OMe > F > H, with no significant alterations to efficacy among the compounds. Among these, compound **24k** (EC<sub>50</sub> = 30 nM) was not only more potent than **4a** but also more potent than **15b**.

Notably, the halogenation of **24e** and **24h** had opposite effects compared to the analogous compounds **24a** and **24b**, respectively, with bulkier di-CF<sub>3</sub> additions at the same positions. Double substitution at the 3,5-positions appeared to be more favorable with the smaller F and Cl additions, whereas larger CF<sub>3</sub> additions at the 2,4-positions were more potent. However, this observation only held for the activity of compounds with double additions to ring C, with single substituents

at the 3-position favoring more sterically hindering groups (as discussed above). Collectively, the results discussed above suggest that ring C can tolerate either electron-donating or electron-withdrawing substituents. In addition, compounds with large groups (e.g., OCF<sub>3</sub> and CF<sub>3</sub>) at the 3-position of ring C showed better GPR52 agonist efficacy.

**Table 3. EC<sub>50</sub> and E<sub>max</sub> of Compounds 24a-k**



Compound	R <sup>3</sup>	ClogP <sup>a</sup>	EC <sub>50</sub> (nM) <sup>b</sup>	E <sub>max</sub> (%) <sup>b</sup>
<b>4a</b>	3-CF <sub>3</sub>	4.10	119 ± 16	100 ± 5
<b>15b</b>	3-CF <sub>3</sub>	4.47	47 ± 8	143 ± 5
<b>24a</b>	3,5-di-CF <sub>3</sub>	5.48	211 ± 51	127 ± 11
<b>24b</b>	2,4-di-CF <sub>3</sub>	5.48	52 ± 11	150 ± 12
<b>24c</b>	4-CF <sub>3</sub>	4.47	220 ± 58	120 ± 9
<b>24d</b>	2-CF <sub>3</sub>	4.47	143 ± 33	122 ± 13
<b>24e</b>	3-Cl, 5-F	4.24	46 ± 8	135 ± 9
<b>24f</b>	3-OMe	3.46	53 ± 10	133 ± 10
<b>24g</b>	H	3.45	278 ± 48	139 ± 9
<b>24h</b>	4-Cl, 2-F	4.24	235 ± 47	131 ± 8
<b>24i</b>	3-F	3.59	136 ± 33	137 ± 7
<b>24j</b>	4-F	3.59	90 ± 17	146 ± 9
<b>24k</b>	3-OCF <sub>3</sub>	4.35	30 ± 8	137 ± 7

<sup>a</sup>ClogP is calculated from a web calculator: <http://biosig.unimelb.edu.au/pkcsm/prediction>.

<sup>b</sup>Values are mean ± SEM from n ≥ 3 independent experiments. E<sub>max</sub> (%) is the efficacy maximum of the compounds in the cAMP assay relative to compound **4a** as 100% and DMSO as 0%.

Overall, opening the indoline ring of **4a** led to an increase in efficacy for GPR52 activation of G protein-mediated cAMP signaling. The rationale for improved efficacy of these compounds can presumably be attributed to the flexibility of the scaffold. Modification to the aminoalcohol moiety generally had negative effects on potency and efficacy compared to **10a** (Figure 3A). Addition of substituents to the 2-position of ring A is essential to improve potency over **4a** and the open-ring scaffold **10a** (Figure 3B). Ring C is amenable to a wide array of modifications, with bulky substitutions at the 3-position being optimal for improving potency (Figure 3C).

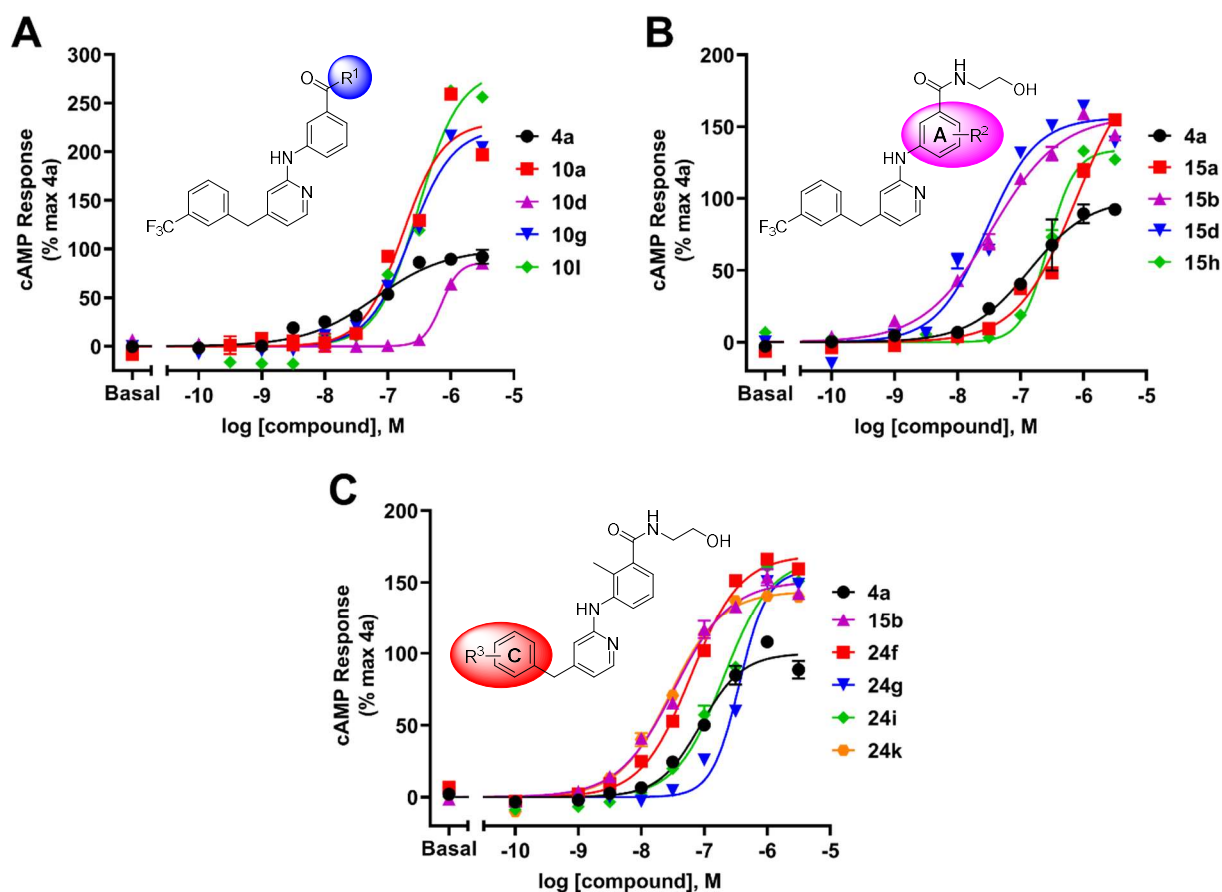


**Figure 3.** Concentration-responses of GPR52 agonists for cAMP signaling in HEK293 cells expressing human GPR52 and the GloSensor cAMP reporter. (A) Opening the indoline ring of **4a** to yield **10a** substantially increased efficacy but reduced potency. Further modification around the aminoalcohol moiety (blue) generally had minimal or negative effects on potency and efficacy compared to **10a**. (B) Addition of substituents around ring A (magenta), particularly at the 2-

position, improved both potency and efficacy over **4a** but did not achieve the efficacy of **10a**. (C) Substitutions to ring C (red) of **15b** generally lost potency while maintaining the increased efficacy relative to **4a**. Results are mean  $\pm$  SEM from triplicate testing in a representative experiment, with similar results observed in  $n \geq 3$  experiments.

***In Vitro* Evaluation of GPR52  $\beta$ -Arrestin Recruitment and Ligand Bias.** In addition to canonical G protein signaling, most agonist-activated GPCRs couple to  $\beta$ -arrestin, a multifunctional scaffolding protein that controls receptor trafficking and activation of various kinases.<sup>32,44</sup> However, to the best of our knowledge, GPR52 recruitment of  $\beta$ -arrestin has not been previously reported. Therefore, we developed a robust method of measuring recruitment of  $\beta$ -arrestin2 to human GPR52, using the transcriptional activation following arrestin translocation (Tango) assay. The Tango assay is a scalable, gene reporter-based assay in which GPCR recruitment of  $\beta$ -arrestin results in transcription of luciferase.<sup>45,46</sup> In initial validation studies, GPR52 displayed high constitutive activity to recruit  $\beta$ -arrestin, significantly elevated above that of another  $G_s$ -coupled receptor, D1R (Supplementary Figure 2A). Concentration response of the positive control agonist **4a** produced robust  $\beta$ -arrestin recruitment to GPR52, approximately 25-fold over basal. This response was specific to GPR52, with no response observed when tested against the D1R (Supplementary Figure 2B). As a quantitative assessment of assay quality, a z-factor of 0.812 was determined testing **4a** agonism at GPR52, indicating the assay had excellent signal-to-noise with low error.<sup>47</sup>

**Table 4.  $\beta$ -Arrestin Recruitment  $EC_{50}$  and  $E_{max}$  and Bias Factors of Selected Compounds**

Compound	$EC_{50}$ (nM) <sup>a</sup>	$E_{max}$ (%) <sup>a</sup>	G Protein Bias Factor	$\beta$ -Arrestin Bias Factor
<b>4a</b>	22 $\pm$ 5	100 $\pm$ 10	1.00	1.00
<b>10a</b>	483 $\pm$ 46	70 $\pm$ 6	25.8	0.039
<b>10g</b>	1585 $\pm$ 250	125 $\pm$ 12	66.3	0.015
<b>10l</b>	1582 $\pm$ 149	127 $\pm$ 7	63.2	0.016
<b>15b</b>	110 $\pm$ 11	109 $\pm$ 3	16.4	0.061

<b>15c</b>	247 ± 62	100 ± 7	31.2	0.032
<b>15d</b>	14 ± 4	92 ± 2	4.10	0.244
<b>15e</b>	335 ± 69	118 ± 5	26.9	0.037
<b>24b</b>	17 ± 3	109 ± 6	2.41	0.415
<b>24e</b>	89 ± 12	120 ± 3	11.7	0.085
<b>24f</b>	1036 ± 136	172 ± 7	81.9	0.012
<b>24j</b>	563 ± 28	142 ± 6	34.7	0.029
<b>24k</b>	349 ± 25	131 ± 4	64.9	0.015

<sup>a</sup>Values are mean ± SEM from  $n \geq 3$  independent experiments.  $E_{\max}$  (%) is the efficacy maximum of the compounds in the  $\beta$ -arrestin recruitment assay relative to compound **4a** as 100% and DMSO as 0%.

Alongside **4a**, twelve of the most potent and efficacious GPR52 ligands for G protein/cAMP signaling were selected for concentration-response screening in the Tango  $\beta$ -arrestin assay. The results are summarized in Table 4, along with calculated bias factors for activation of the G protein/cAMP or  $\beta$ -arrestin pathways. These bias factors provide a scale to compare agonist activity for GPR52 signaling in one pathway versus the other, relative to the parent compound **4a**.<sup>48</sup> All of the tested compounds displayed some degree of GPR52 G protein/cAMP bias, the most biased being **24f** (G protein bias factor = 81.9) and the least biased being **24b** (G protein bias factor = 2.41).

The opening of the indoline ring of **4a** to yield **10a** resulted in a profound 20-fold loss in potency for GPR52  $\beta$ -arrestin activation and a 30% reduction in the maximum response (Figure 4A). Introduction of additional hydroxy groups to the side chain in **10g** and **10l** further decreased  $\beta$ -arrestin potency by more than 70-fold but increased the efficacy relative to both **4a** and **10a**. Substitution of small alkyl groups at the 2-position of ring A (**15b-e**) rescued both potency and efficacy for  $\beta$ -arrestin recruitment that was lost in **10a** (Figure 4B). This increase in  $\beta$ -arrestin potency, along with the identical rank order in potency, was similarly observed in the cAMP assay,

suggesting a significant role of the 2-position of ring A in the ligand-receptor interaction with GPR52. Substitution to ring C of **15b** generally demonstrated limited influence on GPR52  $\beta$ -arrestin efficacy but had variant effects on potency for  $\beta$ -arrestin activation (Figure 4C). A structure-activity trend for  $\beta$ -arrestin recruitment was not clear with ring C modifications. As shown in the cAMP signaling assays, however, ring C is amenable to a wide array of modifications that also maintained activity for  $\beta$ -arrestin recruitment.

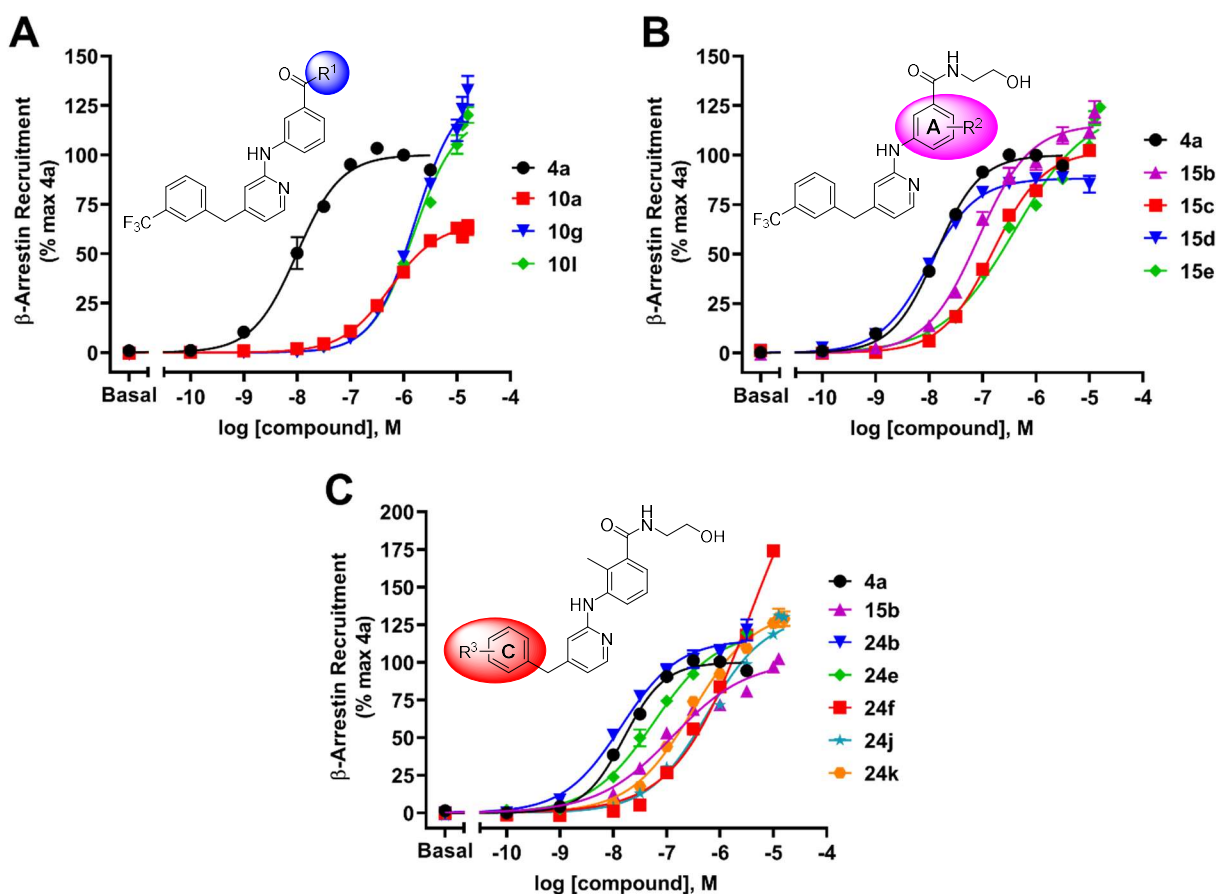


**Figure 4.** Concentration-responses of GPR52 agonists for  $\beta$ -arrestin recruitment in HTLA cells expressing the human GPR52 Tango construct. (A) The open-ring derivatives of **4a** had greatly reduced compound potency and efficacy, and modification of the terminal aminoalcohol moiety (blue) further reduced potency but rescued efficacy. (B) Modifications around ring A (magenta) generally resulted in loss of potency and similar maximal efficacy compared to **4a**. (C) Substitutions to ring C (red) of **15b** generally increased maximal  $\beta$ -arrestin recruitment. Results

are mean  $\pm$  SEM from triplicate testing in a representative experiment, with similar results observed in  $n \geq 3$  experiments.

Interestingly, the parent compound **4a** was more active in the  $\beta$ -arrestin pathway, with roughly 5-fold greater potency for  $\beta$ -arrestin activation than for G protein/cAMP activation (Figure 5A). Simply removing two carbons of the **4a** indoline ring, yielding **10a**, both sharply increased efficacy for cAMP signaling and sharply decreased potency and efficacy for  $\beta$ -arrestin, suggesting that interactions with these carbons may be a driving factor for agonist recruitment of  $\beta$ -arrestin to GPR52 (Figure 5B). Alkyl substitutions at the 2-position of ring A largely recovered this lost  $\beta$ -arrestin activity. This can be seen with the methyl substitution in **15b**, which provided a more balanced profile between the G protein and  $\beta$ -arrestin pathways (Figure 5C). These alkyl substitutions at the 2-position of ring A (**15b**, **15c**, **15d**, **15e**) all enhanced potency both for  $\beta$ -arrestin and G protein activation. These results indicate that the receptor interactions, or possibly the steric hindrance, afforded by substituents at this position are valuable for ligand-receptor binding, rather than for introducing bias for any pathway. Taken together, these pharmacological studies clearly establish that opening the indoline of **4a**, creating more structurally flexible GPR52 agonists, promotes bias for the G protein/cAMP pathway over the  $\beta$ -arrestin pathway.

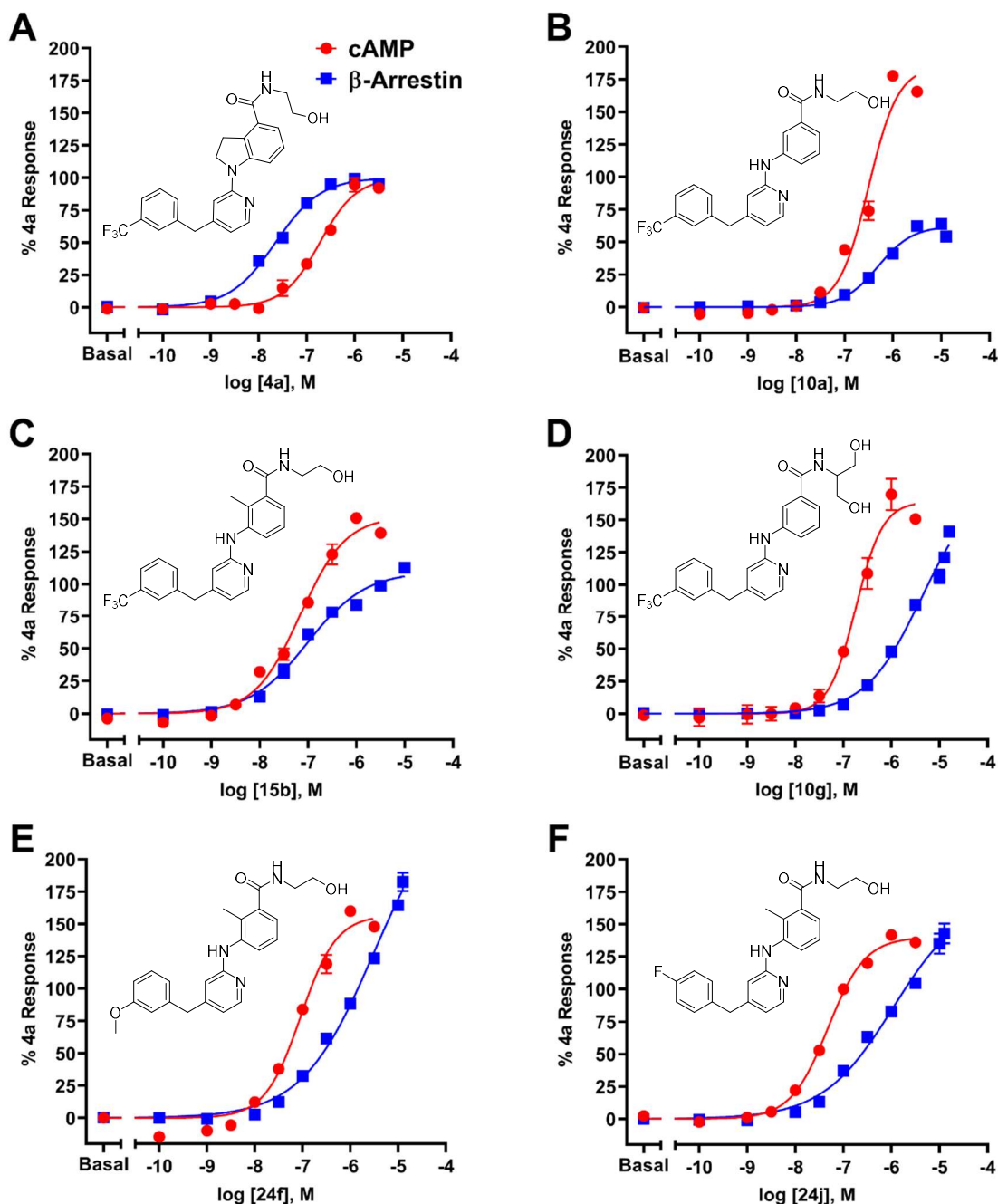


**Figure 5.** Comparison of concentration-responses of select GPR52 agonists for both cAMP signaling and  $\beta$ -arrestin recruitment. (A) Reference compound **4a** showed ~5-fold greater potency for  $\beta$ -arrestin than for cAMP signaling. (B) The removal of the indoline ring in **10a** greatly reduced activity for the  $\beta$ -arrestin pathway but nearly doubled the maximum efficacy for cAMP production. (C) The methyl substitution at ring A in **15b** rescued  $\beta$ -arrestin activity and increased potency for cAMP signaling. (D) **10g** showed similar cAMP signaling activity to **10a**, with greater efficacy for  $\beta$ -arrestin recruitment. (E-F) **24f** and **24j** had similar cAMP signaling activity to **15b**, though the

substitutions at ring C reduced potency for  $\beta$ -arrestin activation. Results are mean  $\pm$  SEM from triplicate testing in a representative experiment, with similar results observed in  $n \geq 3$  experiments.

### Evaluation of G Protein-Biased and Unbiased Agonists on GPR52 Desensitization.

Functional selectivity of agonists for GPCR signaling pathways may provide greater therapeutic efficacy as well as reduced side effect profiles.<sup>33,35,36,38,39</sup> GPCR  $\beta$ -arrestin activation has historically been conceptualized to interrupt G protein signaling and to induce receptor internalization.<sup>34,44,49</sup> Prolonged recruitment of  $\beta$ -arrestin to GPCRs can desensitize receptor signaling responses to agonists,<sup>37,49</sup> potentially leading to tachyphylaxis.<sup>33,34,37,39</sup> To evaluate the functional role of bias for G protein activation over  $\beta$ -arrestin recruitment with our GPR52 agonists, we examined the effect of extended treatment with these compounds on GPR52 desensitization. A schematic shown in Figure 6A outlines agonist-induced recruitment of  $\beta$ -arrestin to GPR52 to inhibit G protein coupling, causing desensitization of GPR52 G protein signaling. Continuous recruitment of  $\beta$ -arrestin is expected to decrease the pool of available receptors for G protein signaling.

To assess potential agonist desensitization, five compounds with a wide range of calculated bias factors were tested for their activity to desensitize GPR52 G protein/cAMP signaling. For this, cells expressing human GPR52 were treated with vehicle (control) or agonists for 2 h with an  $EC_{50}$  concentration previously determined in the cAMP assay. Following compound washout, cells were then challenged with a saturating concentration (1  $\mu$ M) of **4a**, and the cAMP response was measured (Figure 6B). Treatment of cells for 2 h with **4a**, **24b**, and **15b** significantly decreased cAMP responses, whereas the highly G protein-biased agonists **10a** and **24f** showed no significant difference from the vehicle-treated cells. The percent desensitization of GPR52 displayed a similar trend (Figure 6C), with the highest level of desensitization caused by **4a**, **24b**, and **15b**. Notably, the highly G protein-biased agonists **10a** and **24f** showed significantly less desensitization than

parent compound **4a**. The trend in agonist-induced GPR52 desensitization generally follows the trend observed for the G protein bias factor, with less receptor desensitization as the G protein bias factor increases. **10a** showed very low receptor desensitization, likely due to both the reduced potency and partial efficacy for  $\beta$ -arrestin recruitment (see Table 4). Together, these findings suggest the functional bias towards or away from  $\beta$ -arrestin correlates with GPR52 desensitization. To test this, a Pearson's correlation analysis (Figure 6D) was performed comparing the GPR52 cAMP response after agonist pretreatments (see Figure 6B) versus the agonist EC<sub>50</sub> for GPR52  $\beta$ -arrestin recruitment (see Table 4). A significant, positive correlation ( $p = 0.0358$ ) was determined. Prolonged treatment of compounds with greater potency for the GPR52  $\beta$ -arrestin pathway correlated with significantly less G protein-activated cAMP signaling. These results demonstrate that the highly G protein-biased GPR52 agonists, such as **10a** and **24f**, are valuable chemical probes to further investigate the effects of GPR52 signaling bias. These G protein-biased probes could provide sustained agonist activation of GPR52 with reduced desensitization and could reduce the potential for agonist tolerance and tachyphylaxis.

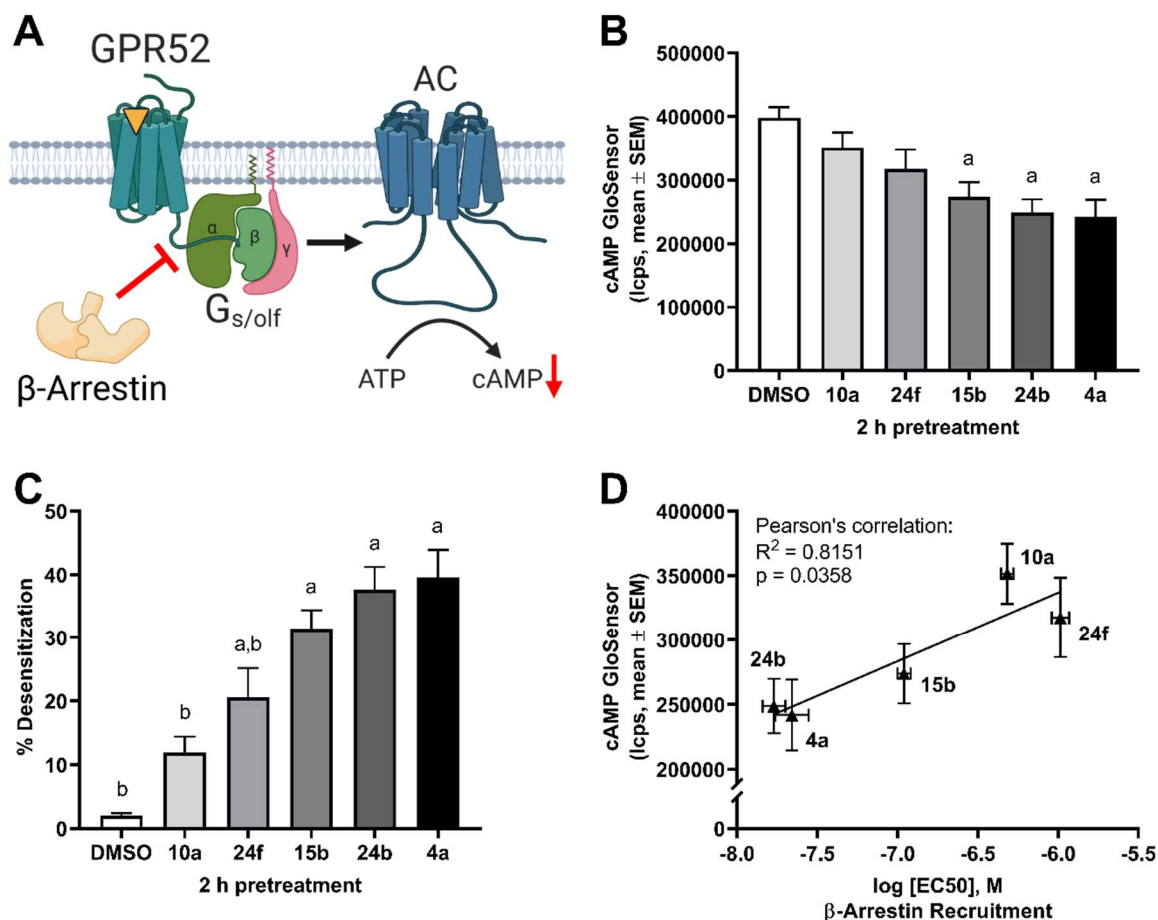


**Figure 6.** Desensitization studies of G protein-biased and balanced GPR52 agonists. (A) GPR52 agonists recruit β-arrestin to the receptor, inhibiting G protein activation and cAMP production. (B) HEK293 cells were pretreated with cAMP assay EC<sub>50</sub> concentrations of GPR52 agonists, washed, then challenged with **4a** (1 μM). (C) Desensitization to the **4a** cAMP response was greatest for **24b** and **4a**, which were the most potent agonists for GPR52 β-arrestin recruitment. Notably, the G protein-biased compounds **10a** and **24f** induced significantly less GPR52 desensitization than 2 h treatments with **4a**. (D) Pearson's correlation analysis reported a significant, positive correlation between compound potency for GPR52 β-arrestin recruitment and the GPR52 cAMP signaling remaining after 2 h pretreatment with compounds. Compounds with greater potency for β-arrestin recruitment showed a greater reduction in GPR52 G protein cAMP signaling. Results are mean ± SEM from n = 3 independent experiments. A, *p* < 0.05 vs. DMSO; b, *p* < 0.05 vs. **4a**; one-way ANOVA with Tukey's post-hoc test.

**Molecular Docking of Compounds 4a, 24f, and 15b with GPR52.** Molecular docking provides significant information about the potential binding mode and receptor-ligand interactions that could assist in structure-based drug design. Recent co-crystal structural analysis of GPR52

bound to compound **2** (PDB code: 6LI0) revealed binding at a narrow side pocket between extracellular loop2 (ECL2), N-terminus, TM1, TM2, and TM7.<sup>21</sup> To ascertain comprehensive docking poses of our compounds with GPR52, Schrödinger Drug Discovery Suite was employed for modeling GPR52 and selected compounds based on the co-crystal structure. For the docking studies, we selected representative compounds **4a** (parent compound) and **24f** (which showed largest G protein bias factor) to find distinct binding modes that could potentially explain the observed differences in bias. Due to its increased potency and efficacy, compound **15b** was also chosen to further examine the molecular interactions with GPR52. **4a**, **15b**, and **24f** demonstrated energetically favorable interactions and occupied similar binding poses to **2** between TM1, TM2, TM7, N-terminus, and ECL2 (Figure 7 and Supplementary Figure 3).

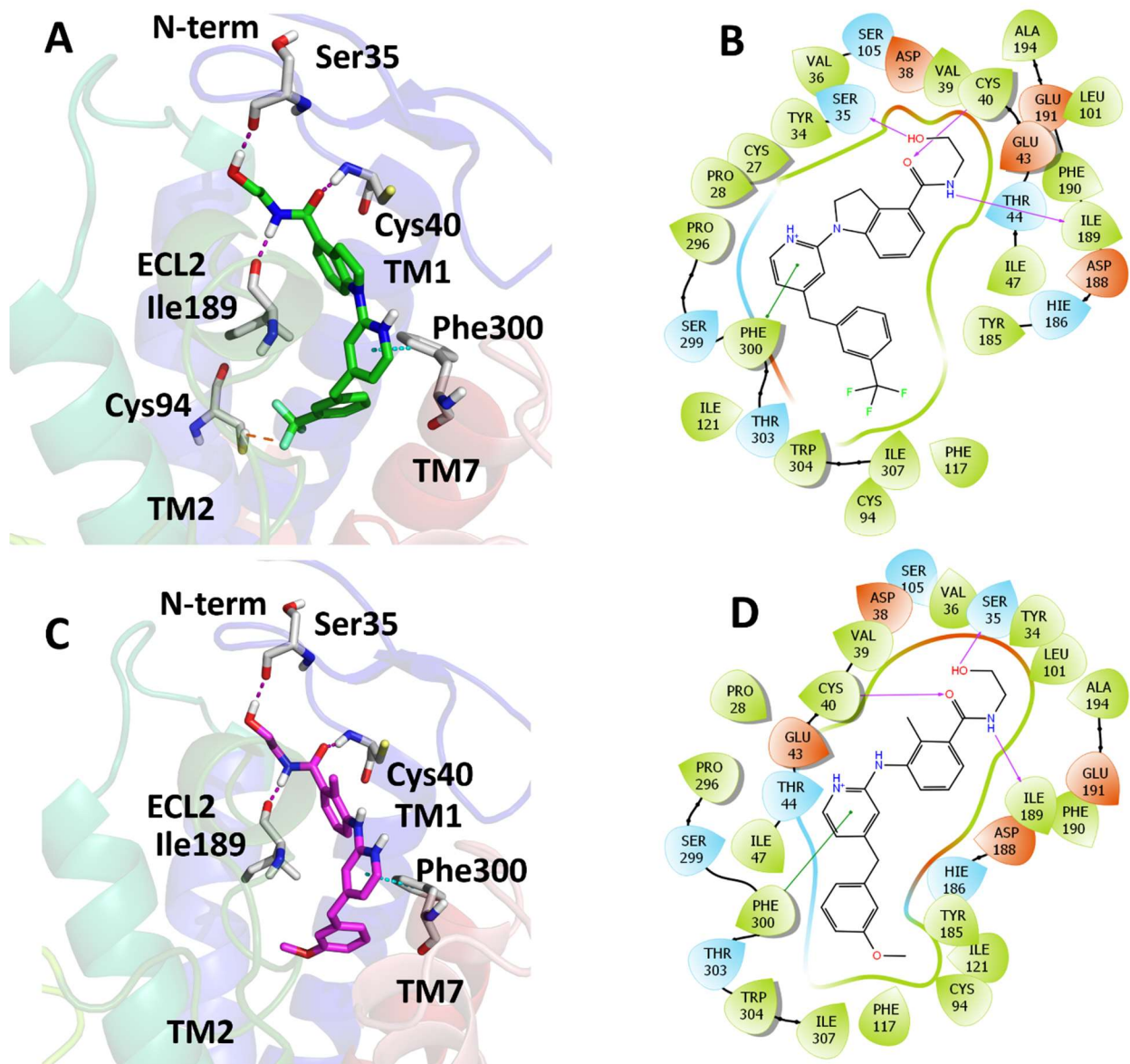


**Figure 7.** Predicted binding mode and molecular docking of **4a** and **24f** with GPR52. (A) Compound **4a** is shown in green docking into the GPR52 binding pocket surrounded by N-terminus, TM1, TM2, TM7, and ECL2 based on the GPR52 crystal structure (PDB: 6LI0). Key interacting residues in the binding site are drawn as gray sticks. Hydrogen bonds are shown as magenta dashed lines, H-F bond is shown as an orange dashed line, and  $\pi$ - $\pi$  stacking is shown as a cyan dashed line. (B) Interaction diagram of **4a** docking into GPR52. Hydrogen bonds are shown as magenta lines, and  $\pi$ - $\pi$  stacking interaction is shown as a green line. (C) Compound **24f** is shown in magenta docking into the binding pocket of GPR52. (D) Interaction diagram of **24f** docking into GPR52.

There were three pair of critical hydrogen bonds between each docked compound and residues within the receptor: the hydroxy group of Ser35 in the N-terminus, the carbonyl group of

the amide in Ile189 at ECL2, and the amine group of the amide in Cys40 in TM1. The flexible aminoalcohol side chain may also form a hydrogen bond with the amine group of the amide in Glu191 in ECL2, rather than with Ser35, with both positions predicted to be equally energetically favorable (Supplementary Figure 3). This binding model may explain the significant activity loss when changing the aminoalcohol moiety to piperidine or morpholine, disrupting hydrogen bonding interactions. The pyridine ring (ring B) of each compound formed a  $\pi$ - $\pi$  stacking interaction with Phe300 of TM7. Ring C of all three compounds pointed into a hydrophobic pocket and formed hydrophobic interactions with residues Ile47, Cys94, Phe117, Ile121, Tyr185, Trp304, and Ile307. This may explain why the ring C could tolerate such varied substitutions and why hydrophobic groups (e.g., OCF<sub>3</sub> and CF<sub>3</sub>) were more favorable for increasing potency. Notably, each of these docked compounds interacted closely with the ECL2 domain through both hydrogen bonds (Ile189 and Glu191) and hydrophobic interactions (Tyr185, His186, Asp188, Ile189, Phe190, and Glu191).

The unusual orientation of ECL2 deep in the canonical class A GPCR orthosteric binding pocket has led to the suggestion that ECL2 acts as a self-agonist for GPR52.<sup>21</sup> The extensive interaction between GPR52 agonists and ECL2 indicates that the ligands may act in an allosteric manner to stabilize receptor self-activation by the ECL2. Based on the results from the cAMP signaling and  $\beta$ -arrestin recruitment assays, the molecular region around ring B appears to be highly important for agonist potency (Figure 3B and Figure 4B). However, no significant receptor interactions with this region were observed in the docking models. Altogether, **4a**, **15b**, and **24f** all showed nearly identical binding modes with this docking exploration, but no obvious changes to account for the variations in signaling bias for G protein or  $\beta$ -arrestin were revealed. However, docking into the GPR52 crystal structure is a structurally rigid, static model, and it does not provide

a wide range of receptor conformations which likely occur for GPR52, limiting these interpretations. More advanced dynamic computational methods may assist in elucidating the exact mechanisms and conformational changes underlying the unique agonist bias for **24f** versus **4a**. For example, the increased flexibility of **24f** between rings A and B, due to the opening of the indoline ring in **4a**, may allow unique interactions that can only be revealed in molecular dynamic simulations. While there were no apparent differences in the docking model, these GPR52 agonists may also have differences in binding kinetics that could affect signaling bias for the G protein or  $\beta$ -arrestin pathways.<sup>50,51</sup> In addition to docking with the GPR52-c17 co-crystal structure (PDB: 6LI0), a similar docking of **24f** and **4a** with the mini-G<sub>s</sub>-coupled active state cryo-EM structure of GPR52 (PDB: 8HMP)<sup>52</sup> was performed, that yielded a similar docking pose and similar ligand interactions (data not shown).

**Counter Screening of Compound 15b.** Considering the *in vitro* activity for GPR52 activation, compound **15b** was chosen as a representative probe out of the active scaffolds for further pharmacological evaluation. To ascertain the selectivity of GPR52 agonist **15b** against other GPCRs and off-targets, broad-panel counter screening was performed by the National Institute of Mental Health Psychoactive Drug Screening Program (NIMH-PDSP).<sup>53</sup> The results revealed that **15b**, at 10  $\mu$ M concentration, displayed no significant binding affinity ( $K_i$ ) at over 30 GPCRs, transporters, and ion channels but showed a moderate interaction with 5-HT<sub>2B</sub> (Table 5). In addition, **15b** did not show inhibition or binding affinity toward the human ether-a-go-go-related gene (hERG) potassium channel, indicating a low risk of cardiovascular toxicity.<sup>54,55</sup> These results are comparable to the lack of off-target activity reported for the structurally related compound **4b**.<sup>40</sup>

**Table 5. Broad-Panel Counter Screening of Compound 15b Against Other GPCRs, Ion Channels, and Transporters**

GPCRs, transporters, ion channels	% inhibition (10 $\mu$ M) <sup>a</sup>	K <sub>i</sub> (nM) <sup>a</sup>	GPCRs, transporters, ion channels	% inhibition (10 $\mu$ M)	K <sub>i</sub> (nM) <sup>a</sup>
5-HT <sub>1A</sub>	35.04	ND	D <sub>1</sub>	7.92	ND
5-HT <sub>1B</sub>	11.55	ND	D <sub>2</sub>	-0.64	ND
5-HT <sub>1D</sub>	29.09	ND	D <sub>3</sub>	10.45	ND
5-HT <sub>1E</sub>	18.55	ND	D <sub>4</sub>	20.65	ND
5-HT <sub>2A</sub>	25.21	ND	D <sub>5</sub>	8.29	ND
5-HT <sub>2B</sub>	91.67	425.4 $\pm$ 81.4	DAT	15.46	ND
5-HT <sub>2C</sub>	41.39	ND	GABA <sub>A</sub>	-17.94	ND
5-HT <sub>3</sub>	22.6	ND	H <sub>1</sub>	15.7	ND
5-HT <sub>5A</sub>	20.55	ND	H <sub>2</sub>	25.13	ND
5-HT <sub>6</sub>	15.34	ND	KOR	18.73	ND
5-HT <sub>7A</sub>	20.68	ND	M <sub>1</sub>	-1.71	ND
$\alpha$ <sub>1A</sub>	16.45	ND	M <sub>2</sub>	3.15	ND
$\alpha$ <sub>1B</sub>	-5.51	ND	M <sub>3</sub>	39.69	ND
$\alpha$ <sub>1D</sub>	-10.52	ND	M <sub>4</sub>	28.71	ND
$\alpha$ <sub>2A</sub>	23	ND	M <sub>5</sub>	-1.37	ND
$\beta$ <sub>1</sub>	10.39	ND	MOR	20.45	ND
$\beta$ <sub>2</sub>	-7.69	ND	hERG	11.04	ND

<sup>a</sup>Values are mean  $\pm$  SEM of at least three independent experiments. SEM < 20% where not listed. “ND” means that a K<sub>i</sub> binding affinity was not determined because off-target inhibition at 10  $\mu$ M did not reach 50%.

***In Vivo* PK Profiles of Compounds 15b and 24f.** Compound **15b** (based on enhanced GPR52 potency and efficacy) and **24f** (based on bias toward G protein signaling pathway) were chosen for further *in vivo* PK profiling. Both compounds were evaluated in rats after a single dose of 20 mg/kg by oral (PO) or 10 mg/kg by intravenous (IV) administration, and the results are summarized in Table 6. **15b** and **24f** displayed acceptable plasma exposure over time after IV

administration ( $AUC_{0-\infty} = 4679$  ng·h/mL and 4746 ng·h/mL, respectively), high maximum serum concentration ( $C_{max} = 6456$  ng/mL and 13733 ng/mL, respectively), and good volume of distribution ( $V_{ss} = 1.85$  L/kg and 0.55 L/kg, respectively). **15b** exhibited good PK parameters after PO ( $AUC_{0-\infty} = 3535$  ng·h/mL,  $C_{max} = 2212$  ng/mL,  $V_{ss} = 9.6$  L/kg), whereas **24f** showed low plasma exposure ( $AUC_{0-\infty} = 662$  ng·h/mL,  $C_{max} = 192$  ng/mL) after PO. This difference appears to be largely due to the reduced oral bioavailability of **24f** compared to **15b** ( $F = 7.0\%$  and 37.6%, respectively).

**Table 6. *In vivo* PK profiles of Compounds 15b or 24f following 20 mg/kg Oral and 10 mg/kg Intravenous Dosing in Rats<sup>a</sup>**

Route	$AUC_{0-\infty}$ (ng·h/mL)	$t_{1/2}$ (h)	$T_{max}$ (h)	$C_{max}$ (ng/mL)	CL (L/h/kg)	$V_{ss}$ (L/kg)	$F$ (%)
<b>15b</b> PO	3535 ± 1411	1.1 ± 0.02	0.5	2212 ± 587	6.2 ± 2.1	9.6 ± 3.2	37.6 ± 15
<b>15b</b> IV	4679 ± 1280	0.6 ± 0.2		6456 ± 988	2.3 ± 0.7	1.8 ± 0.1	
<b>24f</b> PO	662 ± 191	3.3 ± 1.5	1.0	192 ± 109	nd	nd	7.0 ± 2.0
<b>24f</b> IV	4746 ± 268	0.7 ± 0.3		13733 ± 1358	35.2 ± 2.0	0.55 ± 0.08	

<sup>a</sup>Values are mean ± SD from n = 3 biological replicates.  $C_{max}$ , maximum concentration of drug in plasma;  $T_{max}$ , time to maximum concentration of drug in plasma; AUC, area under the curve ( $t = 0$  to 24 h);  $V_{ss}$ , volume of distribution at steady state; CL, plasma clearance;  $t_{1/2}$ , terminal half-life;  $F$ , absolute oral bioavailability; nd, not determined. Formulation for PO and IV: DMSO:20% HP- $\beta$ -CD in saline = 1:9.

In addition, **24f** showed a high plasma clearance rate (CL = 35.2 L/h/kg). **15b** and **24f** demonstrated limited brain exposure (B/P ratio = 0.06 and 0.02, respectively) despite a substantial concentration of the ligand in the brain after the blood-brain barrier (BBB) penetration (Table 7). Therefore, PK profiles of **15b** and **24f** require further optimization to improve oral bioavailability, reduce plasma clearance, and enhance the BBB permeability prior to their application as *in vivo* probes.

**Table 7. Brain Penetration Analysis<sup>a</sup>**

Route	Time (h)	Brain Conc. (ng/g)	Plasma Conc. (ng/g)	Brain/Plasma Ratio
<b>15b</b>	0.25	198 ± 32	3668 ± 845	0.05 ± 0.01
IV	1	62 ± 20	1175 ± 526	0.06 ± 0.04
<b>24f</b>	0.25	124 ± 26	6103 ± 265	0.02 ± 0.003
IV	1	9.0 ± 0.8	376 ± 26	0.02 ± 0.001

<sup>a</sup>Values are mean ± SD from n = 3 biological replicates. Concentrations of compounds **15b** and **24f** in the brain and plasma were determined at 0.25 h and 1 h after a single dose of 10 mg/kg by IV. Formulation: DMSO:20% HP- $\beta$ -CD in saline = 1:9.

## CONCLUSIONS

We conducted a structural optimization of compound **4a**, employing an iterative drug design strategy that led to the discovery of a series of potent GPR52 agonists. Compounds **15b**, **15c**, **15d**, **24b**, **24e**, **24f**, and **24k** were found to be more potent for cAMP signaling than both **4a** and our previously optimized compound **4b**.<sup>40</sup> Our studies into  $\beta$ -arrestin recruitment of this series revealed that the parent compound **4a** was unexpectedly highly potent for GPR52  $\beta$ -arrestin recruitment ( $EC_{50, \beta\text{-arrestin}} = 22$  nM). Opening the indoline ring system to create **10a** profoundly reduced GPR52  $\beta$ -arrestin recruitment potency and efficacy ( $EC_{50, \beta\text{-arrestin}} = 483$  nM,  $E_{\text{max}, \beta\text{-arrestin}} = 70\%$ ). This finding provides a structural basis to generate GPR52 G protein-biased agonist probes and indicates the indoline ring system is important for imparting potent  $\beta$ -arrestin recruitment. To the best of our knowledge, these are the first G protein-biased GPR52 agonists. **10a** and **24f**, with greater bias for G protein/cAMP signaling, also induced significantly less *in vitro* desensitization than **4a**. This bias may be relevant for improving *in vivo* pharmacodynamics by increasing the duration of GPR52 activation and reducing receptor internalization and tachyphylaxis. Molecular docking studies of compounds **4a**, **15b**, and **24f** with GPR52 revealed a conserved binding mode with three pairs of hydrogen bonds,  $\pi$ - $\pi$  stacking, and hydrophobic interactions, providing insights for future structure-based drug design. Compound **15b** was highly selective for GPR52 agonism with no significant off-target effects at other brain GPCRs. **15b** and

**24f** are also bioavailable but have less than optimal brain permeability, requiring further optimization. These balanced and biased GPR52 agonists provide important pharmacological probes to determine the impact of biased agonism on GPR52 function. In addition, these compounds provide an innovative conceptual framework for evaluating reduced  $\beta$ -arrestin-mediated desensitization of GPR52, which may provide sustained agonist efficacy for therapeutic applications.

## EXPERIMENTAL SECTION

**Chemistry.** All commercially available starting materials and solvents were reagent grade and used without further purification. Reactions were performed under a nitrogen atmosphere in dry glassware with magnetic stirring. Preparative column chromatography was performed using silica gel 60, particle size 0.063–0.200 mm (70–230 mesh, flash). Analytical TLC was carried out employing silica gel 60 F254 plates (Merck, Darmstadt). Visualization of the developed chromatograms was performed with detection by UV (254 nm). NMR spectra were recorded on a Bruker-600 ( $^1\text{H}$ , 300 MHz;  $^{13}\text{C}$ , 75 MHz) spectrometer.  $^1\text{H}$  and  $^{13}\text{C}$  NMR spectra were recorded with TMS as an internal reference. Chemical shifts downfield from TMS were expressed in ppm, and  $J$  values were given in Hz. High-resolution mass spectra (HRMS) were obtained from Thermo Fisher LTQ Orbitrap Elite mass spectrometer. Parameters include the following: nano ESI spray voltage was 1.8 kV, capillary temperature was 275 °C, and the resolution was 60000; ionization was achieved by positive mode. Purity of final compounds was determined by analytical HPLC, which was carried out on a Shimadzu HPLC system (model: CBM-20A LC-20AD SPD-20A UV/vis). HPLC analysis conditions: Waters  $\mu$ Bondapak C18 (300 mm  $\times$  3.9 mm), flow rate 0.5 mL/min, UV detection at 270 and 254 nm, linear gradient from 10% acetonitrile in water (0.1%

TFA) to 100% acetonitrile (0.1% TFA) in 20 min, followed by 30 min of the last-named solvent. All biologically evaluated compounds are >95% pure.

**2-Chloro-4-(3-(trifluoromethyl)benzyl)pyridine (7).** A mixture of 1-(bromomethyl)-3-(trifluoromethyl)benzene **5** (287 mg, 1.2 mmol), Na<sub>2</sub>CO<sub>3</sub> (424 mg, 4 mmol), Pd(PPh<sub>3</sub>)<sub>4</sub> (115 mg, 0.05 mmol) and (2-chloropyridin-4-yl)boronic acid **6** (157 mg, 1 mmol) in toluene (5 mL) and ethanol (2.5 mL) was heated to 85 °C for 1.5 h under nitrogen atmosphere. After completion of reaction, it was cooled to room temperature and poured into water, and then extracted with EtOAc (20 mL × 3). The organic phase was washed with brine, dried over anhydrous Na<sub>2</sub>SO<sub>4</sub>, and subsequently concentrated under reduced pressure. The residue was purification by silica gel chromatography (Gradient: 10% to 20% EtOAc in hexane) provided compound **7** as a light-yellow oil (131 mg, 48%). <sup>1</sup>H NMR (300 MHz, Chloroform-*d*) δ 8.32 (d, *J* = 5.1 Hz, 1H), 7.56 (d, *J* = 7.8 Hz, 1H), 7.52 – 7.42 (m, 2H), 7.36 (d, *J* = 7.7 Hz, 1H), 7.16 (s, 1H), 7.04 (d, *J* = 5.0 Hz, 1H), 4.04 (s, 2H).

**Ethyl 3-((4-(3-(trifluoromethyl)benzyl)pyridin-2-yl)amino)benzoate (8).** A mixture of **7** (542 mg, 2 mmol), Pd(OAc)<sub>2</sub> (44 mg, 0.2 mmol), XantPhos (231 mg, 0.4 mmol), Cs<sub>2</sub>CO<sub>3</sub> (1.3 g, 4 mmol) and ethyl 3-aminobenzoate (330 mg, 2 mmol) in 1,4-dioxane (10 mL) was subjected to three rounds of vacuum evacuation followed by introduction of nitrogen. The reaction mixture was then stirred at 100 °C overnight. The reaction was cooled to room temperature and poured in water, and then extracted with EtOAc (20 mL × 3). The organic phase was washed with brine, dried over anhydrous Na<sub>2</sub>SO<sub>4</sub>, and then concentrated under reduced pressure. The residue was purified by silica gel chromatography (Gradient: 10% to 20% EtOAc in hexane) to provide product **8** as a colorless oil (610 mg, 76%). <sup>1</sup>H NMR (300 MHz, Chloroform-*d*) δ 8.16 (d, *J* = 5.1 Hz, 1H), 7.97

(t,  $J = 1.9$  Hz, 1H), 7.75 – 7.61 (m, 2H), 7.56 – 7.35 (m, 6H), 6.72 (s, 1H), 6.66 – 6.58 (m, 2H), 4.39 (q,  $J = 7.0$  Hz, 3H), 3.96 (s, 2H), 1.43 – 1.38 (m, 3H).

**3-((4-(3-(Trifluoromethyl)benzyl)pyridin-2-yl)amino)benzoic acid (9).** To a mixture of **8** (600 mg, 1.5 mmol) in MeOH (4 mL) was added a 4 N solution of NaOH (2 mL), and then resultant mixture was reflux for 2 h. Adjusting pH of the reaction mixture to pH 1 with 2 N HCl solution resulted in the formation of white solid precipitate out of the solution. The white solid was filtered and washed with water, the cake was collected and dried to afford the product **9** as a white solid (445 mg, 80%).  $^1\text{H}$  NMR (300 MHz, DMSO- $d_6$ )  $\delta$  12.77 (s, 1H), 9.20 (s, 1H), 8.26 (t,  $J = 1.9$  Hz, 1H), 8.09 (d,  $J = 5.2$  Hz, 1H), 7.93 (dd,  $J = 7.8, 2.3$  Hz, 1H), 7.70 – 7.51 (m, 4H), 7.45 (d,  $J = 7.6$  Hz, 1H), 7.34 (t,  $J = 7.9$  Hz, 1H), 6.70 (d,  $J = 5.2$  Hz, 1H), 6.63 (s, 1H), 4.03 (s, 2H).

***N*-(2-Hydroxyethyl)-3-((4-(3-(trifluoromethyl)benzyl)pyridin-2-yl)amino)benzamide (10a).** Compound **9** (74 mg, 0.2 mmol) and 2-aminoethan-1-ol (25 mg, 0.4 mmol) were dissolved in DMF (5 mL) and the resultant mixture was cooled to 0 °C using ice bath. HOBt (28 mg, 0.2 mmol), EDCI (39 mg, 0.2 mmol) and DMAP (48 mg, 0.4 mmol) were sequentially added to the reaction mixture at 0 °C. Thereafter, ice bath was removed and reaction was allowed to stir at room temperature overnight. After completion of reaction (detected by TLC), the reaction was quenched by water and then extracted with EtOAc (20 mL  $\times$  3). The combined organic layers were washed with brine, dried anhydrous Na<sub>2</sub>SO<sub>4</sub>, and solvent was removed using rotary evaporator to afford a yellow oil. This material was further purified by preparative TLC plates using CH<sub>2</sub>Cl<sub>2</sub>/MeOH = 50:1 as the eluent to yield **10a** as a colorless oil (71 mg, 87%).  $^1\text{H}$  NMR (300 MHz, Chloroform- $d$ )  $\delta$  8.03 (d,  $J = 5.2$  Hz, 1H), 7.68 (d,  $J = 2.0$  Hz, 1H), 7.60 – 7.45 (m, 2H), 7.44 – 7.29 (m, 4H), 7.28 – 7.13 (m, 3H), 6.60 – 6.47 (m, 2H), 3.86 (s, 3H), 3.69 (t,  $J = 5.0$  Hz, 2H), 3.50 (t,  $J = 5.2$  Hz, 2H);  $^{13}\text{C}$  NMR (75 MHz, CDCl<sub>3</sub>)  $\delta$  168.7, 155.9, 150.8, 147.9, 141.0, 139.9, 135.2, 132.4, 130.9

(d,  $J = 32.1$  Hz), 129.2, 129.1, 125.8, 125.6 (q,  $J = 3.8$  Hz), 123.5 (q,  $J = 3.7$  Hz), 122.2, 120.4, 118.3, 116.1, 109.9, 61.6, 42.8, 40.9; HRMS (ESI) calcd for  $C_{22}H_{21}F_3N_3O_2$  416.1580 (M + H)<sup>+</sup>, found 416.1578.

***N*-((1*R*,4*R*)-4-Hydroxycyclohexyl)-3-((4-(3-(trifluoromethyl)benzyl)pyridin-2-yl)amino)benzamide (10b).** Compound **10b** (41 mg, 65%) was synthesized following the synthetic procedure of compound **10a** as a white solid. <sup>1</sup>H NMR (300 MHz, DMSO-*d*<sub>6</sub>)  $\delta$  9.09 (s, 1H), 8.05 (dd,  $J = 9.1, 6.4$  Hz, 2H), 7.92 (d,  $J = 6.2$  Hz, 2H), 7.68 – 7.53 (m, 4H), 7.28 (d,  $J = 4.6$  Hz, 2H), 6.73 – 6.59 (m, 2H), 4.53 (d,  $J = 4.4$  Hz, 1H), 4.01 (s, 2H), 3.77 – 3.60 (m, 1H), 3.45 – 3.35 (m, 1H), 1.92 – 1.74 (m, 4H), 1.30 (dt,  $J = 24.8, 12.5$  Hz, 4H); <sup>13</sup>C NMR (75 MHz, DMSO)  $\delta$  166.5, 156.5, 150.8, 147.8, 142.2, 141.6, 136.0, 133.6, 130.1, 128.7, 126.0 – 125.6 (m), 123.8 – 123.4 (m), 120.7, 119.2, 117.8, 115.8, 110.8, 68.8, 48.3, 34.7, 30.7; HRMS (ESI) calcd for  $C_{26}H_{27}F_3N_3O_2$  470.2049 (M + H)<sup>+</sup>, found 470.2048.

**(4-Hydroxypiperidin-1-yl)(3-((4-(3-(trifluoromethyl)benzyl)pyridin-2-yl)amino)phenyl)methanone (10c).** Compound **10c** (40 mg, 67%) was synthesized following the synthetic procedure of compound **10a** as a colorless oil. <sup>1</sup>H NMR (300 MHz, Chloroform-*d*)  $\delta$  8.09 (d,  $J = 5.2$  Hz, 1H), 7.53 – 7.38 (m, 5H), 7.37 – 7.25 (m, 2H), 7.21 (s, 1H), 6.96 (d,  $J = 7.5$  Hz, 1H), 6.61 (s, 1H), 6.55 (d,  $J = 5.2$  Hz, 1H), 4.17 (s, 1H), 3.91 (s, 3H), 3.69 (s, 1H), 3.24 (d,  $J = 37.9$  Hz, 2H), 2.75 (s, 1H), 1.85 (d,  $J = 32.6$  Hz, 2H), 1.55 (d,  $J = 22.3$  Hz, 2H); <sup>13</sup>C NMR (75 MHz, CDCl<sub>3</sub>)  $\delta$  170.3, 155.9, 150.6, 148.2, 141.0, 140.0, 136.8, 132.4, 131.1, 130.9 (d,  $J = 32.2$  Hz), 130.7, 129.2, 129.1, 125.6 (d,  $J = 3.8$  Hz), 123.5 (d,  $J = 3.8$  Hz), 120.3, 120.1, 117.7, 116.1, 109.6, 66.9, 45.0, 41.0, 39.5, 34.6, 33.9; HRMS (ESI) calcd for  $C_{25}H_{25}F_3N_3O_2$  456.1893 (M + H)<sup>+</sup>, found 456.1890.

**Morpholino(3-((4-(3-(trifluoromethyl)benzyl)pyridin-2-yl)amino)phenyl)methanone**

**(10d).** Compound **10d** (46 mg, 78%) was synthesized following the synthetic procedure of compound **10a** as a white solid. <sup>1</sup>H NMR (300 MHz, Chloroform-*d*)  $\delta$  8.10 (d, *J* = 5.2 Hz, 1H), 7.51 (d, *J* = 7.3 Hz, 2H), 7.47 – 7.39 (m, 3H), 7.38 – 7.26 (m, 2H), 7.23 (s, 1H), 6.99 (d, *J* = 7.5 Hz, 1H), 6.63 – 6.54 (m, 2H), 3.92 (s, 2H), 3.80 – 3.41 (m, 8H); <sup>13</sup>C NMR (75 MHz, CDCl<sub>3</sub>)  $\delta$  170.3, 155.8, 150.6, 148.2, 141.1, 140.0, 136.0, 132.4, 130.9 (d, *J* = 31.9 Hz), 129.3, 129.1, 125.6 (q, *J* = 3.8 Hz), 123.5 (q, *J* = 3.8 Hz), 120.5, 120.4, 118.0, 116.2, 109.6, 77.5, 77.1, 76.7, 66.9, 41.0; HRMS (ESI) calcd for C<sub>24</sub>H<sub>23</sub>F<sub>3</sub>N<sub>3</sub>O<sub>2</sub> 442.1737 (M + H)<sup>+</sup>, found 442.1734.

**Methyl (3-((4-(3-(trifluoromethyl)benzyl)pyridin-2-yl)amino)benzoyl)-D-allothreoninate**

**(10e).** Compound **10e** (47 mg, 72%) was synthesized following the synthetic procedure of compound **10a** as a colorless oil. <sup>1</sup>H NMR (300 MHz, Chloroform-*d*)  $\delta$  8.04 (d, *J* = 5.2 Hz, 1H), 7.73 (s, 1H), 7.59 (d, *J* = 8.1 Hz, 1H), 7.53 – 7.29 (m, 7H), 7.22 (t, *J* = 7.9 Hz, 1H), 6.61 (s, 1H), 6.53 (d, *J* = 5.2 Hz, 1H), 4.77 (dd, *J* = 8.7, 2.8 Hz, 1H), 4.41 (dd, *J* = 6.6, 2.9 Hz, 1H), 3.88 (s, 2H), 3.69 (s, 4H), 1.23 (d, *J* = 6.4 Hz, 3H); <sup>13</sup>C NMR (75 MHz, CDCl<sub>3</sub>)  $\delta$  171.8, 168.3, 155.8, 150.9, 147.9, 141.0, 139.9, 134.7, 132.4, 131.1, 129.3, 129.1, 125.7 – 125.4 (m), 123.5 (q, *J* = 3.8 Hz), 122.5, 120.6, 118.4, 116.1, 109.6, 68.0, 58.3, 52.5, 41.0, 20.1; HRMS (ESI) calcd for C<sub>25</sub>H<sub>25</sub>F<sub>3</sub>N<sub>3</sub>O<sub>4</sub> 488.1791 (M + H)<sup>+</sup>, found 488.1792.

**N-((1S)-1,3-Dihydroxy-1-phenylpropan-2-yl)-3-((4-(3-(trifluoromethyl)benzyl)pyridin-2-yl)amino)benzamide (10f).** Compound **10f** (38 mg, 55%) was synthesized following the synthetic procedure of compound **10a** as a white solid. <sup>1</sup>H NMR (300 MHz, DMSO-*d*<sub>6</sub>)  $\delta$  9.12 (s, 1H), 8.09 (d, *J* = 5.3 Hz, 1H), 7.98 (s, 1H), 7.86 (d, *J* = 8.0 Hz, 1H), 7.67 – 7.55 (m, 4H), 7.49 (d, *J* = 8.7 Hz, 1H), 7.37 (d, *J* = 7.5 Hz, 2H), 7.24 (dt, *J* = 21.9, 7.2 Hz, 5H), 6.69 (d, *J* = 5.3 Hz, 1H), 6.63 (s, 1H), 5.55 (d, *J* = 5.3 Hz, 1H), 4.96 (t, *J* = 4.5 Hz, 1H), 4.79 (t, *J* = 5.6 Hz, 1H), 4.13 (s, 1H), 4.02

(s, 2H), 3.60 (dt,  $J = 12.5, 6.7$  Hz, 1H), 3.45 – 3.36 (m, 1H);  $^{13}\text{C}$  NMR (75 MHz, DMSO- $d_6$ )  $\delta$  166.9, 156.5, 150.8, 147.8, 144.1, 142.3, 141.6, 135.7, 133.6, 130.1, 128.8, 128.2, 127.1, 126.6, 125.8 (d,  $J = 4.2$  Hz), 123.6 (d,  $J = 4.1$  Hz), 120.8, 119.2, 117.3, 115.9, 110.9, 70.6, 61.0, 57.5; HRMS (ESI) calcd for  $\text{C}_{29}\text{H}_{27}\text{F}_3\text{N}_3\text{O}_3$  522.1999 ( $\text{M} + \text{H}$ ) $^+$ , found 522.2001.

***N*-(1,3-Dihydroxypropan-2-yl)-3-((4-(3-(trifluoromethyl)benzyl)pyridin-2-yl)amino)benzamide (10g).** Compound **10g** (36 mg, 60%) was synthesized following the synthetic procedure of compound **10a** as a white solid.  $^1\text{H}$  NMR (300 MHz, Chloroform- $d$ )  $\delta$  8.03 (d,  $J = 5.4$  Hz, 1H), 7.66 (d,  $J = 16.9$  Hz, 1H), 7.57 – 7.21 (m, 9H), 6.64 – 6.44 (m, 2H), 3.81 (d,  $J = 50.4$  Hz, 9H);  $^{13}\text{C}$  NMR (75 MHz,  $\text{CDCl}_3$ )  $\delta$  168.7, 155.8, 151.1, 147.6, 140.8, 139.8, 135.0, 132.4, 129.2, 129.1, 125.6 (d,  $J = 3.8$  Hz), 123.5 (d,  $J = 3.7$  Hz), 122.3, 120.6, 118.2, 116.0, 109.9, 61.9, 53.1, 40.9; HRMS (ESI) calcd for  $\text{C}_{23}\text{H}_{23}\text{F}_3\text{N}_3\text{O}_3$  446.1682 ( $\text{M} + \text{H}$ ) $^+$ , found 446.1683.

***N*-(2,2-Difluoroethyl)-3-((4-(3-(trifluoromethyl)benzyl)pyridin-2-yl)amino)benzamide (10h).** Compound **10h** (34 mg, 62%) was synthesized following the synthetic procedure of compound **10a** as a white solid.  $^1\text{H}$  NMR (300 MHz, Chloroform- $d$ )  $\delta$  8.12 (d,  $J = 5.1$  Hz, 1H), 7.86 (t,  $J = 1.8$  Hz, 1H), 7.60 – 7.48 (m, 2H), 7.48 – 7.40 (m, 2H), 7.39 – 7.29 (m, 3H), 7.00 (s, 1H), 6.78 (t,  $J = 6.2$  Hz, 1H), 6.65 – 6.53 (m, 2H), 5.96 (tt,  $J = 56.1, 4.1$  Hz, 1H), 3.94 (s, 2H), 3.81 (tdd,  $J = 14.8, 6.2, 4.1$  Hz, 2H);  $^{13}\text{C}$  NMR (75 MHz,  $\text{CDCl}_3$ )  $\delta$  168.1, 166.6, 155.7, 150.8, 148.2, 141.2, 139.9, 134.5, 132.4, 131.2, 130.8, 129.4, 129.2, 125.8, 125.6 (d,  $J = 3.8$  Hz), 123.6 (d,  $J = 3.8$  Hz), 122.6, 120.3, 118.2, 116.9, 116.4, 113.7 (t,  $J = 241.4$  Hz), 110.5, 109.6, 42.23 (t,  $J = 26.7$  Hz), 41.0; HRMS (ESI) calcd for  $\text{C}_{22}\text{H}_{19}\text{F}_5\text{N}_3\text{O}$  436.1443 ( $\text{M} + \text{H}$ ) $^+$ , found 436.1439.

***N*-(2-Methoxyethyl)-3-((4-(3-(trifluoromethyl)benzyl)pyridin-2-yl)amino)benzamide (10i).** Compound **10i** (38 mg, 66%) was synthesized following the synthetic procedure of compound **10a** as a white solid.  $^1\text{H}$  NMR (300 MHz, Chloroform- $d$ )  $\delta$  8.13 (d,  $J = 5.2$  Hz, 1H),

7.82 (t,  $J = 1.9$  Hz, 1H), 7.59 (dt,  $J = 7.0, 2.2$  Hz, 1H), 7.53 – 7.39 (m, 3H), 7.34 (q,  $J = 7.4$  Hz, 3H), 7.07 (s, 1H), 6.72 (t,  $J = 5.5$  Hz, 1H), 6.65 – 6.53 (m, 2H), 3.93 (s, 2H), 3.65 (q,  $J = 5.1$  Hz, 2H), 3.56 (t,  $J = 4.9$  Hz, 2H), 3.39 (s, 3H);  $^{13}\text{C}$  NMR (75 MHz,  $\text{CDCl}_3$ )  $\delta$  167.5, 155.9, 150.7, 148.3, 141.1, 140.0, 135.6, 132.4, 129.3, 129.1, 125.6 (d,  $J = 3.7$  Hz), 123.5 (d,  $J = 3.9$  Hz), 122.3, 120.3, 118.4, 116.2, 109.3, 71.2, 58.8, 41.0, 39.7; HRMS (ESI) calcd for  $\text{C}_{23}\text{H}_{23}\text{F}_3\text{N}_3\text{O}_2$  430.1737 (M + H) $^+$ , found 430.1735.

***N*-(3-Hydroxypropyl)-3-((4-(3-(trifluoromethyl)benzyl)pyridin-2-yl)amino)benzamide**

**(10j).** Compound **10j** (37 mg, 64%) was synthesized following the synthetic procedure of compound **10a** as a white solid.  $^1\text{H}$  NMR (300 MHz, Chloroform-*d*)  $\delta$  8.04 (d,  $J = 5.4$  Hz, 1H), 7.74 (s, 1H), 7.56 (d,  $J = 6.7$  Hz, 1H), 7.38 (dt,  $J = 33.9, 12.4$  Hz, 7H), 7.25 – 7.17 (m, 1H), 6.55 (d,  $J = 13.4$  Hz, 2H), 3.87 (s, 2H), 3.63 (d,  $J = 5.8$  Hz, 2H), 3.50 (t,  $J = 6.1$  Hz, 3H), 1.71 (q,  $J = 5.8$  Hz, 2H);  $^{13}\text{C}$  NMR (75 MHz,  $\text{CDCl}_3$ )  $\delta$  168.7, 166.6, 155.8, 150.9, 147.7, 141.0, 139.9, 135.2, 132.4, 131.1, 129.2, 129.1, 125.6 (d,  $J = 4.1$  Hz), 123.5 (d,  $J = 3.8$  Hz), 122.2, 120.4, 118.2, 116.1, 109.9, 59.8, 41.0, 37.4, 31.8; HRMS (ESI) calcd for  $\text{C}_{23}\text{H}_{23}\text{F}_3\text{N}_3\text{O}_2$  430.1737 (M + H) $^+$ , found 430.1736.

***N*-(4-Hydroxybutyl)-3-((4-(3-(trifluoromethyl)benzyl)pyridin-2-yl)amino)benzamide**

**(10k).** Compound **10k** (41 mg, 69%) was synthesized following the synthetic procedure of compound **10a** as a white solid.  $^1\text{H}$  NMR (300 MHz, Chloroform-*d*)  $\delta$  8.02 (d,  $J = 5.1$  Hz, 1H), 7.75 (s, 1H), 7.40 (ddt,  $J = 45.2, 31.4, 12.5$  Hz, 9H), 6.62 – 6.42 (m, 2H), 3.86 (d,  $J = 4.0$  Hz, 2H), 3.58 (q,  $J = 5.4$  Hz, 2H), 3.35 (t,  $J = 5.8$  Hz, 2H), 3.21 (s, 1H), 1.58 (dt,  $J = 12.7, 6.1$  Hz, 4H);  $^{13}\text{C}$  NMR (75 MHz,  $\text{CDCl}_3$ )  $\delta$  168.1, 155.9, 150.8, 147.8, 141.0, 139.9, 135.7, 132.4, 130.87 (d,  $J = 32.5$  Hz), 129.1, 125.6 (d,  $J = 3.7$  Hz), 123.5 (d,  $J = 3.4$  Hz), 122.0, 120.4, 118.1, 116.0, 110.0,

62.0, 40.9, 39.9, 29.8, 26.1; HRMS (ESI) calcd for C<sub>24</sub>H<sub>25</sub>F<sub>3</sub>N<sub>3</sub>O<sub>2</sub> 444.1893 (M + H)<sup>+</sup>, found 444.1889.

***N*-(2,3-Dihydroxypropyl)-3-((4-(3-(trifluoromethyl)benzyl)pyridin-2-yl)amino)benzamide (10l).** Compound **10l** (40 mg, 67%) was synthesized following the synthetic procedure of compound **10a** as a colorless oil. <sup>1</sup>H NMR (300 MHz, Chloroform-*d*) δ 7.92 – 7.72 (m, 2H), 7.60 – 7.49 (m, 2H), 7.29 (ddd, *J* = 37.2, 22.4, 7.8 Hz, 5H), 7.02 (t, *J* = 7.4 Hz, 1H), 6.48 (s, 1H), 6.36 (d, *J* = 4.9 Hz, 1H), 4.43 (s, 2H), 4.10 (s, 1H), 3.75 (d, *J* = 26.6 Hz, 4H), 3.57 – 3.19 (m, 3H); <sup>13</sup>C NMR (75 MHz, CDCl<sub>3</sub>) δ 169.2, 168.8, 155.7, 150.9, 147.5, 141.0, 139.9, 134.9, 134.7, 132.3, 131.0, 130.6, 129.0, 125.8, 125.5 (d, *J* = 3.6 Hz), 123.4 (d, *J* = 3.7 Hz), 122.2, 122.0, 120.4, 118.4, 115.9, 110.0, 70.9, 63.9, 61.5, 42.8, 40.8; HRMS (ESI) calcd for C<sub>23</sub>H<sub>23</sub>F<sub>3</sub>N<sub>3</sub>O<sub>3</sub> 446.1686 (M + H)<sup>+</sup>, found 446.1683.

**Ethyl 3-amino-2-cyclopropylbenzoate (12d).** A mixture of ethyl 3-amino-2-bromobenzoate **11a** (260 mg, 1.0 mmol), K<sub>3</sub>PO<sub>4</sub> (636 mg, 3 mmol), Pd(dppf)Cl<sub>2</sub> (141 mg, 0.05 mmol) and cyclopropylboronic acid (103 mg, 1.2 mmol) in 1,4-dioxane (2 mL) and water (0.5 mL) was heated to 85 °C for 12 h under nitrogen atmosphere. After completion of reaction, it was cooled to room temperature and poured in water, and then extracted with EtOAc (20 mL × 3). The organic phase was washed with brine, dried over anhydrous Na<sub>2</sub>SO<sub>4</sub>, and then concentrated under reduced pressure. The residue was purified by silica gel chromatography (Gradient: 10% to 20% EtOAc in hexane) to provide compound **12d** as a light yellow oil (96 mg, 47%). <sup>1</sup>H NMR (300 MHz, Chloroform-*d*) δ 7.08 (dt, *J* = 9.9, 4.9 Hz, 1H), 6.97 (d, *J* = 4.7 Hz, 1H), 6.77 (t, *J* = 5.6 Hz, 1H), 4.47 – 4.29 (m, 3H), 4.15 (s, 2H), 1.91 – 1.74 (m, 1H), 1.03 – 0.93 (m, 2H), 0.47 (t, *J* = 5.2 Hz, 2H).

**Methyl 3-amino-2-(furan-2-yl)benzoate (12e).** Compound **12e** (130 mg, 60%) was synthesized following the synthetic procedure of compound **12d** as a yellow oil. <sup>1</sup>H NMR (300 MHz, Chloroform-*d*)  $\delta$  7.54 (d, *J* = 1.8 Hz, 1H), 7.26 – 7.15 (m, 2H), 6.89 (dd, *J* = 7.7, 1.6 Hz, 1H), 6.59 – 6.44 (m, 2H), 4.10 (s, 2H), 3.73 (s, 3H).

**Methyl 2-fluoro-3-((4-(3-(trifluoromethyl)benzyl)pyridin-2-yl)amino)benzoate (13a).** Compound **13a** (154 mg, 38%) was synthesized following the synthetic procedure of compound **8** as a colorless oil. <sup>1</sup>H NMR (300 MHz, Chloroform-*d*)  $\delta$  8.42 (t, *J* = 8.0 Hz, 1H), 8.19 (d, *J* = 5.2 Hz, 1H), 7.58 – 7.36 (m, 5H), 7.17 (t, *J* = 8.0 Hz, 1H), 6.73 – 6.52 (m, 3H), 3.99 (s, 2H), 3.95 (s, 3H).

**Methyl 2-methyl-3-((4-(3-(trifluoromethyl)benzyl)pyridin-2-yl)amino)benzoate (13b).** Compound **13b** (242 mg, 61%) was synthesized following the synthetic procedure of compound **8** as a light-yellow oil. <sup>1</sup>H NMR (300 MHz, Chloroform-*d*)  $\delta$  8.10 (d, *J* = 5.2 Hz, 1H), 7.64 (d, *J* = 7.8 Hz, 1H), 7.53 (dd, *J* = 14.0, 7.7 Hz, 2H), 7.44 (d, *J* = 7.0 Hz, 2H), 7.34 (d, *J* = 7.7 Hz, 1H), 7.24 (t, *J* = 7.9 Hz, 1H), 6.55 (d, *J* = 5.2 Hz, 1H), 6.37 (s, 2H), 3.90 (s, 2H), 2.46 (s, 3H).

**Methyl 2-methoxy-3-((4-(3-(trifluoromethyl)benzyl)pyridin-2-yl)amino)benzoate (13c).** Compound **13c** (157 mg, 75%) was synthesized following the synthetic procedure of compound **8** as a light-yellow oil. <sup>1</sup>H NMR (300 MHz, Chloroform-*d*)  $\delta$  8.36 (dd, *J* = 8.2, 1.6 Hz, 1H), 8.22 – 8.16 (m, 1H), 7.57 – 7.40 (m, 5H), 7.14 (t, *J* = 8.0 Hz, 1H), 7.06 (s, 1H), 6.64 (d, *J* = 4.3 Hz, 2H), 3.99 (s, 2H), 3.95 (s, 3H), 3.90 (s, 3H).

**Ethyl 2-cyclopropyl-3-((4-(3-(trifluoromethyl)benzyl)pyridin-2-yl)amino)benzoate (13d).** Compound **13d** (154 mg, 70%) was synthesized following the synthetic procedure of compound **8** as a light-yellow oil. <sup>1</sup>H NMR (300 MHz, Chloroform-*d*)  $\delta$  8.17 (d, *J* = 5.2 Hz, 1H), 7.84 (dd, *J* = 5.5, 4.1 Hz, 1H), 7.53 (d, *J* = 8.0 Hz, 1H), 7.47 (d, *J* = 6.9 Hz, 2H), 7.38 (d, *J* = 7.5 Hz, 1H),

7.27 – 7.19 (m, 2H), 7.07 (s, 1H), 6.68 (s, 1H), 6.61 (dd,  $J = 5.2, 1.4$  Hz, 1H), 4.39 (s, 2H), 3.97 (s, 2H), 1.97 – 1.86 (m, 1H), 1.42 (s, 3H), 1.11 – 1.01 (m, 2H), 0.55 – 0.45 (m, 2H).

**Methyl 2-(furan-2-yl)-3-((4-(3-(trifluoromethyl)benzyl)pyridin-2-yl)amino)benzoate (13e).** Compound **13e** (83 mg, 37%) was synthesized following the synthetic procedure of compound **8** as a light-yellow oil.  $^1\text{H}$  NMR (300 MHz, Chloroform- $d$ )  $\delta$  8.21 – 8.07 (m, 2H), 7.63 – 7.50 (m, 2H), 7.40 (dt,  $J = 21.8, 7.4$  Hz, 5H), 6.88 (s, 1H), 6.65 – 6.46 (m, 4H), 3.94 (s, 2H), 3.74 (s, 3H).

**Methyl 4-methyl-3-((4-(3-(trifluoromethyl)benzyl)pyridin-2-yl)amino)benzoate (13f).** Compound **13f** (270 mg, 68%) was synthesized following the synthetic procedure of compound **8** as a light-yellow oil.  $^1\text{H}$  NMR (300 MHz, Chloroform- $d$ )  $\delta$  8.23 – 8.02 (m, 2H), 7.73 (dd,  $J = 7.8, 1.7$  Hz, 1H), 7.55 – 7.29 (m, 5H), 6.58 (d,  $J = 5.3$  Hz, 1H), 6.49 (s, 1H), 6.28 (s, 1H), 3.93 (s, 2H), 2.19 (s, 2H).

**Methyl 4-methoxy-3-((4-(3-(trifluoromethyl)benzyl)pyridin-2-yl)amino)benzoate (13g).** Compound **13g** (313 mg, 75%) was synthesized following the synthetic procedure of compound **8** as a light-yellow oil.  $^1\text{H}$  NMR (300 MHz, Chloroform- $d$ )  $\delta$  8.79 (d,  $J = 2.1$  Hz, 1H), 8.22 (d,  $J = 5.2$  Hz, 1H), 7.71 (dd,  $J = 8.5, 2.1$  Hz, 1H), 7.46 (dq,  $J = 21.3, 7.8$  Hz, 4H), 6.92 (d,  $J = 8.6$  Hz, 2H), 6.71 – 6.57 (m, 2H), 3.97 (d,  $J = 5.9$  Hz, 5H), 3.91 (s, 3H).

**Methyl 2-fluoro-5-((4-(3-(trifluoromethyl)benzyl)pyridin-2-yl)amino)benzoate (13h).** Compound **13h** (163 mg, 81%) was synthesized following the synthetic procedure of compound **8** as a light-yellow oil.  $^1\text{H}$  NMR (300 MHz, Chloroform- $d$ )  $\delta$  8.14 (d,  $J = 5.2$  Hz, 1H), 7.87 (dd,  $J = 6.1, 2.9$  Hz, 1H), 7.64 (ddd,  $J = 8.9, 4.1, 3.0$  Hz, 1H), 7.53 (d,  $J = 7.6$  Hz, 1H), 7.48 – 7.44 (m, 2H), 7.38 (d,  $J = 7.7$  Hz, 1H), 7.11 (dd,  $J = 10.1, 8.9$  Hz, 1H), 6.62 (dd,  $J = 5.2, 1.4$  Hz, 1H), 6.50 (d,  $J = 1.3$  Hz, 1H), 6.45 (s, 1H), 3.95 (d,  $J = 3.4$  Hz, 5H).

**2-Fluoro-3-((4-(3-(trifluoromethyl)benzyl)pyridin-2-yl)amino)benzoic acid (14a).**

Compound **14a** (140 mg, 90%) was synthesized following the synthetic procedure of compound **9** as a light yellow solid.  $^1\text{H}$  NMR (300 MHz, DMSO- $d_6$ )  $\delta$  13.11 (s, 1H), 8.74 (s, 1H), 8.36 (t,  $J$  = 8.0 Hz, 1H), 8.04 (d,  $J$  = 5.2 Hz, 1H), 7.69 – 7.53 (m, 4H), 7.39 (t,  $J$  = 6.7 Hz, 1H), 7.19 (q,  $J$  = 8.7, 8.0 Hz, 1H), 6.84 (s, 1H), 6.72 (d,  $J$  = 5.1 Hz, 1H), 4.01 (s, 2H).

**2-Methyl-3-((4-(3-(trifluoromethyl)benzyl)pyridin-2-yl)amino)benzoic acid (14b).**

Compound **14b** (230 mg, 91%) was synthesized following the synthetic procedure of compound **9** as a light yellow solid.  $^1\text{H}$  NMR (300 MHz, DMSO- $d_6$ )  $\delta$  10.45 (s, 1H), 7.90 (d,  $J$  = 6.4 Hz, 1H), 7.81 – 7.68 (m, 2H), 7.59 (dq,  $J$  = 17.1, 7.7 Hz, 4H), 7.38 (t,  $J$  = 7.8 Hz, 1H), 7.01 – 6.76 (m, 2H), 4.16 (s, 2H), 2.37 (s, 3H).

**2-Methoxy-3-((4-(3-(trifluoromethyl)benzyl)pyridin-2-yl)amino)benzoic acid (14c).**

Compound **14c** (179 mg, 89%) was synthesized following the synthetic procedure of compound **9** as a light yellow solid.  $^1\text{H}$  NMR (300 MHz, DMSO- $d_6$ )  $\delta$  13.04 (s, 1H), 10.49 (s, 1H), 7.95 (d,  $J$  = 6.4 Hz, 1H), 7.78 – 7.54 (m, 6H), 7.28 (t,  $J$  = 7.8 Hz, 1H), 7.10 (d,  $J$  = 1.4 Hz, 1H), 6.94 (dd,  $J$  = 6.5, 1.5 Hz, 1H), 4.19 (s, 2H), 3.70 (s, 3H).

**2-Cyclopropyl-3-((4-(3-(trifluoromethyl)benzyl)pyridin-2-yl)amino)benzoic acid (14d).**

Compound **14d** (194 mg, 94%) was synthesized following the synthetic procedure of compound **9** as a light yellow solid.  $^1\text{H}$  NMR (300 MHz, DMSO- $d_6$ )  $\delta$  10.50 (s, 1H), 7.92 (dd,  $J$  = 6.5, 4.6 Hz, 1H), 7.72 (s, 1H), 7.63 (q,  $J$  = 5.3, 4.4 Hz, 3H), 7.56 – 7.41 (m, 3H), 7.01 (s, 1H), 6.93 (dt,  $J$  = 6.5, 1.7 Hz, 1H), 4.19 (s, 2H), 1.89 – 1.74 (m, 1H), 0.78 (d,  $J$  = 8.2 Hz, 2H), 0.40 – 0.22 (m, 2H).

**2-(Furan-2-yl)-3-((4-(3-(trifluoromethyl)benzyl)pyridin-2-yl)amino)benzoic acid (14e).**

Compound **14e** (63 mg, 79%) was synthesized following the synthetic procedure of compound **9**

as a light yellow solid.  $^1\text{H}$  NMR (300 MHz, Chloroform-*d*)  $\delta$  10.34 (s, 1H), 7.81 – 7.61 (m, 2H), 7.56 – 7.38 (m, 4H), 7.24 (t,  $J$  = 10.9 Hz, 3H), 6.68 – 6.15 (m, 4H), 3.84 (s, 2H).

**4-Methyl-3-((4-(3-(trifluoromethyl)benzyl)pyridin-2-yl)amino)benzoic acid (14f).**

Compound **14f** (240 mg, 92%) was synthesized following the synthetic procedure of compound **9** as a light yellow solid.  $^1\text{H}$  NMR (300 MHz, DMSO-*d*<sub>6</sub>)  $\delta$  10.49 (s, 1H), 7.97 – 7.87 (m, 2H), 7.83 (d,  $J$  = 8.0 Hz, 1H), 7.72 (s, 1H), 7.61 (q,  $J$  = 7.4, 5.3 Hz, 3H), 7.49 (d,  $J$  = 8.0 Hz, 1H), 7.05 – 6.74 (m, 2H), 4.16 (s, 2H), 2.26 (s, 3H).

**4-Methoxy-3-((4-(3-(trifluoromethyl)benzyl)pyridin-2-yl)amino)benzoic acid (14g).**

Compound **14g** (254 mg, 81%) was synthesized following the synthetic procedure of compound **9** as a light yellow solid.  $^1\text{H}$  NMR (300 MHz, DMSO-*d*<sub>6</sub>)  $\delta$  10.00 (s, 1H), 8.06 (s, 1H), 7.90 (t,  $J$  = 7.7 Hz, 2H), 7.77 – 7.53 (m, 4H), 7.26 (d,  $J$  = 8.7 Hz, 1H), 7.00 – 6.82 (m, 2H), 4.15 (s, 2H), 3.85 (s, 3H).

**2-Fluoro-5-((4-(3-(trifluoromethyl)benzyl)pyridin-2-yl)amino)benzoic acid (14h).**

Compound **14h** (181 mg, 93%) was synthesized following the synthetic procedure of compound **9** as a light yellow solid.  $^1\text{H}$  NMR (300 MHz, DMSO-*d*<sub>6</sub>)  $\delta$  10.27 (s, 1H), 8.03 – 7.91 (m, 2H), 7.77 – 7.69 (m, 2H), 7.62 (d,  $J$  = 5.7 Hz, 3H), 7.36 (dd,  $J$  = 10.5, 8.7 Hz, 1H), 6.95 – 6.82 (m, 2H), 4.13 (s, 2H).

**2-Fluoro-N-(2-hydroxyethyl)-3-((4-(3-(trifluoromethyl)benzyl)pyridin-2-yl)amino)benzamide (15a).** Compound **15a** (33 mg, 38%) was synthesized following the synthetic procedure of compound **10a** as a colorless oil (33 mg, 38%).  $^1\text{H}$  NMR (300 MHz, Chloroform-*d*)  $\delta$  8.09 (q,  $J$  = 7.1, 5.8 Hz, 2H), 7.62 – 7.30 (m, 5H), 7.20 (dt,  $J$  = 10.4, 5.6 Hz, 1H), 7.07 (t,  $J$  = 8.0 Hz, 1H), 6.97 (s, 1H), 6.69 – 6.47 (m, 2H), 3.92 (s, 2H), 3.75 (t,  $J$  = 5.0 Hz, 2H), 3.57 (q,  $J$  = 5.2 Hz, 3H);  $^{13}\text{C}$  NMR (75 MHz, CDCl<sub>3</sub>)  $\delta$  164.6, 164.6, 155.4, 152.8, 150.9, 148.0,

139.8, 132.4, 129.4, 129.2, 125.6 (d,  $J = 3.6$  Hz), 124.3 (d,  $J = 4.2$  Hz), 123.9, 123.6 (d,  $J = 3.9$  Hz), 123.4, 121.7 (d,  $J = 11.1$  Hz), 116.7, 110.1, 61.5, 42.7, 40.9; HRMS (ESI) calcd for  $C_{22}H_{20}F_4N_3O_2$  434.1486 (M + H)<sup>+</sup>, found 434.1481.

***N*-(2-Hydroxyethyl)-2-methyl-3-((4-(3-(trifluoromethyl)benzyl)pyridin-2-yl)amino)benzamide (15b).** Compound **15b** (33 mg, 77%) was synthesized following the synthetic procedure of compound **10a** as a white solid. <sup>1</sup>H NMR (300 MHz, Chloroform-*d*) δ 8.03 (d,  $J = 5.4$  Hz, 1H), 7.43 (td,  $J = 24.9, 22.2, 7.7$  Hz, 5H), 7.24 – 7.09 (m, 2H), 6.86 (s, 1H), 6.62 – 6.38 (m, 3H), 4.16 (s, 1H), 3.91 (s, 2H), 3.79 (t,  $J = 5.0$  Hz, 2H), 3.57 (q,  $J = 5.3$  Hz, 2H), 2.30 (s, 3H); <sup>13</sup>C NMR (75 MHz, CDCl<sub>3</sub>) δ 171.0, 166.6, 156.8, 151.2, 147.9, 139.9, 139.1, 138.5, 132.3, 129.3, 129.1, 126.5, 124.6, 122.9, 115.6, 108.2, 62.1, 42.6, 41.1, 14.7; HRMS (ESI) calcd for  $C_{23}H_{23}F_3N_3O_2$  430.1737 (M + H)<sup>+</sup>, found 430.1734.

***N*-(2-Hydroxyethyl)-2-methoxy-3-((4-(3-(trifluoromethyl)benzyl)pyridin-2-yl)amino)benzamide (15c).** Compound **15c** (36 mg, 60%) was synthesized following the synthetic procedure of compound **10a** as a white solid. <sup>1</sup>H NMR (300 MHz, Chloroform-*d*) δ 8.16 (d,  $J = 5.2$  Hz, 1H), 8.05 (dt,  $J = 8.1, 3.1$  Hz, 2H), 7.61 (dd,  $J = 7.9, 1.6$  Hz, 1H), 7.54 – 7.37 (m, 4H), 7.16 (t,  $J = 8.0$  Hz, 1H), 6.96 (s, 1H), 6.63 (dd,  $J = 6.7, 1.4$  Hz, 2H), 3.97 (s, 2H), 3.82 (d,  $J = 8.3$  Hz, 5H), 3.65 (t,  $J = 5.0$  Hz, 2H); <sup>13</sup>C NMR (75 MHz, CDCl<sub>3</sub>) δ 166.4, 155.6, 150.9, 148.4, 147.9, 139.9, 134.2, 132.4, 129.2, 126.6, 125.6 (d,  $J = 3.7$  Hz), 124.9, 123.9, 123.6 (d,  $J = 3.8$  Hz), 122.7, 116.5, 109.6, 62.2, 61.7, 42.7, 41.0; HRMS (ESI) calcd for  $C_{23}H_{23}F_3N_3O_3$  446.1686 (M + H)<sup>+</sup>, found 446.1682.

**2-Cyclopropyl-*N*-(2-hydroxyethyl)-3-((4-(3-(trifluoromethyl)benzyl)pyridin-2-yl)amino)benzamide (15d).** Compound **15d** (42 mg, 69%) was synthesized following the synthetic procedure of compound **10a** as a white solid. <sup>1</sup>H NMR (300 MHz, Chloroform-*d*) δ 8.13

(d,  $J = 5.2$  Hz, 1H), 7.74 (dd,  $J = 8.2, 1.3$  Hz, 1H), 7.53 (d,  $J = 7.7$  Hz, 1H), 7.48 – 7.42 (m, 2H), 7.38 (d,  $J = 7.6$  Hz, 1H), 7.19 (t,  $J = 7.9$  Hz, 1H), 7.09 – 6.99 (m, 2H), 6.66 (d,  $J = 5.1$  Hz, 1H), 6.61 (dd,  $J = 5.2, 1.4$  Hz, 1H), 6.52 (t,  $J = 5.6$  Hz, 1H), 3.97 (d,  $J = 5.5$  Hz, 2H), 3.80 (t,  $J = 4.9$  Hz, 2H), 3.61 – 3.54 (m, 2H), 1.87 – 1.73 (m, 1H), 1.03 (dd,  $J = 8.3, 1.8$  Hz, 2H), 0.62 – 0.47 (m, 2H);  $^{13}\text{C}$  NMR (75 MHz,  $\text{CDCl}_3$ )  $\delta$  171.2, 155.8, 150.8, 148.4, 141.3, 139.9, 139.5, 132.4, 129.2, 128.6, 127.3, 125.6, 123.5, 121.2, 120.6, 116.3, 109.3, 62.1, 42.9, 41.1, 10.4, 7.2; HRMS (ESI) calcd for  $\text{C}_{25}\text{H}_{25}\text{F}_3\text{N}_3\text{O}_2$  456.1893 ( $\text{M} + \text{H}$ ) $^+$ , found 456.1890.

**2-(Furan-2-yl)-*N*-(2-hydroxyethyl)-3-((4-(3-(trifluoromethyl)benzyl)pyridin-2-yl)amino)benzamide (15e).** Compound **15e** (26 mg, 54%) was synthesized following the synthetic procedure of compound **10a** as a white solid.  $^1\text{H}$  NMR (300 MHz, Chloroform-*d*)  $\delta$  8.06 (d,  $J = 5.1$  Hz, 1H), 7.86 (d,  $J = 8.2$  Hz, 1H), 7.56 – 7.39 (m, 4H), 7.31 (dd,  $J = 19.7, 7.8$  Hz, 2H), 7.14 (d,  $J = 7.6$  Hz, 1H), 6.93 (s, 1H), 6.63 – 6.41 (m, 4H), 6.33 (t,  $J = 5.8$  Hz, 1H), 3.91 (s, 2H), 3.52 (d,  $J = 5.0$  Hz, 2H), 3.31 (d,  $J = 5.2$  Hz, 2H), 3.16 (s, 1H);  $^{13}\text{C}$  NMR (75 MHz,  $\text{CDCl}_3$ )  $\delta$  170.3, 155.6, 150.8, 148.4, 148.2, 143.2, 139.9, 139.3, 138.4, 131.0 (d,  $J = 31.9$  Hz), 129.2, 125.7 – 125.5 (m), 123.5 (d,  $J = 4.0$  Hz), 121.6, 121.3, 118.8, 116.6, 111.5, 111.0, 109.7, 61.6, 42.7, 41.0; HRMS (ESI) calcd for  $\text{C}_{26}\text{H}_{23}\text{F}_3\text{N}_3\text{O}_3$  482.1686 ( $\text{M} + \text{H}$ ) $^+$ , found 482.1686.

***N*-(2-Hydroxyethyl)-4-methyl-3-((4-(3-(trifluoromethyl)benzyl)pyridin-2-yl)amino)benzamide (15f).** Compound **15f** (37 mg, 86%) was synthesized following the synthetic procedure of compound **10a** as a white solid.  $^1\text{H}$  NMR (300 MHz, Chloroform-*d*)  $\delta$  8.04 (d,  $J = 5.3$  Hz, 1H), 7.88 (d,  $J = 1.9$  Hz, 1H), 7.57 – 7.30 (m, 5H), 7.20 (d,  $J = 7.9$  Hz, 1H), 6.98 (t,  $J = 5.6$  Hz, 1H), 6.72 (s, 1H), 6.53 (d,  $J = 5.3$  Hz, 1H), 6.41 (s, 1H), 4.31 (s, 1H), 3.89 (s, 2H), 3.75 (t,  $J = 5.0$  Hz, 2H), 3.55 (q,  $J = 5.2$  Hz, 2H), 2.23 (s, 3H);  $^{13}\text{C}$  NMR (75 MHz,  $\text{CDCl}_3$ )  $\delta$  168.3, 156.6, 151.1, 148.0, 139.9, 138.5, 134.9, 133.1, 132.3, 131.1, 129.1, 125.6 (d,  $J = 3.9$  Hz), 123.5 (d,  $J =$

3.7 Hz), 122.7, 121.4, 115.8, 108.6, 62.0, 42.9, 41.1, 18.0; HRMS (ESI) calcd for C<sub>23</sub>H<sub>23</sub>F<sub>3</sub>N<sub>3</sub>O<sub>2</sub> 430.1737 (M + H)<sup>+</sup>, found 430.1734.

***N*-(2-Hydroxyethyl)-4-methoxy-3-((4-(3-(trifluoromethyl)benzyl)pyridin-2-yl)amino)benzamide (15g).** Compound **15g** (36 mg, 41%) was synthesized following the synthetic procedure of compound **10a** as a white solid. <sup>1</sup>H NMR (300 MHz, Chloroform-*d*) δ 8.56 (d, *J* = 2.2 Hz, 1H), 8.10 (d, *J* = 5.2 Hz, 1H), 7.56 – 7.32 (m, 5H), 7.22 (t, *J* = 5.6 Hz, 1H), 7.02 (s, 1H), 6.81 (d, *J* = 8.5 Hz, 1H), 6.56 (d, *J* = 5.3 Hz, 2H), 3.92 (s, 3H), 3.85 (s, 3H), 3.75 (t, *J* = 4.9 Hz, 2H), 3.54 (d, *J* = 5.1 Hz, 2H); <sup>13</sup>C NMR (75 MHz, CDCl<sub>3</sub>) δ 168.7, 155.5, 150.7, 147.8, 139.9, 132.4, 130.9 (d, *J* = 32.4 Hz) 129.8, 129.1, 126.9, 125.6 (d, *J* = 3.8 Hz), 123.5 (d, *J* = 3.8 Hz), 121.2, 116.5, 116.2, 110.6, 109.6, 62.1, 55.8, 43.0, 41.0; HRMS (ESI) calcd for C<sub>23</sub>H<sub>23</sub>F<sub>3</sub>N<sub>3</sub>O<sub>3</sub> 446.1686 (M + H)<sup>+</sup>, found 446.1683.

**2-Fluoro-*N*-(2-hydroxyethyl)-5-((4-(3-(trifluoromethyl)benzyl)pyridin-2-yl)amino)benzamide (15h).** Compound **15h** (37 mg, 64%) was synthesized following the synthetic procedure of compound **10a** as a white solid. <sup>1</sup>H NMR (300 MHz, Chloroform-*d* and MeOD) δ 8.07 (d, *J* = 5.6 Hz, 1H), 7.88 (dd, *J* = 6.6, 2.9 Hz, 1H), 7.69 (ddd, *J* = 8.8, 4.3, 2.9 Hz, 1H), 7.50 (d, *J* = 7.7 Hz, 1H), 7.46 – 7.39 (m, 2H), 7.35 (d, *J* = 7.8 Hz, 1H), 7.31 – 7.20 (m, 2H), 7.00 (dd, *J* = 11.3, 8.9 Hz, 1H), 6.56 (dd, *J* = 3.9, 1.6 Hz, 2H), 3.91 (s, 2H), 3.80 (t, *J* = 5.1 Hz, 2H), 3.63 (d, *J* = 5.3 Hz, 2H); <sup>13</sup>C NMR (75 MHz, CDCl<sub>3</sub>) δ 164.4, 157.4, 156.0, 154.2, 150.8, 148.1, 139.9, 137.5, 132.4, 131.1, 129.1, 125.6 (d, *J* = 3.9 Hz), 124.5 (d, *J* = 8.6 Hz), 123.5 (d, *J* = 3.8 Hz), 122.6, 121.1 (d, *J* = 12.5 Hz), 116.7, 116.3, 116.1, 109.2, 61.8, 42.9, 41.0; HRMS (ESI) calcd for C<sub>22</sub>H<sub>20</sub>F<sub>4</sub>N<sub>3</sub>O<sub>2</sub> 434.1486 (M + H)<sup>+</sup>, found 434.1483.

**Methyl 4-((4-(3-(trifluoromethyl)benzyl)pyridin-2-yl)amino)benzoate (17).** Compound **17** (168 mg, 87%) was synthesized following the synthetic procedure of compound **8** as a white solid.

$^1\text{H}$  NMR (300 MHz, Chloroform-*d*)  $\delta$  8.26 – 8.17 (m, 1H), 8.04 – 7.94 (m, 2H), 7.61 – 7.33 (m, 6H), 6.80 – 6.64 (m, 3H), 4.00 (s, 2H), 3.91 (s, 3H).

**4-((4-(3-(Trifluoromethyl)benzyl)pyridin-2-yl)amino)benzoic acid (18).** Compound **18** (169 mg, 91%) was synthesized following the synthetic procedure of compound **9** as a white solid.  $^1\text{H}$  NMR (300 MHz, DMSO-*d*<sub>6</sub>)  $\delta$  10.03 (s, 1H), 8.10 (d,  $J = 5.7$  Hz, 1H), 7.96 – 7.84 (m, 2H), 7.76 – 7.50 (m, 6H), 6.89 (dd,  $J = 7.5, 2.0$  Hz, 2H), 4.11 (s, 2H).

***N*-(2-Hydroxyethyl)-4-((4-(3-(trifluoromethyl)benzyl)pyridin-2-yl)amino)benzamide (19).** Compound **19** (43 mg, 77%) was synthesized following the synthetic procedure of compound **10a** as a white solid.  $^1\text{H}$  NMR (300 MHz, Chloroform-*d* and MeoD)  $\delta$  8.03 (dd,  $J = 5.1, 2.3$  Hz, 1H), 7.67 (dd,  $J = 8.8, 2.5$  Hz, 2H), 7.50 – 7.25 (m, 7H), 6.71 – 6.50 (m, 2H), 3.90 (d,  $J = 2.3$  Hz, 2H), 3.68 (d,  $J = 2.4$  Hz, 2H), 3.50 – 3.44 (m, 2H);  $^{13}\text{C}$  NMR (75 MHz, CDCl<sub>3</sub> and MeoD)  $\delta$  168.6, 155.3, 151.1, 147.8, 144.0, 139.8, 132.4, 129.1, 128.3, 126.5, 125.5 (d,  $J = 3.8$  Hz), 123.5 (d,  $J = 3.5$  Hz), 117.7, 116.5, 110.4, 61.3, 42.5, 40.9; HRMS (ESI) calcd for C<sub>22</sub>H<sub>21</sub>F<sub>3</sub>N<sub>3</sub>O<sub>2</sub> 416.1580 (M + H)<sup>+</sup>, found 416.1576.

**4-(3,5-Bis(trifluoromethyl)benzyl)-2-chloropyridine (21a).** Compound **21a** (540 mg, 80%) was synthesized following the synthetic procedure of compound **7** as a colorless oil.  $^1\text{H}$  NMR (300 MHz, Chloroform-*d*)  $\delta$  8.37 (d,  $J = 5.1$  Hz, 1H), 7.83 (s, 1H), 7.64 (s, 2H), 7.17 (s, 1H), 7.08 – 6.96 (m, 1H), 4.11 (s, 2H).

**4-(2,4-Bis(trifluoromethyl)benzyl)-2-chloropyridine (21b).** Compound **21b** (260 mg, 77%) was synthesized following the synthetic procedure of compound **7** as a colorless oil.  $^1\text{H}$  NMR (300 MHz, Chloroform-*d*)  $\delta$  8.34 (d,  $J = 5.1$  Hz, 1H), 8.00 (s, 1H), 7.80 (d,  $J = 8.1$  Hz, 1H), 7.37 (d,  $J = 8.1$  Hz, 1H), 7.10 (s, 1H), 6.99 (d,  $J = 5.1$  Hz, 1H), 4.24 (s, 2H).

**2-Chloro-4-(4-(trifluoromethyl)benzyl)pyridine (21c).** Compound **21c** (81 mg, 75%) was synthesized following the synthetic procedure of compound **7** as a colorless oil.  $^1\text{H}$  NMR (300 MHz, Chloroform-*d*)  $\delta$  8.34 – 8.27 (m, 1H), 7.61 (d,  $J = 8.0$  Hz, 2H), 7.31 (d,  $J = 8.0$  Hz, 2H), 7.15 (dd,  $J = 1.6, 0.7$  Hz, 1H), 7.08 – 7.00 (m, 1H), 4.04 (s, 2H).

**2-Chloro-4-(2-(trifluoromethyl)benzyl)pyridine (21d).** Compound **21d** (64 mg, 79%) was synthesized following the synthetic procedure of compound **7** as a colorless oil.  $^1\text{H}$  NMR (300 MHz, Chloroform-*d*)  $\delta$  8.29 (d,  $J = 5.1$  Hz, 1H), 7.73 (dd,  $J = 7.9, 1.4$  Hz, 1H), 7.54 (td,  $J = 7.6, 1.4$  Hz, 1H), 7.42 (t,  $J = 7.6$  Hz, 1H), 7.22 (d,  $J = 7.7$  Hz, 1H), 7.12 – 7.05 (m, 1H), 6.99 (dd,  $J = 5.1, 1.5$  Hz, 1H), 4.18 (s, 2H).

**2-Chloro-4-(3-chloro-5-fluorobenzyl)pyridine (21e).** Compound **21e** (70 mg, 91%) was synthesized following the synthetic procedure of compound **7** as a colorless oil.  $^1\text{H}$  NMR (300 MHz, Chloroform-*d*)  $\delta$  8.33 (d,  $J = 5.1$  Hz, 1H), 7.14 (dd,  $J = 1.6, 0.7$  Hz, 1H), 7.08 – 6.94 (m, 3H), 6.79 (dt,  $J = 8.9, 1.9$  Hz, 1H), 3.93 (s, 2H).

**2-Chloro-4-(3-methoxybenzyl)pyridine (21f).** Compound **21f** (60 mg, 86%) was synthesized following the synthetic procedure of compound **7** as a colorless oil.  $^1\text{H}$  NMR (300 MHz, Chloroform-*d*)  $\delta$  8.28 (d,  $J = 5.1$  Hz, 1H), 7.32 – 7.25 (m, 1H), 7.20 – 7.14 (m, 1H), 7.05 (dd,  $J = 5.1, 1.4$  Hz, 1H), 6.90 – 6.68 (m, 3H), 3.94 (s, 2H), 3.81 (s, 3H).

**4-Benzyl-2-chloropyridine (21g).** Compound **21g** (53 mg, 87%) was synthesized following the synthetic procedure of compound **7** as a colorless oil.  $^1\text{H}$  NMR (300 MHz, Chloroform-*d*)  $\delta$  8.28 (d,  $J = 5.1$  Hz, 1H), 7.40 – 7.26 (m, 3H), 7.23 – 7.12 (m, 3H), 7.05 (dd,  $J = 5.1, 1.4$  Hz, 1H), 3.97 (s, 2H).

**2-Chloro-4-(4-chloro-2-fluorobenzyl)pyridine (21h).** Compound **21h** (59 mg, 77%) was synthesized following the synthetic procedure of compound **7** as a colorless oil.  $^1\text{H}$  NMR (300

MHz, Chloroform-*d*)  $\delta$  8.29 (d,  $J = 5.1$  Hz, 1H), 7.18 – 7.09 (m, 4H), 7.04 (dd,  $J = 5.1, 1.4$  Hz, 1H), 3.95 (d,  $J = 1.3$  Hz, 2H).

**2-Chloro-4-(3-fluorobenzyl)pyridine (21i).** Compound **21i** (54 mg, 80%) was synthesized following the synthetic procedure of compound **7** as a colorless oil.  $^1\text{H}$  NMR (300 MHz, Chloroform-*d*)  $\delta$  8.30 (d,  $J = 5.1$  Hz, 1H), 7.37 – 7.27 (m, 1H), 7.17 – 7.12 (m, 1H), 7.08 – 6.93 (m, 3H), 6.88 (dt,  $J = 9.6, 2.1$  Hz, 1H), 3.96 (s, 2H).

**2-Chloro-4-(4-fluorobenzyl)pyridine (21j).** Compound **21j** (35 mg, 53%) was synthesized following the synthetic procedure of compound **7** as a colorless oil.  $^1\text{H}$  NMR (300 MHz, Chloroform-*d*)  $\delta$  8.29 (d,  $J = 5.1$  Hz, 1H), 7.20 – 7.10 (m, 3H), 7.09 – 6.98 (m, 3H), 3.95 (s, 2H).

**2-Chloro-4-(3-(trifluoromethoxy)benzyl)pyridine (21k).** Compound **21k** (80 mg, 93%) was synthesized following the synthetic procedure of compound **7** as a colorless oil.  $^1\text{H}$  NMR (300 MHz, Chloroform-*d*)  $\delta$  8.31 (d,  $J = 5.1$  Hz, 1H), 7.38 (t,  $J = 7.9$  Hz, 1H), 7.19 – 7.08 (m, 3H), 7.04 (dd,  $J = 5.1, 1.5$  Hz, 2H), 3.99 (s, 2H).

**Methyl 3-((4-(3,5-bis(trifluoromethyl)benzyl)pyridin-2-yl)amino)-2-methylbenzoate (22a).** Compound **22a** (110 mg, 79%) was synthesized following the synthetic procedure of compound **8** as a colorless oil.  $^1\text{H}$  NMR (300 MHz, Chloroform-*d*)  $\delta$  8.15 (d,  $J = 5.2$  Hz, 1H), 7.77 (s, 1H), 7.69 (s, 1H), 7.62 (s, 2H), 7.55 (d,  $J = 8.0$  Hz, 1H), 7.24 (d,  $J = 8.1$  Hz, 1H), 6.54 (d,  $J = 5.3$  Hz, 1H), 6.34 (s, 2H), 3.97 (s, 2H), 3.93 (s, 3H), 2.47 (s, 3H).

**Methyl 3-((4-(2,4-bis(trifluoromethyl)benzyl)pyridin-2-yl)amino)-2-methylbenzoate (22b).** Compound **22b** (91 mg, 65%) was synthesized following the synthetic procedure of compound **8** as a colorless oil.  $^1\text{H}$  NMR (300 MHz, Chloroform-*d*)  $\delta$  8.13 (d,  $J = 5.2$  Hz, 1H), 7.66 (dd,  $J = 7.8, 1.3$  Hz, 1H), 7.56 (dd,  $J = 8.2, 1.3$  Hz, 1H), 7.26 – 7.20 (m, 3H), 7.05 (d,  $J = 11.4$  Hz,

1H), 6.55 (dd,  $J = 5.2, 1.4$  Hz, 1H), 6.34 (d,  $J = 5.0$  Hz, 2H), 3.93 (s, 3H), 3.90 (s, 2H), 2.47 (s, 3H).

**Methyl 2-methyl-3-((4-(4-(trifluoromethyl)benzyl)pyridin-2-yl)amino)benzoate (22c).**

Compound **22c** (88 mg, 73%) was synthesized following the synthetic procedure of compound **8** as a colorless oil.  $^1\text{H}$  NMR (300 MHz, Chloroform-*d*)  $\delta$  8.11 (d,  $J = 5.2$  Hz, 1H), 7.65 (dd,  $J = 7.8, 1.3$  Hz, 1H), 7.61 – 7.52 (m, 3H), 7.34 – 7.20 (m, 4H), 6.55 (dd,  $J = 5.2, 1.4$  Hz, 1H), 6.36 (s, 1H), 6.32 (s, 1H), 3.93 (s, 3H), 3.91 (s, 2H), 2.47 (s, 3H).

**Methyl 2-methyl-3-((4-(2-(trifluoromethyl)benzyl)pyridin-2-yl)amino)benzoate (22d).**

Compound **22d** (86 mg, 72%) was synthesized following the synthetic procedure of compound **8** as a colorless oil.  $^1\text{H}$  NMR (300 MHz, Chloroform-*d*)  $\delta$  8.10 (d,  $J = 5.2$  Hz, 1H), 7.73 – 7.55 (m, 3H), 7.47 (d,  $J = 7.5$  Hz, 1H), 7.37 (d,  $J = 7.6$  Hz, 1H), 7.26 – 7.17 (m, 2H), 6.52 (d,  $J = 5.2$  Hz, 1H), 6.37 (s, 1H), 6.27 (s, 1H), 4.07 (s, 2H), 3.93 (s, 3H), 2.47 (s, 3H).

**Methyl 3-((4-(3-chloro-5-fluorobenzyl)pyridin-2-yl)amino)-2-methylbenzoate (22e).**

Compound **22e** (85 mg, 74%) was synthesized following the synthetic procedure of compound **8** as a colorless oil.  $^1\text{H}$  NMR (300 MHz, Chloroform-*d*)  $\delta$  8.12 (d,  $J = 5.2$  Hz, 1H), 7.66 (dd,  $J = 7.8, 1.3$  Hz, 1H), 7.58 (dd,  $J = 8.0, 1.3$  Hz, 1H), 7.28 (d,  $J = 4.1$  Hz, 1H), 6.98 (dd,  $J = 7.6, 2.0$  Hz, 2H), 6.77 (dt,  $J = 9.4, 2.0$  Hz, 1H), 6.55 (dd,  $J = 5.2, 1.4$  Hz, 1H), 6.40 – 6.28 (m, 2H), 3.93 (s, 3H), 3.81 (s, 2H), 2.48 (s, 3H).

**Methyl 3-((4-(3-methoxybenzyl)pyridin-2-yl)amino)-2-methylbenzoate (22f).** Compound **22f** (48 mg, 67%) was synthesized following the synthetic procedure of compound **8** as a colorless oil.  $^1\text{H}$  NMR (300 MHz, Chloroform-*d*)  $\delta$  8.09 (d,  $J = 5.2$  Hz, 1H), 7.61 (td,  $J = 8.2, 1.3$  Hz, 2H), 7.24 (td,  $J = 7.8, 3.9$  Hz, 2H), 6.78 (ddd,  $J = 7.4, 5.6, 2.0$  Hz, 2H), 6.71 (t,  $J = 2.1$  Hz, 1H), 6.59

(dd,  $J = 5.2, 1.4$  Hz, 1H), 6.43 (s, 1H), 6.28 (s, 1H), 3.93 (s, 3H), 3.83 (s, 2H), 3.80 (s, 3H), 2.47 (s, 3H).

**Methyl 3-((4-benzylpyridin-2-yl)amino)-2-methylbenzoate (22g).** Compound **22g** (72 mg, 72%) was synthesized following the synthetic procedure of compound **8** as a colorless oil.  $^1\text{H}$  NMR (300 MHz, Chloroform-*d*)  $\delta$  8.09 (d,  $J = 5.2$  Hz, 1H), 7.61 (ddd,  $J = 10.4, 8.1, 1.3$  Hz, 2H), 7.37 – 7.21 (m, 4H), 7.20 – 7.13 (m, 2H), 6.58 (dd,  $J = 5.2, 1.3$  Hz, 1H), 6.46 – 6.39 (m, 1H), 6.28 (s, 1H), 3.93 (s, 3H), 3.86 (s, 2H), 2.47 (s, 3H).

**Methyl 3-((4-(4-chloro-2-fluorobenzyl)pyridin-2-yl)amino)-2-methylbenzoate (22h).** Compound **22h** (61 mg, 80%) was synthesized following the synthetic procedure of compound **8** as a colorless oil.  $^1\text{H}$  NMR (300 MHz, Chloroform-*d*)  $\delta$  8.10 (d,  $J = 5.2$  Hz, 1H), 7.65 (dd,  $J = 7.7, 1.4$  Hz, 1H), 7.58 (dd,  $J = 8.0, 1.3$  Hz, 1H), 7.24 (d,  $J = 7.9$  Hz, 1H), 7.11 – 7.03 (m, 3H), 6.56 (dd,  $J = 5.2, 1.4$  Hz, 1H), 6.40 (s, 1H), 6.30 (s, 1H), 3.93 (s, 3H), 3.83 (s, 2H), 2.47 (s, 3H).

**Methyl 3-((4-(3-fluorobenzyl)pyridin-2-yl)amino)-2-methylbenzoate (22i).** Compound **22i** (54 mg, 77%) was synthesized following the synthetic procedure of compound **8** as a colorless oil.  $^1\text{H}$  NMR (300 MHz, Chloroform-*d*)  $\delta$  8.11 (d,  $J = 5.2$  Hz, 1H), 7.64 (dd,  $J = 7.9, 1.3$  Hz, 1H), 7.61 – 7.56 (m, 1H), 7.28 – 7.21 (m, 2H), 6.95 (dd,  $J = 8.0, 2.0$  Hz, 2H), 6.87 (d,  $J = 9.6$  Hz, 1H), 6.57 (dd,  $J = 5.2, 1.4$  Hz, 1H), 6.40 (s, 1H), 6.29 (s, 1H), 3.93 (s, 3H), 3.84 (s, 2H), 2.47 (s, 3H).

**Methyl 3-((4-(4-fluorobenzyl)pyridin-2-yl)amino)-2-methylbenzoate (22j).** Compound **22j** (58 mg, 83%) was synthesized following the synthetic procedure of compound **8** as a colorless oil.  $^1\text{H}$  NMR (300 MHz, Chloroform-*d*)  $\delta$  8.09 (d,  $J = 5.2$  Hz, 1H), 7.64 (dd,  $J = 7.8, 1.3$  Hz, 1H), 7.57 (dd,  $J = 8.0, 1.3$  Hz, 1H), 7.24 (d,  $J = 7.8$  Hz, 1H), 7.12 (dd,  $J = 8.5, 5.5$  Hz, 2H), 7.00 (t,  $J = 8.7$  Hz, 2H), 6.55 (dd,  $J = 5.2, 1.4$  Hz, 1H), 6.36 (d,  $J = 8.6$  Hz, 2H), 3.93 (s, 3H), 3.82 (s, 2H), 2.46 (s, 3H).

**Methyl 2-methyl-3-((4-(3-(trifluoromethoxy)benzyl)pyridin-2-yl)amino)benzoate (22k).**

Compound **22k** (68 mg, 82%) was synthesized following the synthetic procedure of compound **8** as a colorless oil. <sup>1</sup>H NMR (300 MHz, Chloroform-*d*) δ 8.09 (d, *J* = 5.2 Hz, 1H), 7.64 (dd, *J* = 7.8, 1.3 Hz, 1H), 7.56 (dd, *J* = 7.9, 1.4 Hz, 1H), 7.32 (dd, *J* = 7.8, 3.6 Hz, 1H), 7.23 (d, *J* = 7.7 Hz, 1H), 7.11 – 7.07 (m, 2H), 7.02 (s, 1H), 6.55 (dd, *J* = 5.3, 1.4 Hz, 2H), 6.37 (s, 1H), 3.92 (s, 3H), 3.86 (s, 2H), 2.46 (s, 3H).

**3-((4-(3,5-Bis(trifluoromethyl)benzyl)pyridin-2-yl)amino)-2-methylbenzoic acid (23a).**

Compound **23a** (76 mg, 84%) was synthesized following the synthetic procedure of compound **9** as a white solid. <sup>1</sup>H NMR (300 MHz, DMSO-*d*<sub>6</sub>) δ 10.55 (s, 1H), 8.01 (d, *J* = 11.6 Hz, 2H), 7.92 – 7.88 (m, 1H), 7.82 – 7.78 (m, 1H), 7.57 – 7.52 (m, 2H), 7.42 (d, *J* = 7.7 Hz, 1H), 6.98 – 6.93 (m, 2H), 4.29 (s, 2H), 2.36 (s, 3H).

**3-((4-(2,4-Bis(trifluoromethyl)benzyl)pyridin-2-yl)amino)-2-methylbenzoic acid (23b).**

Compound **23b** (78 mg, 86%) was synthesized following the synthetic procedure of compound **9** as a white solid. <sup>1</sup>H NMR (300 MHz, DMSO-*d*<sub>6</sub>) δ 10.69 (d, *J* = 4.5 Hz, 1H), 7.91 (dd, *J* = 6.5, 4.5 Hz, 1H), 7.80 (ddd, *J* = 7.8, 4.1, 1.4 Hz, 1H), 7.66 – 7.54 (m, 4H), 7.47 – 7.40 (m, 1H), 7.00 – 6.88 (m, 2H), 4.19 (s, 2H), 2.38 (s, 3H).

**2-Methyl-3-((4-(4-(trifluoromethyl)benzyl)pyridin-2-yl)amino)benzoic acid (23c).**

Compound **23c** (70 mg, 91%) was synthesized following the synthetic procedure of compound **9** as a white solid. <sup>1</sup>H NMR (300 MHz, DMSO-*d*<sub>6</sub>) δ 13.14 (s, 1H), 10.63 (s, 1H), 7.89 (dd, *J* = 6.5, 4.3 Hz, 1H), 7.83 – 7.69 (m, 3H), 7.56 (ddd, *J* = 13.2, 8.0, 1.4 Hz, 3H), 7.42 (q, *J* = 7.5 Hz, 1H), 7.00 – 6.83 (m, 2H), 4.17 (s, 2H), 2.37 (s, 3H).

**2-Methyl-3-((4-(2-(trifluoromethyl)benzyl)pyridin-2-yl)amino)benzoic acid (23d).**

Compound **23d** (59 mg, 76%) was synthesized following the synthetic procedure of compound **9**

as a white solid.  $^1\text{H}$  NMR (300 MHz,  $\text{DMSO-}d_6$ )  $\delta$  13.04 (s, 1H), 10.27 (s, 1H), 7.87 (d,  $J = 6.4$  Hz, 1H), 7.83 – 7.66 (m, 3H), 7.61 – 7.47 (m, 3H), 7.39 (t,  $J = 7.8$  Hz, 1H), 6.79 (dd,  $J = 6.5, 1.6$  Hz, 1H), 6.68 (s, 1H), 4.26 (s, 2H), 2.34 (s, 3H).

**3-((4-(3-Chloro-5-fluorobenzyl)pyridin-2-yl)amino)-2-methylbenzoic acid (23e).**

Compound **23e** (58 mg, 78%) was synthesized following the synthetic procedure of compound **9** as a white solid.  $^1\text{H}$  NMR (300 MHz,  $\text{DMSO-}d_6$ )  $\delta$  13.11 (s, 1H), 10.51 (s, 1H), 7.88 (dd,  $J = 6.5, 4.5$  Hz, 1H), 7.80 (dd,  $J = 7.8, 1.4$  Hz, 1H), 7.56 (dd,  $J = 7.9, 1.4$  Hz, 1H), 7.47 – 7.29 (m, 3H), 7.24 (dt,  $J = 9.6, 1.8$  Hz, 1H), 6.98 – 6.85 (m, 2H), 4.08 (s, 2H), 2.38 (s, 3H).

**3-((4-(3-Methoxybenzyl)pyridin-2-yl)amino)-2-methylbenzoic acid (23f).** Compound **23f** (58 mg, 83%) was synthesized following the synthetic procedure of compound **9** as a white solid.  $^1\text{H}$  NMR (300 MHz,  $\text{DMSO-}d_6$ )  $\delta$  10.58 (s, 1H), 7.83 (td,  $J = 7.6, 7.1, 2.1$  Hz, 2H), 7.54 (dd,  $J = 7.9, 1.5$  Hz, 1H), 7.42 (t,  $J = 7.8$  Hz, 1H), 7.27 (t,  $J = 7.8$  Hz, 1H), 6.95 – 6.78 (m, 4H), 6.68 (dd,  $J = 4.5, 1.9$  Hz, 1H), 4.02 (s, 2H), 3.75 (s, 3H), 2.37 (s, 3H).

**3-((4-(4-Benzylpyridin-2-yl)amino)-2-methylbenzoic acid (23g).** Compound **23g** (59 mg, 93%) was synthesized following the synthetic procedure of compound **9** as a white solid.  $^1\text{H}$  NMR (300 MHz,  $\text{DMSO-}d_6$ )  $\delta$  13.02 (s, 1H), 10.65 (s, 1H), 7.87 (dd,  $J = 6.5, 4.0$  Hz, 1H), 7.79 (ddd,  $J = 6.1, 4.8, 1.4$  Hz, 1H), 7.61 – 7.52 (m, 1H), 7.44 – 7.25 (m, 6H), 6.95 (d,  $J = 1.6$  Hz, 1H), 6.87 (dt,  $J = 6.5, 1.7$  Hz, 1H), 4.05 (s, 2H), 2.37 (s, 3H).

**3-((4-(4-Chloro-2-fluorobenzyl)pyridin-2-yl)amino)-2-methylbenzoic acid (23h).**

Compound **23h** (54 mg, 73%) was synthesized following the synthetic procedure of compound **9** as a white solid.  $^1\text{H}$  NMR (300 MHz,  $\text{DMSO-}d_6$ )  $\delta$  13.14 (s, 1H), 10.29 (s, 1H), 7.82 (dd,  $J = 18.5, 7.1$  Hz, 2H), 7.57 – 7.32 (m, 5H), 6.91 – 6.77 (m, 2H), 4.09 (s, 2H), 2.36 (s, 3H).

**3-((4-(3-Fluorobenzyl)pyridin-2-yl)amino)-2-methylbenzoic acid (23i).** Compound **23i** (59 mg, 88%) was synthesized following the synthetic procedure of compound **9** as a white solid. <sup>1</sup>H NMR (300 MHz, DMSO-*d*<sub>6</sub>) δ 13.06 (s, 1H), 10.52 (s, 1H), 7.92 – 7.76 (m, 2H), 7.55 (dd, *J* = 7.9, 1.4 Hz, 1H), 7.47 – 7.35 (m, 2H), 7.24 – 7.06 (m, 3H), 6.97 – 6.83 (m, 2H), 4.08 (s, 2H), 2.37 (s, 3H).

**3-((4-(4-Fluorobenzyl)pyridin-2-yl)amino)-2-methylbenzoic acid (23j).** Compound **23j** (53 mg, 79%) was synthesized following the synthetic procedure of compound **9** as a white solid. <sup>1</sup>H NMR (300 MHz, DMSO-*d*<sub>6</sub>) δ 13.00 (s, 1H), 10.44 (s, 1H), 7.92 – 7.73 (m, 2H), 7.54 (dd, *J* = 7.9, 1.4 Hz, 1H), 7.46 – 7.32 (m, 3H), 7.24 – 7.13 (m, 2H), 6.87 (d, *J* = 7.3 Hz, 2H), 4.05 (s, 2H), 2.36 (s, 3H).

**2-Methyl-3-((4-(3-(trifluoromethoxy)benzyl)pyridin-2-yl)amino)benzoic acid (23k).** Compound **23k** (68 mg, 85%) was synthesized following the synthetic procedure of compound **9** as a white solid. <sup>1</sup>H NMR (300 MHz, DMSO-*d*<sub>6</sub>) δ 13.04 (s, 1H), 10.42 (s, 1H), 7.90 – 7.77 (m, 2H), 7.58 – 7.47 (m, 2H), 7.43 – 7.34 (m, 3H), 7.28 (d, *J* = 8.2 Hz, 1H), 6.90 (d, *J* = 6.5 Hz, 2H), 4.13 (s, 2H), 2.37 (s, 3H).

**3-((4-(3,5-Bis(trifluoromethyl)benzyl)pyridin-2-yl)amino)-N-(2-hydroxyethyl)-2-methylbenzamide (24a).** Compound **24a** (68 mg, 68%) was synthesized following the synthetic procedure of compound **10a** as a white solid. <sup>1</sup>H NMR (300 MHz, Chloroform-*d* and MeOD) δ 7.98 (d, *J* = 5.3 Hz, 1H), 7.75 (s, 1H), 7.61 (s, 2H), 7.34 (t, *J* = 4.7 Hz, 1H), 7.15 (d, *J* = 4.6 Hz, 2H), 6.49 (dd, *J* = 5.3, 1.4 Hz, 1H), 6.44 (s, 1H), 3.95 (s, 2H), 3.71 (t, *J* = 5.1 Hz, 2H), 3.50 (t, *J* = 5.3 Hz, 2H), 2.23 (s, 3H); <sup>13</sup>C NMR (75 MHz, CDCl<sub>3</sub> and MeOD) δ 171.4, 171.3, 166.6, 157.1, 149.9, 148.3, 141.5, 138.8, 138.5, 132.1, 131.6, 130.0, 129.3, 129.0, 126.4, 125.2, 125.0, 123.3,

121.4, 120.7, 115.2, 108.4, 61.3, 42.4, 40.8, 14.7; HRMS (ESI) calcd for C<sub>24</sub>H<sub>22</sub>F<sub>6</sub>N<sub>3</sub>O<sub>2</sub> 498.1611 (M + H)<sup>+</sup>, found 498.1609.

**3-((4-(2,4-Bis(trifluoromethyl)benzyl)pyridin-2-yl)amino)-N-(2-hydroxyethyl)-2-methylbenzamide (24b).** Compound **24b** (50 mg, 75%) was synthesized following the synthetic procedure of compound **10a** as a white solid. <sup>1</sup>H NMR (300 MHz, Chloroform-*d*) δ 7.99 (d, *J* = 5.2 Hz, 1H), 7.37 (dd, *J* = 6.7, 2.6 Hz, 1H), 7.26 – 7.16 (m, 2H), 7.14 – 7.00 (m, 3H), 6.90 (t, *J* = 5.6 Hz, 1H), 6.71 (s, 1H), 6.50 (dd, *J* = 5.3, 1.4 Hz, 1H), 6.44 (s, 1H), 3.87 (s, 2H), 3.69 (t, *J* = 5.0 Hz, 2H), 3.48 (d, *J* = 5.2 Hz, 2H), 3.23 (s, 1H), 2.21 (s, 3H); <sup>13</sup>C NMR (75 MHz, CDCl<sub>3</sub>) δ 171.1, 164.2, 160.9, 157.0, 150.1, 148.3, 142.8 (d, *J* = 7.4 Hz), 139.0, 138.5, 129.4, 126.4, 124.7, 123.0, 121.5 – 121.4 (m), 119.4 (d, *J* = 20.9 Hz), 115.5, 111.10 (d, *J* = 24.7 Hz), 108.4, 61.5, 42.5, 40.8, 14.7; HRMS (ESI) calcd for C<sub>24</sub>H<sub>22</sub>F<sub>6</sub>N<sub>3</sub>O<sub>2</sub> 498.1611 (M + H)<sup>+</sup>, found 498.1609.

**N-(2-Hydroxyethyl)-2-methyl-3-((4-(4-(trifluoromethyl)benzyl)pyridin-2-yl)amino)benzamide (24c).** Compound **24c** (54 mg, 93%) was synthesized following the synthetic procedure of compound **10a** as a white solid. <sup>1</sup>H NMR (300 MHz, Chloroform-*d* and MeOD) δ 7.92 (d, *J* = 5.3 Hz, 1H), 7.53 (d, *J* = 8.0 Hz, 2H), 7.34 – 7.23 (m, 3H), 7.17 – 7.07 (m, 2H), 6.49 (dd, *J* = 5.3, 1.4 Hz, 1H), 6.43 (s, 1H), 3.87 (s, 2H), 3.69 (t, *J* = 5.2 Hz, 2H), 3.48 (t, *J* = 5.1 Hz, 2H), 2.21 (s, 3H); <sup>13</sup>C NMR (75 MHz, CDCl<sub>3</sub> and MeOD) δ 171.4, 156.9, 151.2, 147.8, 143.1, 138.9, 138.4, 129.8, 129.3, 129.1, 128.7, 126.3, 125.9, 125.5 (q, *J* = 3.8 Hz), 125.1, 123.2, 115.5, 108.6, 61.2, 42.5, 42.3, 41.0, 14.7; HRMS (ESI) calcd for C<sub>23</sub>H<sub>23</sub>F<sub>3</sub>N<sub>3</sub>O<sub>2</sub> 430.1737 (M + H)<sup>+</sup>, found 430.1735.

**N-(2-Hydroxyethyl)-2-methyl-3-((4-(2-(trifluoromethyl)benzyl)pyridin-2-yl)amino)benzamide (24d).** Compound **24d** (67 mg, 78%) was synthesized following the synthetic procedure of compound **10a** as a white solid. <sup>1</sup>H NMR (300 MHz, Chloroform-*d*) δ 7.93

(d,  $J = 5.3$  Hz, 1H), 7.66 (dd,  $J = 7.9, 1.4$  Hz, 1H), 7.50 – 7.42 (m, 1H), 7.34 (dd,  $J = 8.5, 6.2$  Hz, 2H), 7.19 (d,  $J = 7.7$  Hz, 1H), 7.11 – 6.96 (m, 3H), 6.72 (s, 1H), 6.50 – 6.37 (m, 2H), 4.03 (s, 2H), 3.64 (t,  $J = 5.1$  Hz, 3H), 3.44 (t,  $J = 5.2$  Hz, 2H), 2.17 (s, 3H);  $^{13}\text{C}$  NMR (75 MHz,  $\text{CDCl}_3$ )  $\delta$  171.2, 156.7, 151.1, 147.7, 139.1, 138.4, 137.1, 132.0, 131.8, 129.0, 128.6, 126.8, 126.3, 126.2, 126.1 (q,  $J = 5.8, 5.3$  Hz), 124.3, 122.7, 115.7, 108.9, 61.4, 42.5, 37.5, 37.4, 14.7; HRMS (ESI) calcd for  $\text{C}_{23}\text{H}_{23}\text{F}_3\text{N}_3\text{O}_2$  430.1737 ( $\text{M} + \text{H}$ ) $^+$ , found 430.1735.

**3-((4-(3-Chloro-5-fluorobenzyl)pyridin-2-yl)amino)-N-(2-hydroxyethyl)-2-methylbenzamide (24e).** Compound **24e** (55 mg, 66%) was synthesized following the synthetic procedure of compound **10a** as a white solid.  $^1\text{H}$  NMR (300 MHz, Chloroform- $d$ )  $\delta$  7.94 (d,  $J = 5.3$  Hz, 1H), 7.34 (dd,  $J = 7.0, 2.3$  Hz, 1H), 7.14 – 7.02 (m, 3H), 6.94 (dp,  $J = 4.4, 2.0$  Hz, 2H), 6.87 – 6.70 (m, 2H), 6.52 – 6.39 (m, 2H), 3.76 (s, 2H), 3.64 (t,  $J = 5.1$  Hz, 3H), 3.43 (q,  $J = 5.0$  Hz, 2H), 2.18 (s, 3H);  $^{13}\text{C}$  NMR (75 MHz,  $\text{CDCl}_3$ )  $\delta$  171.2, 166.6, 164.3, 161.0, 156.9, 150.4, 148.1, 142.7 (d,  $J = 8.2$  Hz), 139.1, 138.4, 135.0 (d,  $J = 10.8$  Hz), 129.4, 126.4, 125.0 (d,  $J = 3.1$  Hz), 124.7, 122.9, 115.5, 114.6 (d,  $J = 6.4$  Hz), 114.3 (d,  $J = 3.2$  Hz), 108.6, 61.3, 42.5, 40.7, 14.8; HRMS (ESI) calcd for  $\text{C}_{22}\text{H}_{22}\text{ClFN}_3\text{O}_2$  414.1379 ( $\text{M} + \text{H}$ ) $^+$ , found 414.1377.

**N-(2-Hydroxyethyl)-3-((4-(3-methoxybenzyl)pyridin-2-yl)amino)-2-methylbenzamide (24f).** Compound **24f** (20 mg, 38%) was synthesized following the synthetic procedure of compound **10a** as a white solid.  $^1\text{H}$  NMR (300 MHz, Chloroform- $d$ )  $\delta$  8.00 (s, 1H), 7.41 (t,  $J = 5.4$  Hz, 1H), 7.31 – 6.92 (m, 4H), 6.80 – 6.41 (m, 6H), 3.97 – 3.62 (m, 7H), 3.52 (t,  $J = 5.2$  Hz, 2H), 3.05 (s, 1H), 2.24 (d,  $J = 3.9$  Hz, 3H);  $^{13}\text{C}$  NMR (75 MHz,  $\text{CDCl}_3$ )  $\delta$  171.1, 159.8, 156.5, 152.1, 147.8, 140.5, 139.2, 138.4, 129.6, 128.9, 126.4, 124.2, 122.6, 121.4, 116.0, 114.9, 111.7, 108.6, 61.9, 55.2, 42.6, 41.4, 14.7; HRMS (ESI) calcd for  $\text{C}_{23}\text{H}_{26}\text{N}_3\text{O}_3$  392.1969 ( $\text{M} + \text{H}$ ) $^+$ , found 392.1964.

**3-((4-Benzylpyridin-2-yl)amino)-N-(2-hydroxyethyl)-2-methylbenzamide (24g).**

Compound **24g** (37 mg, 77%) was synthesized following the synthetic procedure of compound **10a** as a white solid.  $^1\text{H}$  NMR (300 MHz, Chloroform-*d*)  $\delta$  7.94 (d,  $J$  = 5.3 Hz, 1H), 7.35 (dd,  $J$  = 7.1, 2.2 Hz, 1H), 7.33 – 7.27 (m, 2H), 7.26 – 7.20 (m, 1H), 7.19 – 7.13 (m, 2H), 7.12 – 7.04 (m, 2H), 6.96 (t,  $J$  = 5.6 Hz, 1H), 6.54 (dd,  $J$  = 5.3, 1.3 Hz, 2H), 6.47 (s, 1H), 3.83 (s, 2H), 3.66 (t,  $J$  = 5.0 Hz, 2H), 3.45 (d,  $J$  = 5.2 Hz, 3H);  $^{13}\text{C}$  NMR (75 MHz,  $\text{CDCl}_3$ )  $\delta$  171.2, 156.6, 152.2, 147.7, 139.2, 139.0, 138.4, 129.0, 129.0, 128.6, 126.6, 126.3, 124.4, 122.7, 115.9, 108.8, 61.5, 42.5, 41.4, 14.8; HRMS (ESI) calcd for  $\text{C}_{22}\text{H}_{24}\text{N}_3\text{O}_2$  362.1863 ( $\text{M} + \text{H}$ ) $^+$ , found 362.1862.

**3-((4-(4-Chloro-2-fluorobenzyl)pyridin-2-yl)amino)-N-(2-hydroxyethyl)-2-methylbenzamide (24h).** Compound **24h** (36 mg, 65%) was synthesized following the synthetic procedure of compound **10a** as a white solid.  $^1\text{H}$  NMR (300 MHz, Chloroform-*d*)  $\delta$  7.96 (d,  $J$  = 5.3 Hz, 1H), 7.37 (dd,  $J$  = 7.2, 2.1 Hz, 1H), 7.18 – 7.03 (m, 5H), 6.87 (t,  $J$  = 5.7 Hz, 1H), 6.72 – 6.50 (m, 2H), 6.46 (s, 1H), 3.81 (s, 2H), 3.69 (t,  $J$  = 5.0 Hz, 2H), 3.48 (q,  $J$  = 5.2 Hz, 2H), 3.20 (s, 1H), 2.20 (s, 3H);  $^{13}\text{C}$  NMR (75 MHz,  $\text{CDCl}_3$ )  $\delta$  171.1, 159.0, 156.7, 150.3, 148.0, 138.8 (d,  $J$  = 53.6 Hz), 133.4 (d,  $J$  = 10.0 Hz), 131.7 (d,  $J$  = 5.3 Hz), 129.1, 126.4, 124.9, 124.7 (d,  $J$  = 3.5 Hz), 124.4, 122.7, 116.3 (d,  $J$  = 25.6 Hz), 115.4, 108.4, 61.6, 42.6, 34.0, 34.0, 14.7; HRMS (ESI) calcd for  $\text{C}_{22}\text{H}_{22}\text{ClFN}_3\text{O}_2$  414.1379 ( $\text{M} + \text{H}$ ) $^+$ , found 414.1377.

**3-((4-(3-Fluorobenzyl)pyridin-2-yl)amino)-N-(2-hydroxyethyl)-2-methylbenzamide (24i).** Compound **24i** (33 mg, 65%) was synthesized following the synthetic procedure of compound **10a** as a white solid.  $^1\text{H}$  NMR (300 MHz, Chloroform-*d*)  $\delta$  7.93 (s, 1H), 7.33 (dd,  $J$  = 6.7, 2.7 Hz, 1H), 7.24 (td,  $J$  = 8.2, 6.2 Hz, 1H), 7.11 – 7.03 (m, 3H), 6.96 – 6.89 (m, 2H), 6.88 – 6.74 (m, 2H), 6.55 – 6.38 (m, 2H), 3.80 (s, 2H), 3.64 (t,  $J$  = 5.1 Hz, 3H), 3.43 (q,  $J$  = 5.2 Hz, 2H), 2.18 (s, 3H);  $^{13}\text{C}$  NMR (75 MHz,  $\text{CDCl}_3$ )  $\delta$  171.2, 164.5, 161.3, 156.8, 151.4, 147.8, 141.4 (d,  $J$  = 7.2 Hz), 139.1,

138.4, 130.1 (d,  $J = 8.4$  Hz), 129.3, 126.3, 124.7, 124.6, 122.8, 115.8 (d,  $J = 21.3$  Hz), 113.5 (d,  $J = 21.0$  Hz), 108.7, 61.3, 42.5, 41.0, 14.8; HRMS (ESI) calcd for  $C_{22}H_{23}FN_3O_2$  380.1769 (M + H)<sup>+</sup>, found 380.1765.

**3-((4-(4-Fluorobenzyl)pyridin-2-yl)amino)-N-(2-hydroxyethyl)-2-methylbenzamide (24j).** Compound **24j** (27 mg, 71%) was synthesized following the synthetic procedure of compound **10a** as a white solid. <sup>1</sup>H NMR (300 MHz, Chloroform-*d*)  $\delta$  7.97 (d,  $J = 5.2$  Hz, 1H), 7.38 (dd,  $J = 7.2$ , 2.2 Hz, 1H), 7.16 – 7.04 (m, 4H), 7.03 – 6.92 (m, 2H), 6.83 (t,  $J = 5.6$  Hz, 1H), 6.64 – 6.47 (m, 2H), 6.44 (s, 1H), 3.81 (s, 2H), 3.70 (t,  $J = 5.0$  Hz, 2H), 3.49 (q,  $J = 5.3$  Hz, 2H), 3.00 (s, 1H), 2.21 (s, 3H); <sup>13</sup>C NMR (75 MHz, CDCl<sub>3</sub>)  $\delta$  171.2, 166.6, 163.2, 160.0, 156.7, 152.0, 147.9, 139.2, 138.4, 134.7 (d,  $J = 3.2$  Hz), 130.4 (d,  $J = 8.0$  Hz), 129.1, 126.4, 124.4, 122.7, 115.7, 115.6, 115.3, 108.5, 61.6, 42.6, 40.5, 14.7; HRMS (ESI) calcd for  $C_{22}H_{23}FN_3O_2$  380.1769 (M + H)<sup>+</sup>, found 380.1765.

**N-(2-Hydroxyethyl)-2-methyl-3-((4-(3-(trifluoromethoxy)benzyl)pyridin-2-yl)amino)benzamide (24k).** Compound **24k** (47 mg, 78%) was synthesized following the synthetic procedure of compound **10a** as a white solid. <sup>1</sup>H NMR (300 MHz, Chloroform-*d*)  $\delta$  8.01 (d,  $J = 4.5$  Hz, 1H), 7.44 – 7.25 (m, 2H), 7.20 – 6.97 (m, 5H), 6.78 (d,  $J = 5.1$  Hz, 1H), 6.65 – 6.37 (m, 3H), 3.85 (d,  $J = 3.6$  Hz, 2H), 3.71 (d,  $J = 5.1$  Hz, 2H), 3.50 (t,  $J = 5.1$  Hz, 2H), 3.26 (s, 1H), 2.23 (t,  $J = 2.8$  Hz, 3H); <sup>13</sup>C NMR (75 MHz, CDCl<sub>3</sub>)  $\delta$  171.1, 166.6, 156.8, 151.1, 149.4, 148.1, 141.3, 139.1, 138.4, 129.9, 129.1, 127.4, 126.4, 124.4, 122.8, 121.4, 119.0, 115.7, 108.5, 61.7, 42.6, 41.0, 14.7; HRMS (ESI) calcd for  $C_{23}H_{23}F_3N_3O_3$  446.1686 (M + H)<sup>+</sup>, found 446.1682.

**Molecular Docking.** The molecular docking study was performed using Schrödinger Small-Molecule Drug Discovery Suite (Schrödinger, LLC, New York, NY, 2020). The co-crystal structure of GPR52 bound with compound **2** (PDB code: 6LI0) was downloaded from RCS PDB

bank. The co-crystal structure was preprocessed and minimized with Schrödinger Protein Preparation Wizard using default settings. The grid center was chosen on the centroid of existing ligand and the size of grid box was set to 30 Å on each side. The 3D structure of ligands **4a**, **15b**, and **24f** were created using Schrödinger Maestro and a low energy conformation was calculated using LigPrep. Docking was employed with Glide using the SP precision. Docked poses were incorporated into Schrödinger Maestro for visualization and analysis of binding site interactions.

**Cell Culture and Plasmids.** Wildtype (WT) human embryonic kidney 293 (HEK293) cells were a generous gift from Dr. Asuka Inoue, Tohoku University.<sup>56</sup> The wild type HEK293 cells were cultured in DMEM (Gibco, Carlsbad, CA) with 10% FBS (Omega Scientific, Tarzana, CA) and 1% penicillin/streptomycin (Gibco, Carlsbad, CA) in a humidified incubator at 37°C in 5% CO<sub>2</sub>. HTLA cells (HEK293 cells stably expressing tTA-dependent luciferase reporter and a  $\beta$ -arrestin2-TEV fusion gene) were a generous gift from Dr. Bryan Roth, University of North Carolina at Chapel Hill.<sup>46</sup> The HTLA cells were cultured in DMEM with 10% FBS, 1% penicillin/streptomycin, 100  $\mu$ g/ml hygromycin (Thermofisher, Waltham, MA), and 2  $\mu$ g/ml puromycin (Gibco/Fisher Scientific, Hampton, NH) in a humidified incubator at 37 °C in 5% CO<sub>2</sub>. The human GPR52 Tango plasmid was purchased from Addgene (Watertown, MA). A human GPR52 WT construct was generated from the GPR52 Tango plasmid via placement of a stop codon following the receptor coding sequence, as previously described.<sup>40</sup>

**Transfection.** For the cAMP GloSensor assays,  $6.5 \times 10^5$  wildtype HEK293 cells were plated in 6-well plates (Corning, Oneonta, NY) 24 h before transfection to achieve 70-80% confluency the following day. Each well of wildtype HEK293 cells was transiently transfected with 0.10  $\mu$ g of wild type human GPR52 WT plasmid and 1  $\mu$ g of 22F GloSensor plasmid (Promega, Madison, WI) using 10  $\mu$ L of Lipofectamine 2000 (Invitrogen, Waltham, MA) in 0.4 mL of Opti-MEM

(Gibco, Carlsbad, CA) and 2 mL of growth media. For the Tango  $\beta$ -arrestin recruitment assays,  $6.5 \times 10^5$  HTLA cells were plated in 6-well plates 24 h before transfection to achieve 70-80% confluency the following day. Each well was transiently transfected with 0.25  $\mu$ g of GPR52 Tango plasmid using 10  $\mu$ L of Lipofectamine 2000 in 0.4 mL of Opti-MEM and 2 mL of growth media.

**cAMP GloSensor Assay.** 18 h after transfection, wildtype HEK293 cells with GPR52 and GloSensor plasmids (see transfections above) were seeded at 50,000 cells/well in growth media into poly-*L*-lysine (Trevigen, Gaithersburg, MD) coated 96-well white clear-bottomed cell culture plates (Greiner Bio-One, Monroe, NC). 4 h later, complete media was aspirated and replaced with 90  $\mu$ L/well of 1% GloSensor reagent (Promega, Madison, WI) in Hanks balanced salt solution (HBSS, Gibco/Fisher Scientific, Hampton, NH) and 20 mM HEPES. Cells were serum starved for 2 h at room temperature in the dark. Test compounds were weighed and diluted to 2 mM in DMSO. Serial dilutions of each test compound were prepared in 1% GloSensor reagent/20 mM HEPES in HBSS and were transferred to a 96-well source plate. Cells were incubated with compound solutions for 15 min. Luminescence in light counts per second (lcps) was recorded on a MicroBeta2 Microplate counter (Perkin Elmer, Waltham, MA). Data from at least three independent experiments ( $n = 3-24$ ) conducted in technical triplicate are presented as percentage of compound **4a** response (compound **4a** response set to 100%). All *in vitro* pharmacological data were analyzed using GraphPad Prism 8.4.3 software (La Jolla, CA). Data from cAMP ligand concentration-response assays are presented as the half maximum ( $EC_{50}$ , nM) and maximum effect ( $E_{max}$ ) (means  $\pm$  SEM) as computed by GraphPad using a four-parameter nonlinear regression curve-fitting algorithm.

**Tango  $\beta$ -Arrestin Recruitment Assay.** 18 h after transfection, HTLA cells expressing GPR52 Tango plasmid (see transfections above) were seeded at 80,000 cells/well in 100  $\mu$ L/well growth

media into poly-*L*-lysine coated 96-well white clear-bottomed cell culture plates. Test compounds were weighed and diluted to 2 mM in DMSO. Serial dilutions of each compound were prepared in growth media in a 96-well source plate. At 24 h post-transfection, cells were treated with compound solutions and returned to the incubator. After 20 h incubation, growth media was aspirated and the cells were lysed with 50  $\mu$ L/well of 40-fold diluted Bright-Glo luciferase substrate (Promega, Madison, WI) in HBSS for 20 min at room temperature. Luminescence in light counts per second (lcps) was recorded on a MicroBeta2 Microplate counter. Data from at least three independent experiments ( $n = 3-6$ ) conducted in technical triplicate are presented as percentage of compound **4a** response (compound **4a** response set to 100%). All data were analyzed using GraphPad Prism 8.4.3 software. Data from  $\beta$ -arrestin recruitment concentration-response assays are presented as the half maximum ( $EC_{50}$ , nM) and maximum effect ( $E_{max}$ ) (means  $\pm$  SEM) as computed by GraphPad using a four-parameter nonlinear regression curve-fitting algorithm. Notably, some compounds when tested for  $\beta$ -arrestin recruitment did not show saturating concentration-responses; in these cases, the curve-fitting algorithm in GraphPad Prism was constrained by defining the maximum efficacy as the maximal observed luminescence.

**GPR52 Desensitization Studies.** 18 h after transfection of wildtype HEK293 cells with GPR52 and GloSensor plasmids (see transfections above), cells were seeded at 50,000 cells/well into poly-*L*-lysine coated 96-well white clear-bottomed cell culture plates in growth media (Greiner Bio-One, Monroe, NC). 4 h later, complete media was aspirated and replaced with 90  $\mu$ L/well serum-free DMEM media. Compounds were diluted in serum-free media to respective  $EC_{50}$  concentrations determined from the cAMP concentration-response assays (see above). Cells were incubated at room temperature in the dark with the  $EC_{50}$  concentration (determined in cAMP assays) of compounds for 2 h to induce GPR52 desensitization. During the final 60 min of

compound pretreatment, cells were also incubated in 1% GloSensor reagent/20 mM HEPES in HBSS to load cells with substrate for the cAMP assay. Following the 2 h pretreatments, buffer was aspirated, and wells were washed for 5 min intervals three times with 20 mM HEPES in HBSS. After washing, cells were challenged with 1  $\mu$ M compound **4a** for 15 min to determine remaining GPR52 G protein/cAMP signaling activity. Luminescence in light counts per second (lcps) was recorded on a MicroBeta2 Microplate counter. Data from three independent experiments ( $n = 3$ ) conducted in technical quadruplicate are presented as raw counts (lcps) or percent desensitization (normalized to 100% DMSO control response). All data were analyzed using GraphPad Prism 8.4.3 software. Statistically significant differences were determined by one-way ANOVA with Tukey's post-hoc test. A Pearson's correlation analysis was used to compare the GPR52 cAMP response after agonist pretreatments versus the agonist  $EC_{50}$  for GPR52  $\beta$ -arrestin recruitment. The resulting correlation  $p$ -value and a coefficient of determination ( $R^2$ ) were determined.

**Bias Factor Calculations.** Mean efficacy ( $E_{max}$ ) and potency ( $EC_{50}$ ) were taken from at least three independent experiments for all compounds tested in both the cAMP and  $\beta$ -arrestin recruitment assays. Formulas for bias factor calculations were adapted from Kenakin (2017).<sup>48</sup> The bias factor calculation method requires an agonist to have an  $E_{max} > 35\%$  compared to the reference agonist, which all tested compounds displayed.  $E_{max}$  and  $EC_{50}$  values for each compound were entered into the equation  $\log(E_{max}/EC_{50})$  for both cAMP and  $\beta$ -arrestin recruitment assays, then subtracted from the respective  $\log(E_{max}/EC_{50})$  for the reference compound **4a** to obtain a  $\Delta\log(E_{max}/EC_{50})$  for each compound. A  $\Delta\Delta\log(E_{max}/EC_{50})$  value for each compound was calculated by subtraction of  $\Delta\log(E_{max}/EC_{50})_{\beta\text{-arrestin}}$  from  $\Delta\log(E_{max}/EC_{50})_{cAMP}$ . The inverse log of this  $\Delta\Delta\log(E_{max}/EC_{50})$  value is the G protein bias factor. Conversely, the  $\beta$ -arrestin bias factor is calculated from the inverse log of  $\Delta\Delta\log(E_{max}/EC_{50})$  when  $\Delta\log(E_{max}/EC_{50})_{cAMP}$  is subtracted from

$\Delta\log(E_{\max}/EC_{50})_{\beta\text{-arrestin}}$ . The calculated bias factors represent relative propensity to activate one pathway over another in reference to compound **4a**.

***In Vivo* PK Studies.** Male Sprague-Dawley rats (n = 3 per treatment group; Beijing Vital River Laboratory, Animal Technology Co., Ltd, Beijing, China) weighing 200-250 g at the beginning of the experiment were housed three per cage in a pathogen-free, temperature-controlled (20-26°C), and humidity-controlled (40-70%) environment with a 12 h light–dark cycle and ad libitum access to food and filtered water. Rats were randomly assigned to treatment groups. Vehicle (10% dimethyl sulfoxide (DMSO) and 90% 2-hydroxypropyl- $\beta$ -cyclodextrin (HP- $\beta$ -CD); Cyclodextrin Technologies Development, Inc., High Springs, FL, USA) or compound **15b/24f** dissolved in vehicle was administered to rats IV at 10 mg/kg or PO at 20 mg/kg. The rat was restrained manually at the designated time points (0.08, 0.25, 0.5, 1.0, 2.0, 4.0, 8.0, and 24 h post-dosing for IV; 0.25, 0.5, 1.0, 2.0, 4.0, 8.0, and 24 h post-dosing for PO). 300  $\mu$ L of blood (yielding ~50  $\mu$ L of plasma) samples are taken from the animal’s jugular vein and placed into micro K<sub>2</sub>EDTA tubes. Blood samples were placed on ice and centrifuged at 6000 rpm for 5 min at 4°C to generate plasma sample within 0.5 h of collection. Brain samples were collected at 0.25 and 1 h post-dosing. All samples were stored at –80 °C. The concentration of **15b/24f** in each sample was analyzed by Sundia MediTech Co., Ltd. The study and the related standard operating procedures were reviewed and approved by the Sundia Institutional Animal Care and Use Committee. The Sundia animal facility is approved with yearly inspection by the Shanghai Laboratory Animal Management Committee. All treatment assignments were blinded to investigators who performed PK assays and end point statistical analyses.

The PK parameters of compounds **15b** and **24f** were calculated according to a non-compartmental model using WinNonlin (Pharsight Corporation, ver 8.1, Mountain View, CA,

USA). The peak concentration ( $C_{\max}$ ) was directly obtained by visual inspection of the plasma concentration-time profile. The elimination rate constant ( $\lambda$ ) was obtained by the least-squares fitted terminal log-linear portion of the slope of the plasma concentration-time profile. The elimination half-life ( $t_{1/2}$ ) was evaluated according to  $0.693/\lambda$ . The area under the plasma concentration-time curve from 0 to time t ( $AUC_{0-t}$ ) was evaluated using the linear trapezoidal rule and further extrapolated to infinity ( $AUC_{0-\infty}$ ) according to the following equation:  $AUC_{0-\infty} = AUC_{0-t} + C_{\text{last}}/\lambda$ . The pharmacokinetic parameters are presented as mean  $\pm$  SEM.

## ASSOCIATED CONTENT

### Supporting Information

The Supporting Information is available free of charge at <https://pubs.acs.org/>. Figures S1-S3, HPLC analysis spectra of representative compounds,  $^1\text{H}$  and  $^{13}\text{C}$  NMR spectra of all new compounds, and molecular formula strings. Authors will release the atomic coordinates for docked compounds upon article publication.

## AUTHOR INFORMATION

### Corresponding Authors

Jia Zhou – Center for Addiction Sciences and Therapeutics, Department of Pharmacology and Toxicology, University of Texas Medical Branch, Galveston, Texas 77555, United States; Phone: (409) 772-9748; Email: [jizhou@utmb.edu](mailto:jizhou@utmb.edu)

John A. Allen – Center for Addiction Sciences and Therapeutics, Department of Pharmacology and Toxicology, School of Medicine, University of Texas Medical Branch, Galveston, Texas 77555, United States; Phone: (409) 772-9621; Email: [joaallen@utmb.edu](mailto:joaallen@utmb.edu)

### Present Addresses

PW: Ocean University of China, Qingdao, Shangdong 266003, China.

DEF: Neurocrine Biosciences, San Diego, California 92130.

### **Author Contributions**

<sup>1</sup>REM, PW, and SA contributed equally and should be considered as co-first authors.

\*JAA and JZ are equal contributors and co-corresponding authors.

### **ACKNOWLEDGMENTS**

This work was supported by grants U18 DA052543 (JAA and JZ) and T32 DA 007287 (DEF), a 2022 Predoctoral Fellowship from the PhRMA foundation (REM), and the Center for Addiction Sciences and Therapeutics at the University of Texas Medical Branch (UTMB). J.Z. is also partially supported by the John D. Stobo, M. D., Distinguished Chair Endowment and the Edith & Robert Zinn Chair Endowment in Drug Discovery. The authors would also like to acknowledge Dr. Asuka Inoue, Tohoku University, for the generous gift of the HEK cell line, Dr. Bryan Roth, UNC-Chapel Hill, for the generous gift of the HTLA cell line, Dr. Lawrence C. Sowers at the UTMB Department of Pharmacology and Toxicology as well as Dr. Tianzhi Wang at the NMR core facility of UTMB for the NMR spectroscopy assistance, and Dr. Xuemei Luo at UTMB Mass Spectrometry Core with funding support from University of Texas System Proteomics Network for the HRMS analysis.

### **ABBREVIATIONS USED**

cAMP, cyclic adenosine monophosphate; CNS, central nervous system; DMAP, 4-dimethylaminopyridine; DMF, *N,N*-dimethylformamide; EC<sub>50</sub>, half maximal effective concentration; ECL2, extracellular loop 2; EDCI, *N*-(3-dimethylaminopropyl)-*N'*-ethylcarbodiimide hydrochloride; GPCRs, G-protein-coupled receptors; HD, Huntington's disease; HEK293, human embryonic kidney 293; hERG, human ether-a-go-go-related gene; HOBt, 1-hydroxybenzotriazole; IV, intravenous; mHTT, mutant huntingtin; MSNs, medium spiny

neurons; NAc, nucleus accumbens; NIMH, national institute of mental health; Pd(dppf)<sub>2</sub>Cl<sub>2</sub>, 1,1'-bis(diphenylphosphino)ferrocene-palladium(II)dichloride dichloromethane complex; PDSP, psychoactive drug screening program; PK, pharmacokinetic; PO, oral ; SAR, structure-activity relationship; SUD, substance-use disorder; SZ, schizophrenia; TM, transmembrane helix; WT, Wildtype; XantPhos, 4,5-bis(diphenylphosphino)-9,9-dimethylxanthene.

## REFERENCES

- (1) Ali, S.; Wang, P.; Murphy, R. E.; Allen, J. A.; Zhou, J. Orphan GPR52 as an emerging neurotherapeutic target. *Drug Discov. Today* **2024**, *29*, 103922.
- (2) Wang, P.; Lv, L.; Li, H.; Wang, C. Y.; Zhou, J. Opportunities and challenges in drug discovery targeting the orphan receptor GPR12. *Drug Discov. Today* **2023**, *28*, 103698.
- (3) Bolinger, A. A.; Frazier, A.; La, J. H.; Allen, J. A.; Zhou, J. Orphan G Protein-Coupled Receptor GPR37 as an Emerging Therapeutic Target. *ACS Chem. Neurosci.* **2023**, *14*, 3318-3334.
- (4) Ye, N.; Li, B.; Mao, Q.; Wold, E. A.; Tian, S.; Allen, J. A.; Zhou, J. Orphan Receptor GPR88 as an Emerging Neurotherapeutic Target. *ACS Chem. Neurosci.* **2019**, *10*, 190-200.
- (5) Alavi, M. S.; Shamsizadeh, A.; Azhdari-Zarmehri, H.; Roohbakhsh, A. Orphan G protein-coupled receptors: The role in CNS disorders. *Biomed. Pharmacother.* **2018**, *98*, 222-232.
- (6) Sutton, L. P.; Orlandi, C.; Song, C.; Oh, W. C.; Muntean, B. S.; Xie, K.; Filippini, A.; Xie, X.; Satterfield, R.; Yaeger, J. D. W.; et al. Orphan receptor GPR158 controls stress-induced depression. *eLife* **2018**, *7*.
- (7) Jeong, E.; Kim, Y.; Jeong, J.; Cho, Y. Structure of the class C orphan GPCR GPR158 in complex with RGS7-Gβ5. *Nat. Commun.* **2021**, *12*, 6805.

- (8) Lees, J. A.; Dias, J. M.; Rajamohan, F.; Fortin, J.-P.; O'Connor, R.; Kong, J. X.; Hughes, E. A. G.; Fisher, E. L.; Tuttle, J. B.; Lovett, G.; et al. An inverse agonist of orphan receptor GPR61 acts by a G protein-competitive allosteric mechanism. *Nat. Commun.* **2023**, *14*, 5938.
- (9) Margolin, D. H.; Brice, N. L.; Davidson, A. M.; Matthews, K. L.; Carlton, M. B. L. A Phase I, First-in-Human, Healthy Volunteer Study to Investigate the Safety, Tolerability, and Pharmacokinetics of CVN424, a Novel G Protein-Coupled Receptor 6 Inverse Agonist for Parkinson's Disease. *J. Pharmacol. Exp. Ther.* **2022**, *381*, 33-41.
- (10) Sawzdargo, M.; Nguyen, T.; Lee, D. K.; Lynch, K. R.; Cheng, R.; Heng, H. H.; George, S. R.; O'Dowd, B. F. Identification and cloning of three novel human G protein-coupled receptor genes GPR52,  $\Psi$ GPR53 and GPR55: GPR55 is extensively expressed in human brain. *Mol. Brain Res.* **1999**, *64*, 193-198.
- (11) Komatsu, H.; Maruyama, M.; Yao, S.; Shinohara, T.; Sakuma, K.; Imaichi, S.; Chikatsu, T.; Kuniyeda, K.; Siu, F. K.; Peng, L. S.; et al. Anatomical transcriptome of G protein-coupled receptors leads to the identification of a novel therapeutic candidate GPR52 for psychiatric disorders. *PLoS One* **2014**, *9*, e90134.
- (12) Yang, R. Y.; Quan, J.; Sodaei, R.; Aguet, F.; Segrè, A. V.; Allen, J. A.; Lanz, T. A.; Reinhart, V.; Crawford, M.; Hasson, S.; et al. A systematic survey of human tissue-specific gene expression and splicing reveals new opportunities for therapeutic target identification and evaluation. *bioRxiv* **2018**, 311563.
- (13) Spark, D. L.; Mao, M.; Ma, S.; Sarwar, M.; Nowell, C. J.; Shackelford, D. M.; Sexton, P. M.; Nithianantharajah, J.; Stewart, G. D.; Langmead, C. J. In the Loop: Extrastriatal Regulation of Spiny Projection Neurons by GPR52. *ACS Chem. Neurosci.* **2020**.

- (14) Murphy, R. F., DE; Allen JA. Bi-directional cAMP signaling crosstalk between dopamine D2 receptors and the constitutively active orphan receptor GPR52. *FASEB J.* **2021**, *35*.
- (15) Pardinás, A. F.; Holmans, P.; Pocklington, A. J.; Escott-Price, V.; Ripke, S.; Carrera, N.; Legge, S. E.; Bishop, S.; Cameron, D.; Hamshere, M. L.; et al. Common schizophrenia alleles are enriched in mutation-intolerant genes and in regions under strong background selection. *Nat. Genet.* **2018**, *50*, 381-389.
- (16) Felsing, D. E.; Jain, M. K.; Allen, J. A. Advances in Dopamine D1 Receptor Ligands for Neurotherapeutics. *Curr. Top. Med. Chem.* **2019**, *19*, 1365-1380.
- (17) Surmeier, D. J.; Ding, J.; Day, M.; Wang, Z.; Shen, W. D1 and D2 dopamine-receptor modulation of striatal glutamatergic signaling in striatal medium spiny neurons. *Trends Neurosci.* **2007**, *30*, 228-235.
- (18) Yao, Y.; Cui, X.; Al-Ramahi, I.; Sun, X.; Li, B.; Hou, J.; DiFiglia, M.; Palacino, J.; Wu, Z. Y.; Ma, L.; et al. A striatal-enriched intronic GPCR modulates huntingtin levels and toxicity. *eLife* **2015**, *4*.
- (19) Li, G.; Marlin, M. C. Rab family of GTPases. *Methods Mol. Biol.* **2015**, *1298*, 1-15.
- (20) Song, H.; Li, H.; Guo, S.; Pan, Y.; Fu, Y.; Zhou, Z.; Li, Z.; Wen, X.; Sun, X.; He, B.; et al. Targeting Gpr52 lowers mutant HTT levels and rescues Huntington's disease-associated phenotypes. *Brain* **2018**, *141*, 1782-1798.
- (21) Lin, X.; Li, M.; Wang, N.; Wu, Y.; Luo, Z.; Guo, S.; Han, G. W.; Li, S.; Yue, Y.; Wei, X.; et al. Structural basis of ligand recognition and self-activation of orphan GPR52. *Nature* **2020**, *579*, 152-157.
- (22) Krumm, B.; Roth, B. L. A self-activating orphan receptor. *Nature* **2020**, *579*, 35-36.

- (23) Setoh, M.; Ishii, N.; Kono, M.; Miyanoohana, Y.; Shiraishi, E.; Harasawa, T.; Ota, H.; Odani, T.; Kanzaki, N.; Aoyama, K.; et al. Discovery of the first potent and orally available agonist of the orphan G-protein-coupled receptor 52. *J. Med. Chem.* **2014**, *57*, 5226-5237.
- (24) Nakahata, T.; Tokumaru, K.; Ito, Y.; Ishii, N.; Setoh, M.; Shimizu, Y.; Harasawa, T.; Aoyama, K.; Hamada, T.; Kori, M.; et al. Design and synthesis of 1-(1-benzothiophen-7-yl)-1H-pyrazole, a novel series of G protein-coupled receptor 52 (GPR52) agonists. *Bioorg. Med. Chem.* **2018**, *26*, 1598-1608.
- (25) Tokumaru, K.; Ito, Y.; Nomura, I.; Nakahata, T.; Shimizu, Y.; Kurimoto, E.; Aoyama, K.; Aso, K. Design, synthesis, and pharmacological evaluation of 4-azolyl-benzamide derivatives as novel GPR52 agonists. *Bioorg. Med. Chem.* **2017**, *25*, 3098-3115.
- (26) Nishiyama, K.; Suzuki, H.; Harasawa, T.; Suzuki, N.; Kurimoto, E.; Kawai, T.; Maruyama, M.; Komatsu, H.; Sakuma, K.; Shimizu, Y.; et al. FTBMT, a novel and selective GPR52 agonist, demonstrates antipsychotic-like and procognitive effects in rodents, revealing a potential therapeutic agent for schizophrenia. *J. Pharmacol. Exp. Ther.* **2017**, *363*, 253-264.
- (27) Xiong, Y. G., A. J.; Korman, H.; Lehmann, J.; Ren, A. S.; Semple, G. 1-Heteroaryl-indoline-4-carboxamines as modulators of GPR52 useful for the treatment or prevention of disorders related thereto. WO2016176571 A1, 2016.
- (28) Poulter, S.; Austin, N.; Armstrong, R.; Barnes, M.; Bucknell, S. J.; Higuieruelo, A.; Banerjee, J.; Mead, A.; Mould, R.; MacSweeney, C.; et al. The Identification of GPR52 Agonist HTL0041178, a Potential Therapy for Schizophrenia and Related Psychiatric Disorders. *ACS Med. Chem. Lett.* **2023**, *14*, 499-505.
- (29) Sosei Heptares Doses First Subject in Phase I Trial with HTL0048149, a First-in-Class GPR52 Agonist for Schizophrenia: <https://soseiheptares.com/news/851/129/Sosei-Heptares-Doses-First->

[Subject-in-Phase-I-Trial-with-HTL0048149-a-First-in-Class-GPR52-Agonist-for-Schizophrenia.html](#). 2023.

(30) Watson, S. P.; Swain, N. A.; O'Brien, M. A. GPR52 modulator compounds. WO 2023/041909 A1, 2023.

(31) Gerlach, K.; Berta, D. G.; Ferrara, M.; Gutsche, K.; Mueller-Vieira, U.; Hobson, S.; Runge, F.; Semple, G.; Vintonyak, V.; Xiong, Y. 3-Phenoxyazetid-1-yl-heteroaryl pyrrolidine derivatives and the use thereof as medicament. WO 2023/041432 A1, 2023.

(32) DeWire, S. M.; Ahn, S.; Lefkowitz, R. J.; Shenoy, S. K.  $\beta$ -Arrestins and Cell Signaling. *Annu. Rev. Physiol.* **2007**, *69*, 483-510.

(33) Peterson, Y. K.; Luttrell, L. M. The Diverse Roles of Arrestin Scaffolds in G Protein–Coupled Receptor Signaling. *Pharmacol. Rev.* **2017**, *69*, 256-297.

(34) Wess, J.; Oteng, A.-B.; Rivera-Gonzalez, O.; Gurevich, E. V.; Gurevich, V. V.  $\beta$ -Arrestins: Structure, Function, Physiology, and Pharmacological Perspectives. *Pharmacol. Rev.* **2023**, *75*, 854-884.

(35) Urban, J. D.; Clarke, W. P.; von Zastrow, M.; Nichols, D. E.; Kobilka, B.; Weinstein, H.; Javitch, J. A.; Roth, B. L.; Christopoulos, A.; Sexton, P. M.; et al. Functional selectivity and classical concepts of quantitative pharmacology. *J. Pharmacol. Exp. Ther.* **2007**, *320*, 1-13.

(36) Schmid, C. L.; Kennedy, N. M.; Ross, N. C.; Lovell, K. M.; Yue, Z.; Morgenweck, J.; Cameron, M. D.; Bannister, T. D.; Bohn, L. M. Bias Factor and Therapeutic Window Correlate to Predict Safer Opioid Analgesics. *Cell* **2017**, *171*, 1165-1175 e1113.

(37) Gray, D. L., Allen, J.A.; Mente, S.; O'Connor, R. E.; DeMarco, G. J.; Efremov, I.; Tierney, P.; Volfson, D.; Davoren, J.; Guilmette, E.; Salafia, M.; et al. Impaired  $\beta$ -arrestin recruitment and

reduced desensitization by non-catechol agonists of the D1 dopamine receptor. *Nat. Commun.* **2018**, *9*, 674.

(38) Rajagopal, S.; Rajagopal, K.; Lefkowitz, R. J. Teaching old receptors new tricks: biasing seven-transmembrane receptors. *Nat. Rev. Drug Discov.* **2010**, *9*, 373-386.

(39) Rankovic, Z.; Brust, T. F.; Bohn, L. M. Biased agonism: An emerging paradigm in GPCR drug discovery. *Bioorg. Med. Chem. Lett.* **2016**, *26*, 241-250.

(40) Wang, P.; Felsing, D. E.; Chen, H.; Stutz, S. J.; Murphy, R. E.; Cunningham, K. A.; Allen, J. A.; Zhou, J. Discovery of Potent and Brain-Penetrant GPR52 Agonist that Suppresses Psychostimulant Behavior. *J. Med. Chem.* **2020**, *63*, 13951-13972.

(41) Zhou, J.; Allen, J. A.; Wang, P.; Felsing, D. E. Heterocyclic G-protein-coupled receptor 52 (GPR52) agonists. US 2022/0112164 A1, 2022.

(42) Ali, S.; Zhou, J. Highlights on U.S. FDA-approved fluorinated drugs over the past five years (2018-2022). *Eur. J. Med. Chem.* **2023**, *256*, 115476.

(43) Ali, S.; Bolinger, A. A.; Zhou, J. Highlights on Fluorine-Containing Drugs Approved by U.S. FDA in 2023. *Curr. Top. Med. Chem.* **2024**, *24*, 1-7.

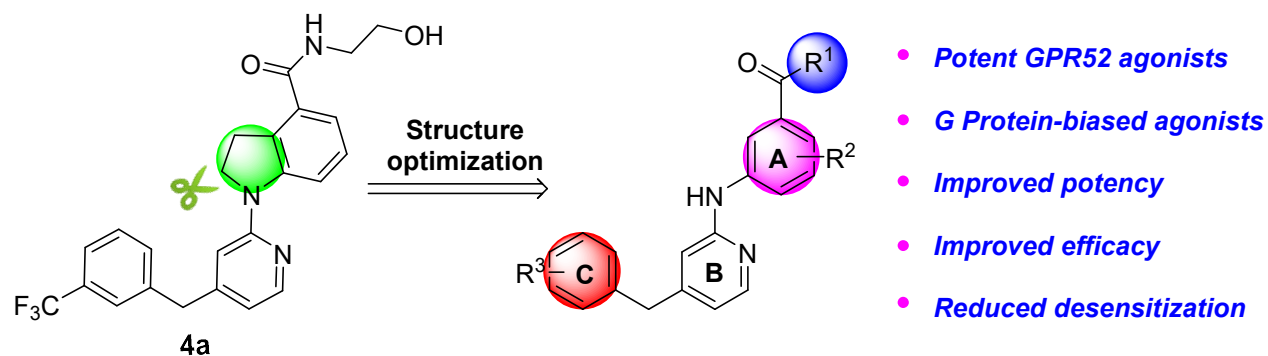
(44) Ferguson, S. S.; Downey, W. E., 3rd; Colapietro, A. M.; Barak, L. S.; Menard, L.; Caron, M. G. Role of  $\beta$ -Arrestin in Mediating Agonist-Promoted G Protein-Coupled Receptor Internalization. *Science* **1996**, *271*, 363-366.

(45) Kroeze, W. K.; Sassano, M. F.; Huang, X. P.; Lansu, K.; McCorvy, J. D.; Giguere, P. M.; Sciaky, N.; Roth, B. L. PRESTO-Tango as an open-source resource for interrogation of the druggable human GPCRome. *Nat. Struct. Mol. Biol.* **2015**, *22*, 362-369.

- (46) Barnea, G.; Strapps, W.; Herrada, G.; Berman, Y.; Ong, J.; Kloss, B.; Axel, R.; Lee, K. J. The genetic design of signaling cascades to record receptor activation. *Proc. Natl. Acad. Sci. U. S. A.* **2008**, *105*, 64-69.
- (47) Zhang, J. H.; Chung, T. D.; Oldenburg, K. R. A Simple Statistical Parameter for Use in Evaluation and Validation of High Throughput Screening Assays. *J. Biomol. Screen.* **1999**, *4*, 67-73.
- (48) Kenakin, T. A Scale of Agonism and Allosteric Modulation for Assessment of Selectivity, Bias, and Receptor Mutation. *Mol. Pharmacol.* **2017**, *92*, 414-424.
- (49) Lohse, M. J.; Benovic, J. L.; Codina, J.; Caron, M. G.; Lefkowitz, R. J.  $\beta$ -Arrestin: a Protein that Regulates  $\beta$ -adrenergic Receptor Function. *Science* **1990**, *248*, 1547-1550.
- (50) Klein Herenbrink, C.; Sykes, D. A.; Donthamsetti, P.; Canals, M.; Coudrat, T.; Shonberg, J.; Scammells, P. J.; Capuano, B.; Sexton, P. M.; Charlton, S. J.; et al. The role of kinetic context in apparent biased agonism at GPCRs. *Nat. Commun.* **2016**, *7*, 10842.
- (51) Wacker, D.; Wang, S.; McCorvy, J. D.; Betz, R. M.; Venkatakrishnan, A. J.; Levit, A.; Lansu, K.; Schools, Z. L.; Che, T.; Nichols, D. E.; et al. Crystal Structure of an LSD-Bound Human Serotonin Receptor. *Cell* **2017**, *168*, 377-389.e312.
- (52) Fan, Y.; Lin, X.; Pan, B.; Chen, B.; Liu, D.; Wuthrich, K.; Xu, F. Allosteric coupling between G-protein binding and extracellular ligand binding sites in GPR52 revealed by (19)F-NMR and cryo-electron microscopy. *MedComm* **2023**, *4*, e260.
- (53) Besnard, J.; Ruda, G. F.; Setola, V.; Abecassis, K.; Rodriguiz, R. M.; Huang, X. P.; Norval, S.; Sassano, M. F.; Shin, A. I.; Webster, L. A.; et al. Automated design of ligands to polypharmacological profiles. *Nature* **2012**, *492*, 215-220.

- (54) Kalyaanamoorthy, S.; Barakat, K. H. Development of Safe Drugs: The hERG Challenge. *Med. Res. Rev.* **2018**, *38*, 525-555.
- (55) Garrido, A.; Lepailleur, A.; Mignani, S. M.; Dallemagne, P.; Rochais, C. hERG toxicity assessment: Useful guidelines for drug design. *Eur. J. Med. Chem.* **2020**, *195*, 112290.
- (56) Grundmann, M.; Merten, N.; Malfacini, D.; Inoue, A.; Preis, P.; Simon, K.; Rüttiger, N.; Ziegler, N.; Benkel, T.; Schmitt, N. K.; et al. Lack of beta-arrestin signaling in the absence of active G proteins. *Nat. Commun.* **2018**, *9*, 341.

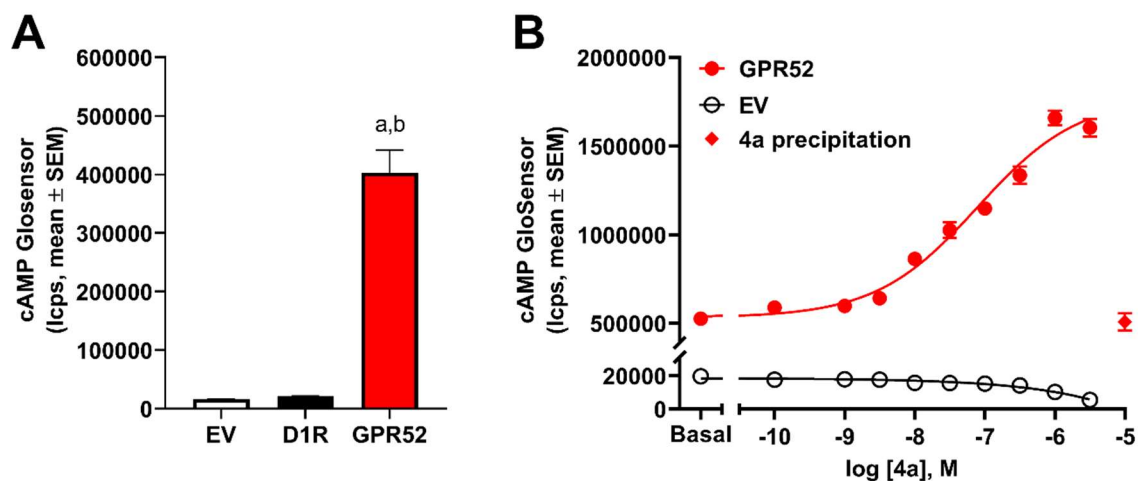
## Graphic Abstract



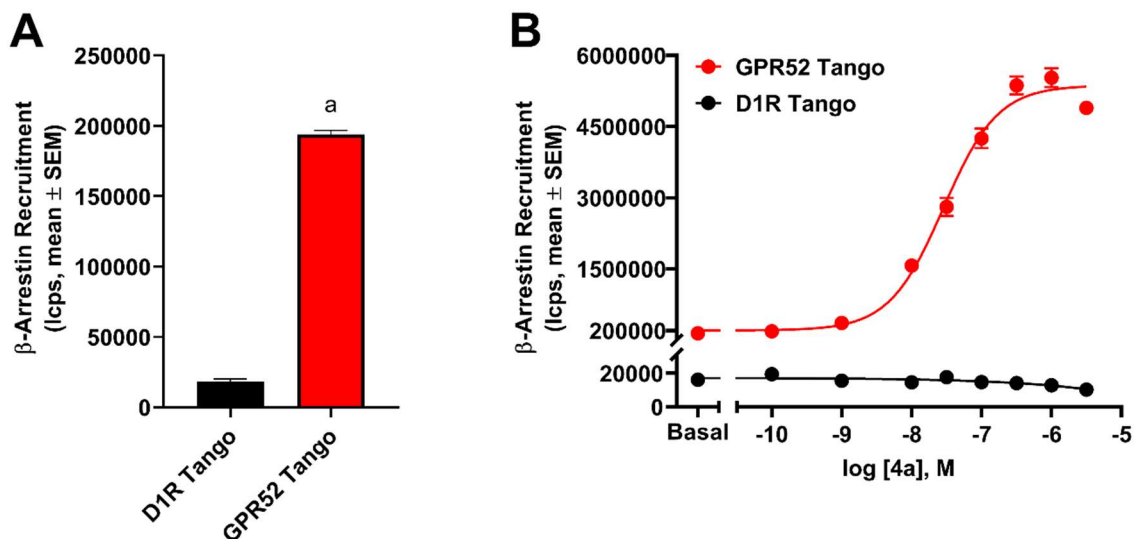
# *Supporting Information*

## **Table of Contents**

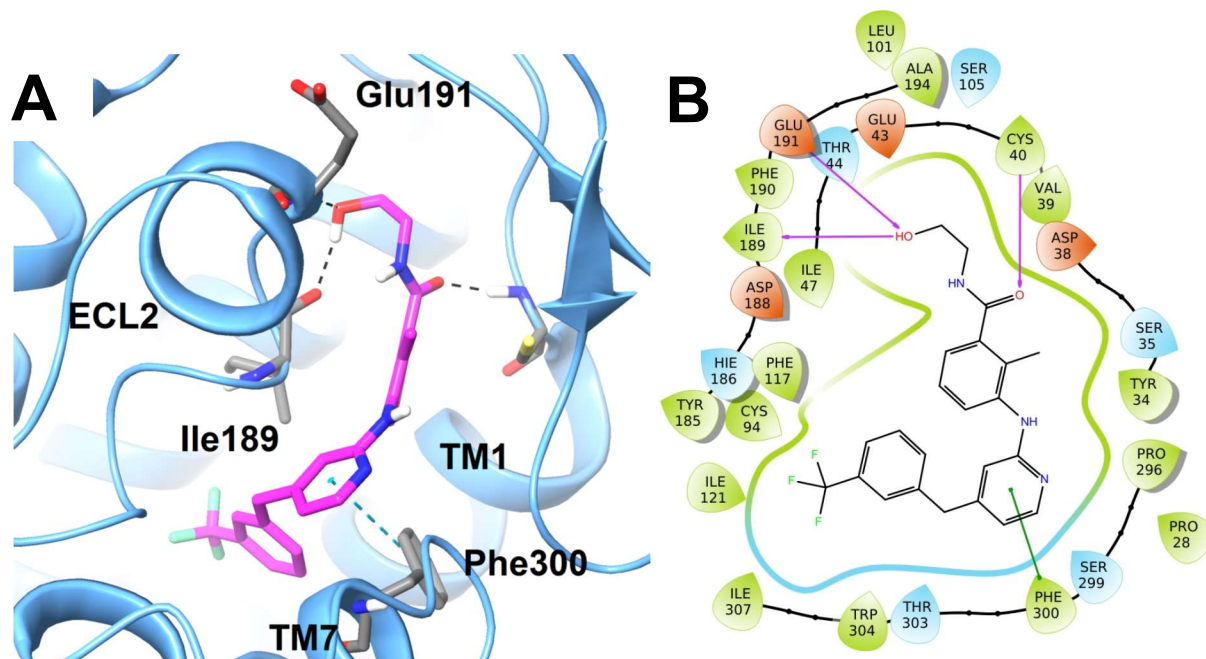
Figure S1	77
Figure S2	78
Figure S3	79



**Supplementary Figure 1.** GloSensor cAMP assay validation in HEK293 cells transiently transfected with GloSensor 22F reporter and GPR52, dopamine D<sub>1</sub> receptor (D<sub>1</sub>R), or empty vector (EV). (A) Expression of GPR52 significantly elevated basal cAMP levels >20-fold above that of both EV and G<sub>s</sub>-coupled D<sub>1</sub>R. *a*,  $p < 0.05$  vs. EV; *b*,  $p < 0.05$  vs. D<sub>1</sub>R; one-way ANOVA with Tukey's post-hoc test. (B) Representative concentration-response plot of parent compound **4a**, which displayed a robust, ~3-fold response in GPR52 cells and no activity in EV cells. Limited solubility of **4a** caused visible precipitation and decreased GloSensor response at high concentration.



**Supplementary Figure 2.** Tango  $\beta$ -arrestin recruitment assay validation in HTLA cells transiently transfected with GPR52 Tango or D1R Tango plasmids. (A) GPR52 Tango expression significantly increased basal  $\beta$ -arrestin activity  $\sim$ 10-fold over D1R TANGO. *a*,  $p < 0.05$  vs. D1R; Student's T test. (B) Representative concentration-response plot of parent compound **4a**, showing  $\sim$ 25-fold signal response in GPR52 Tango cells with no activity in the D1R Tango control cells.



**Supplemental Figure 3.** Predicted binding mode and molecular docking of compound **15b** with GPR52 (PDB: 6LI0). (A) Docking of compound **15b** (magenta) into the binding pocket of GPR52 surrounded by N-terminus, TM1, TM2, TM7, and ECL2. Important residues are drawn as gray sticks. Hydrogen bonds are shown as dashed black lines, while  $\pi$ - $\pi$  interactions are shown as dashed cyan lines. (B) Interaction diagram of compound **15b** docked into the binding pocket of GPR52. Hydrogen bonds are shown as magenta lines and  $\pi$ - $\pi$  stacking interaction is shown as a green line.